Modelling the Synaptic Plasticity Underlying Habituation, Sensitization and Classical Conditioning of the *Aplysia Californica* Gill Siphon Withdrawal Reflex

by

J. H. Boyle

BSc.Eng, University of Cape Town (2002)

Submitted to the Department of Electrical Engineering
in partial fulfillment of the requirements for the degree of

Master of Science

at the

UNIVERSITY OF CAPE TOWN

December 2005

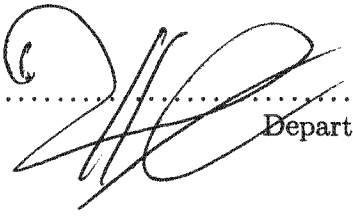

Signature of Author .....
Department of Electrical Engineering
31 August 2005

Accepted by .....

Modelling the Synaptic Plasticity Underlying Habituation, Sensitization and Classical Conditioning of the *Aplysia Californica* Gill Siphon Withdrawal Reflex

by

J. H. Boyle

Submitted to the Department of Electrical Engineering
on 31 August 2005, in partial fulfillment of the
requirements for the degree of
Master of Science

Abstract

Part I of this thesis aims to familiarize the reader with some of the basics of neuroscience. It includes a simplified description of the functioning of real neurons, as well as an introduction to several of the well known neuron models, including the Hodgkin Huxley equations and the Leaky Integrate-and-Fire model. Also included is a brief description of some neural coding schemes. The next chapter explains the basic functioning of synapses and introduces some common forms of synaptic plasticity. This is followed by a discussion of some properties of learning and memory. Note that these chapters are intended as an introduction for the non-neuroscientist, and are therefore kept as simple as possible.

The second half of Part I is dedicated to the organism on which the model of Part II is based. After a brief discussion of the role of invertebrates in neuroscience, the Californian Sea Hair, or *Aplysia Californica*, is introduced. Next, the use of simple reflexes as model systems is justified. This is followed by an analysis of the Gill Siphon Withdrawal Reflex and the learning it exhibits, first from a behavioral and then from a cellular point of view.

Part II covers the original work done by the author. The scope of the project is first restricted to modelling the short-term forms of habituation, sensitization and classical conditioning of the monosynaptic portion of the reflex. This is followed by a breakdown of the neural circuit into functional modules. Simple models are presented for the sensory and motor neurons, as these are not the emphasis of the model but are required as a framework for the synapse model. The "structure" of the synapse is modelled first, with attention paid to the properties of the Postsynaptic Current. The core of this research is the synaptic plasticity underlying the reflex's ability to learn. The mechanisms of short term plasticity are examined and described in as much detail as possible. This is done separately for each mechanism, and is followed by a description of the modelling process, and presentation of the equations. Habituation is handled first, followed by dishabituation and sensitization and finally classical conditioning. Once all three mechanisms have been addressed, the model is summarized in its entirety.

The model is evaluated by presenting it with stimulus patterns similar to those in the experimental literature. This evaluation is conducted on the complete model, and the interactions between the three mechanisms are also considered. The model is found to be a success, despite certain specific flaws which are discussed.

Statement of Originality

I know the meaning of plagiarism and declare that all work in this document, save for that which is properly acknowledged, is my own.

To my dear brother, Jed. Always remember that there is life beyond high-school. I know you will make us all proud.

Acknowledgements

The author wishes to thank the following:

- My parents, Loesje and Brendan, for making my education possible, and helping me become the person I am today.
- Professor J. Tapson, for his continued guidance, financial support and understanding.
- The Postgraduate Funding Office at the University of Cape Town, for their substantial financial contributions.
- Gareth Goldswain, for his proof reading, input and friendship - one of the best things to come of my postgrad experience.
- Bonny, my angel, without you I would just fade away.

Contents

Part I

Background

Chapter 1

Introduction

The past 75 years have seen enormous advances in computing and in neuroscience, which have allowed these two fields to cross paths. Artificial Neural Networks (ANNs) were the first technology to emerge from this union. Despite being initally controvertial, ANNs are now a completely accepted computational tool. However, since their conception ANNs have moved into mainstream computer science and away from the biological neurons on which they are based. While improvements in computer power continue to make ANNs more useful, advances in neuroscience have not been reflected in ANNs. Recent years have seen the emergence of fields such as Neurocomputing and Neuromorphic Engineering, which aim to create neural networks that more accurately mimic real neural systems. An interesting aspect of these new fields is that they are highly multi-disciplinary, attracting researchers from diverse backgrounds such as psychology, medicine, neurobiology, computer science and engineering.

Much work has been done on models of individual neurons, as these are obviously the building blocks of a neural network, but less attention has been paid to synapses. It has been known for some time that synapses participate in information storage. When an ANN is trained, it is the synaptic weights which are altered. However, the process of adjusting synaptic weights according to some learning algorithm does not do justice to the complexity of real synapses. The ability of a synapse to alter its efficiency in response to stimulation is often referred to as synaptic plasticity.

Real synapses exhibit plasticity over a very wide range of time scales, from milliseconds

to years, and a single synapse can exhibit several different types of plasticity. Some ANN learning rules, such as the well known Hebb's Rule, are a fair approximation to their biological counterpart, but they still only account for modifications on the slowest time scales. Far more attention needs to be paid to the short- and medium-term plasticity exhibited by real synapses.

Most people would agree that the human brain is the most advanced neural network on earth. It therefore seems odd that neuroscientists and psychologists would endeavor to understand the human brain before understanding, say, the brain of a rat. In fact, the brains of all mammals are far beyond our current ability to comprehend in their entirety. Eric Kandel was the first to show the validity of using simple invertibrate organisms in the study of learning and memory (see [52] for a review). Kandel's primary justification came from the finding that there are no major differences between the neurons of invertebrates and humans. The author of this work comes from an electrical engineering background and is primarily interested in using biologically inspired neural networks in robotics. Invertibrate-level intelligence would be ample for many robotic applications, providing further motivation for the use of a simple organism as the subject of this research.

The author's goal was to realistically model the plasticity displayed by a specific synapse. Before this could be done, it was necessary to become familiar with the basic operation of real nervous systems. The author was unable to find a work which provided a suitable introduction to contemprary neuroscience for the non-neuroscientist. The first half of Part I aims to be such an introduciton, and is based on a variety of sourses. The second half of Part I is about *Aplysia Californica*, a well known and extensively documented sea slug, on which the model is based. Part II details the modelling process undertaken by the author.

Chapter 2

Neurons and Neuron Models

Neurons are the basic building blocks of all animal behaviours, from the pulsing of a jellyfish to the work of Van Gogh. In a sense their role is comparable to that of the transistor in electronics. In contrast to transistors, however, a neuron is an incredibly complex molecular machine whose inner workings we are just beginning to understand. To further complicate matters there is no such thing as a typical neuron, and countless variations are found depending on the exact makeup of the nerve cell in question. Despite their internal complexity, the true power of neurons only emerges from interactions within large neural networks. Human intelligence, for example, is the product of around 10^{11} neurons in the brain alone [14].

Any model of a neuron is likely to be incomplete, due to the incredible complexity of that which it models. Still, some extremely complex models of individual neurons have been made, but these require a lot of processor time to simulate, making the simulation or implementation of moderate to large networks nigh impossible. It is from the two competing requirements of simplicity and realism that the huge diversity of neuron models originates, ranging from trivially simple to hugely complex.

2.1 Biological Background

While real neurons come in countless varieties, they still have much in common and it is these common aspects that are presented here. This "basic" neuron is loosely based on motor neurons found in the mammalian spinal cord and is very similar to many of the simpler neurons found

in nervous systems. Most other, more complex neurons build on this basic substrate.

2.1.1 Operation of Single Neurons

The following is a fairly typical description of neural behaviour and is not overly complicated. It draws primarily from [7, 40, 58], but similar material is presented in many other sources.

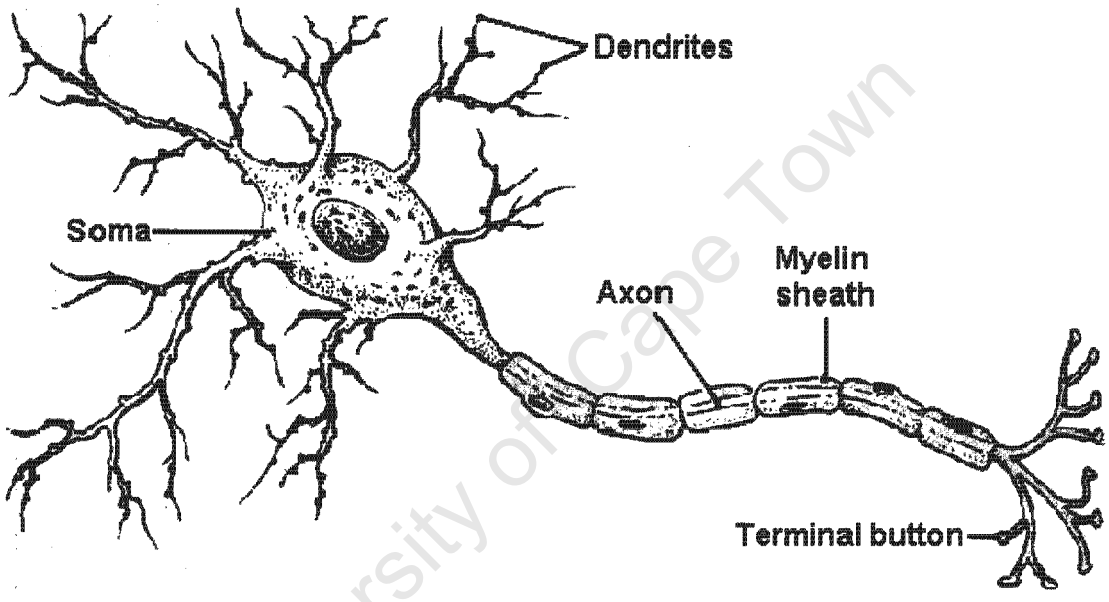

Figure 2-1: Sketch of a typical neuron (reproduced from [28])

A sketch of a typical neuron, taken from [28] is shown in Figure 2-1. Structurally, a neuron consists of three parts, called the axon, the soma and the dendritic tree. The soma is the cell body and performs the metabolic tasks required to keep the cell alive. Extending from the soma in a branching structure are the dendrites which, together with the soma, are the possible sites of input to the neuron. Also extending from the cell body at a site called the axon hillock is the axon. The axon has a structure similar to a tap root, with a single primary fibre extending from the cell and smaller branches protruding from this. At the tips of these branches are the synaptic boutons which make connections with (or synapse onto) other neurons. Thus the axon is the output surface for the neuron. Like all cells the neuron is enclosed by its cell membrane

which functions much like our skin. This membrane forms the boundary of the cell and keeps the intracellular fluid separate from the extracellular fluid. These fluids contain an assortment of ions, primarily Na^+, K^+ and Ca^{2+} which, thanks to the cell membrane, can have substantially different concentrations inside and outside the cell. Having different concentrations of these ions means that there can exist a potential difference across the membrane, often called the membrane potential. In the absence of stimulation, the membrane potential will settle at a specific value called the rest potential (U_{rest}) which is typically around -65mV with respect to the extracellular fluid. While the cell membrane does serve to insulate the inside of the cell from the outside, it is actually much more than merely an insulator.

Spanning the membrane (from inside to outside, like portholes in a ship) are complex molecular structures called ion channels. Composed of proteins, these constructs can selectively allow ions to pass through them, into or out of the cell. More importantly (and the key to a neuron's dynamic nature) these channels can alter their conductivity in response to certain "signals" or as a function of membrane potential. In addition to the ion channels, which can be viewed as dynamic conductances spanning the membrane, are other proteins including pumps, exchangers and transporters. While operating on somewhat different time scales, pumps and exchangers perform similar tasks. Together they are responsible for maintaining the electrical and chemical gradients of the cell by moving specific ions through the membrane. At rest they counteract the leakage of ions through the ion channels and after neural activity they are responsible for returning the cell to its resting state. Transporters are somewhat different as they move various transmitter molecules, rather than ions, into the cell.

Let us now consider a neuron which is receiving some sort of input, the result of which is to raise the membrane potential. A neuron whose potential is higher than rest is said to be depolarized, while one whose potential is lower than rest is said to be hyperpolarized. Inputs are received at sites called synapses where the membranes of two neurons meet. In most cases this involves the axon of the presynaptic neuron and the dendrite of the postsynaptic neuron. In the case of a depolarizing input, the action of the synapse allows an influx of positive ions which raises the membrane potential. It must be noted that conduction within a neuron is not instantaneous as it relies on the diffusion of ions. Rather, the potential spreads much like heat conduction. A neuron typically receives inputs from around 1000 others and the dendritic tree

sums their contributions and propagates them to the soma. If the membrane potential at the axon hillock exceeds a certain value (called the threshold or firing threshold) then an interesting regenerative process begins, leading to the generation of an action potential (AP), often called a spike.

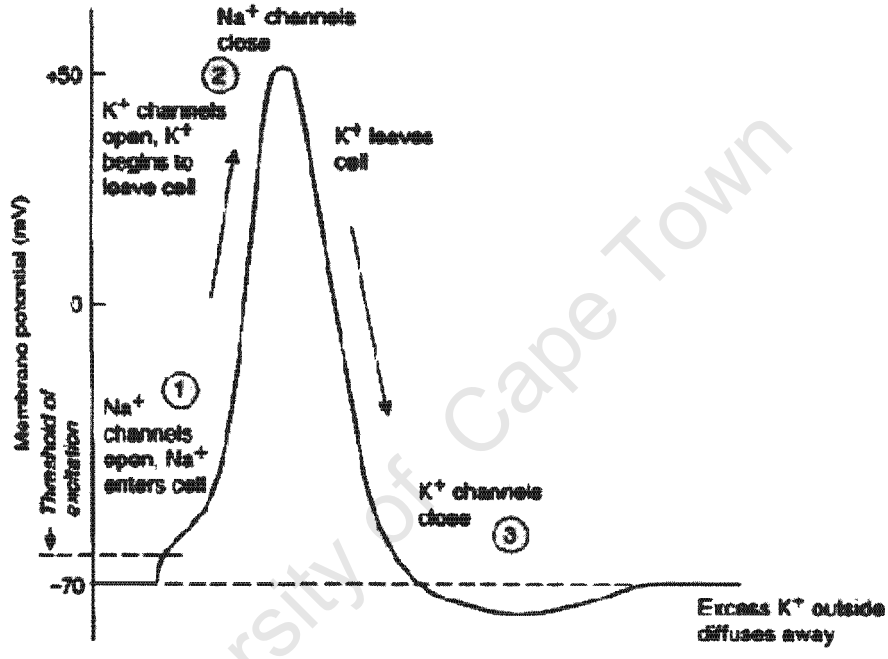

Figure 2-2: Diagram of an action potential showing activity of ion channels during firing (reproduced from [28]).

A diagram of an AP, showing the associated ion channel activity, is shown in Figure 2-2 (reproduced from [28]). As the membrane potential approaches threshold, which is typically around -50mV relative to the extracellular fluid, the Na^+ channel begins to open (or activate), increasing its conductance and allowing an influx of sodium ions. This influx of positive ions acts to further increase the membrane potential, which in turn further increases the conductance and so on. This positive-feedback effect results in the large and sudden positive excursion of the cell membrane potential, which constitutes half of the AP. After about one millisecond, the Na^+ channel closes (or deactivates) of its own accord, stopping the influx of ions. At about the same time that the Na^+ channel deactivates, the K^+ channel begins to activate, allowing K^+

ions to leave the cell. This K^+ efflux brings the potential back to the rest potential and slightly below[1], while the pumps and exchangers work to restore balance. Immediately after firing a spike, the channels are still recovering and so it is impossible to elicit another spike. This is called the absolute refractory period. Lasting slightly longer is the relative refractory period, during which firing is possible, but requires much stronger stimulation. Within a few tens of milliseconds the neuron will have fully recovered and returned to its rest potential, ready to fire again. This whole process occurs initially at the axon hillock, but rather than being passively propagated as in the dendrite, the AP at the axon hillock triggers the same process in the axon, and again in each of its branches. Thus the AP propagates quickly and without losing amplitude down the length of the axon and to all of the many synapses. The propagation of the spike down the axon is far from instantaneous, but is accelerated by a factor of about 50 if the axon is myelinated[2].

This mechanism of AP generation, involving the sodium and potassium currents, is common to most spiking neurons and can be augmented by the addition of other ion channels with specific characteristics. This can lead to all sorts of additional behaviours, such as a tendency to fire in bursts, or to adapt to constant levels of stimulation.

2.1.2 Neural Coding

It is generally accepted that the shape of the action potential does not contain any information. As a result, all neural information is contained in the firing times. There are several different ways that information can be encoded by firing times and these are introduced below. None of these are at all exclusive however, and different codes can be used at different points in the network. The neural codes presented in this section are taken from [58].

Firing Rate Codes

In its simplest sense a rate code converts a single "input variable" to a firing rate. However there are multiple definitions of firing rate, each with different implications. The most obvious

[1] This hyperpolarised state, more negative than the resting potential, is generally refered to as the spike afterpotential (SAP)

[2] Myelin is a fatty, electrically insulating substance which is produced by glial cells and forms a sheath around the axon of myelinated neurons. Its primary role is to speed up axonal conduction.

definition would be the number of spikes per second. The problem with this approach is that in order to perceive a firing rate it is necessary to count the number of spikes occurring within a certain time window. The time required for the system to respond to a change in input is determined by the length of this window. As we make the window shorter, the number of spikes occurring within the window will decrease, which will reduce the accuracy and resolution of the signal. At the extreme end of the scale would be the use of instantaneous firing rate, which is simply the inverse of the time between two spikes.

It must be pointed out that neural systems in nature have no "end user" and the information is only significant to the system itself. While the author has found this a tricky concept to get to grips with, it is significant here because it means that there is no outside observer to perform functions like windowing. Neural systems are not clocked like digital systems, so any averaging functions must be performed in a moving average manner, with the "window", or filter constant, being determined by the receiving neuron's time constant.

As a trivialized example, consider a stretch receptor[3] that encodes muscle extension as a mean firing rate. Such a signal will not vary too quickly, so let us assume a hypothetical "window" of about 50ms. Next let's assume that some part of the brain wants to know when the stretching reaches dangerous levels. This threshold detection task could be performed by a single neuron whose "leakiness" is such that an input firing rate of F is required for it to reach threshold, and hence fire. However, due to the 50ms averaging, a sudden increase in muscle stretch could possibly take up to 50ms to register.

Instantaneous firing rate offers a much quicker response, but the downside is that a small amount of temporal jitter can render the information inaccurate. The situation can be improved by using multiple neurons in parallel, which is frequently the case in neural systems. This brings us to the next section.

Population Codes

Population codes are similar to rate codes in the sense that they both represent information in terms of the number of spikes in a time interval. The difference is that a population code

[3] A stretch receptor is a specific type of sensory neuron which provides feedback as to the degree to which a muscle is extended.

makes use of a large group of neurons where the rate is expressed as the number of neurons firing at one time. Obviously if we have a finite population of neurons, it is unlikely that any two will fire at exactly the same time, so there must still be a window of some sort. However for a large population of fast-spiking neurons we could hope to use a window of 5-10ms duration and still receive a representative number of spikes. The key with this method is that all the neurons in the population must receive the same input and must have the same (or very similar) characteristics. What is interesting here is that if the neurons were identical and received identical input, all the members of the population would be doing exactly the same thing and would be firing at the same time. However in the noisy environment of a biological neural network such synchronization is unlikely to occur. If we have a neural network where all neurons' membrane potentials have a white noise component added, we can determine the probability that the neuron will fire in response to a given input. If the population is homogenous, all members will have this same probability of firing and so this probability can be converted into a percentage of the population that will be firing. Thus population codes are particularly useful in a stochastic system.

Time to First Spike

In certain circumstances it would be possible to encode information as the delay from the onset of some stimulus to the first action potential. This obviously requires that the network "knows" the time of the stimulus onset (t_0). Assuming for a moment that something signals this time (e.g. the spiking of a different neuron), then the intensity of the stimulus can be represented by the time to first spike. This is intuitive since a stronger stimulus will cause membrane potential to move more quickly to the firing threshold. A stimulus that is too weak will elicit no response at all. If we do not have a marker for t_0, this coding scheme can still indicate the relative strength of two stimuli which both began at the same time. Assuming that two identical neurons each receive an input, the neuron with the stronger stimulus will fire first. Of course two neurons will never be identical, but for this scheme to work they need only be similar enough that errors become insignificant.

Phase Coding

The notion of phase coding is similar to the time to first spike scheme. If, rather than a singular reference point, we have some periodic reference, then the phase of another spike train in relation to the reference can encode information. This is plausible considering the fact that detectable rhythms exist in the human brain, such as the alpha and beta waves that change according to state of conciousness. In the absence of a usable background oscillation, the relative phase between two spike trains of the same frequency could be used.

Spatiotemporal Coding

These are coding schemes where information is represented by the specific firing pattern of a group of neurons relative to each other. We may assume for the present that neural mechanisms exist which can detect the simultaneous occurrence of a certain number of spikes, and which can delay the transmission of spikes by a specific time period. Using these mechanisms, it becomes possible to detect whether spikes from a group of neurons occur with a specific spatiotemporal pattern. This is achieved by introducing transmission delays in the paths of the various spikes which are the inverse of the pattern to be detected. Thus when the correct pattern is presented, all the spikes reach the coincidence detector at the same time. If the detector has been appropriately tuned, it will fire only if all the required spikes arrive simultaneously.

Discussion of Coding Schemes

The schemes introduced above are unlikely to be all-inclusive. In real organisms, different schemes are used in different parts of the nervous system and variations on those above surely exist. Another important point is that these schemes are not mutually exclusive. A single neural pathway could, for example, encode stimulus intensity as mean firing rate and spatial information about the stimulus as relative phase.

2.2 Compartmental and Point Models

The following discussion regarding compartmental and point models is based on [7, 58, 75]. Unfortunately for the reductionists among us, the physical layout of a neuron is significant to its

function. The main reason for this is that unlike a metal conductor, the neuron can (and usually does) have different membrane potentials at different locations. This is particularly significant for neurons with large dendritic trees. The spread of charge in the dendritic tree can be described by the cable equation[4], but it is necessary to discretize the dendrite into compartments if one wishes to solve the equations. However, modelling the dendrites as transmission lines requires rather specific knowledge of the tree's shape and structure. If this is the case it will add drastically to the complexity of the model. A typical compartmental model will include many compartments for the dendritic tree and axon, and probably one each for the soma and axon hillock.

Point models on the other hand assume that all parts of the neuron have the same potential, and hence neglect the physical structure. Models such as these are obviously much simpler, but also less realistic. While the computational neuroscientist may well be willing to sacrifice simplicity in favour of a detailed compartmental model, neural computation may be impractical with such complex models. The key then is to determine how necessary the spatial structure is. A single point model is arguably sufficient for describing the behaviour at the axon hillock (where APs originate) as its small size limits the effect of electrical gradient. The main inaccuracies of point models are in representing the axon and the dendritic tree. A synapse's location on the tree can have a major effect on the amplitude and time course of the postsynaptic potential (PSP) elicited by activity at that synapse. In fact, dendritic processing is key to several processing functions such as computation of Inter Aural Time Differences (used in sound localization). The role the dendrite plays in such computation is to differentially delay inputs from different synapses, based on their proximity to the soma. A successful network model would need to account for such delays, but dendritic processing and modelling is a topic in itself, and is outside the scope of this work.

The models introduced on the following pages are all point neurons and are typically presented as such in the literature. However, multicompartment conductance-based models provide the closest approximation to reality, and are often used by computational neuroscientists. It is the author's opinion that dendrites, axons and synapses all require more attention if we are

[4]The cable equation models the dendritic tree as a transmission line. The line has characteristic resistance, capacitance and cross resistance and is discretized into compartments for the purposes of solving the equations.

to create networks of comparable ability to those in nature, but this dissertation focuses on synapses and their plastic nature. The following can be thought of as models of the soma and axon hillock.

2.3 Conductance-Based Models

This is a class of model whose dynamics are determined by various membrane conductances and are therefore the most biologically accurate. The archetype of this class is the Hodgkin – Huxley (HH) model [47], which describes the membrane behaviour as a system of four coupled non-linear differential equations (DEs). Hodgkin and Huxley performed their ground-breaking experiments on the giant axon of the giant squid, a neuron that is unusual due to its macroscopic size. While their equations reproduce the behaviour of this particular neuron very well, the giant axon is considerably simpler than most vertebrate cortical neurons. Fortunately the neuron they modelled is similar to the simpler neurons of other species, including ourselves. In addition, the mechanism of spike generation (involving Na^+ and K^+ conductances) is conserved across species and neurons. Models of more complex neurons, which can have considerably more ion channels, are still of the same form as the HH model.

2.3.1 The Hodgkin Huxley Model

The HH model is as ubiquitous as Ohm's Law and can be found in many papers, books and web sites, but was originally presented in [47]. There are three conductances involved in the HH model. The combination of these three relationships, with a fourth equation for the dependence of the membrane potential on the ionic currents, produces the membrane behaviour of the model. The cell membrane is capacitive in nature, so as current is injected into the cell, either via synapses from presynaptic neurons or as an external current input, it charges the capacitor and changes the membrane potential. The membrane however is not a perfect insulator and has various ion channels, effectively in parallel with the membrane capacitance. As described previously the different potentials inside and outside the cell are produced by differing concentrations of ions.

Hodgkin and Huxley found that in the case of the giant axon there are two primary ion

channels involved, namely Na^+ and K^+, and the minor contributions of other ions could be combined into a single "leak conductance". This leak conductance is not dynamic, so the leak current depends only on the membrane voltage.

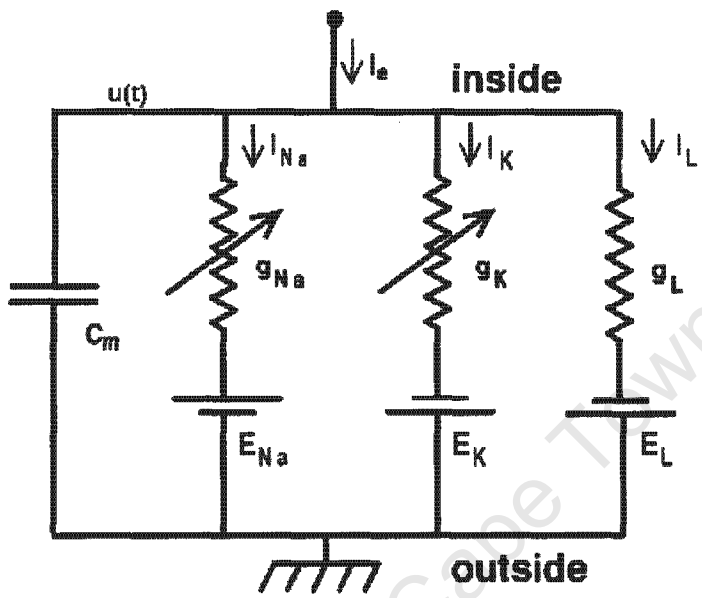

Figure 2-3: Electrical circuit representation of the HH model. C_m is the membrane capacitance, I_e is the input current, g_x are the ionic conductances, I_x are the ionic currents and E_x are the reversal potentials (x = L, K or Na)

An electrical-circuit representation of the membrane is shown in Figure 2-3. The potentials, E_x, in series with the conductances are the associated reversal potentials for each channel. Reversal potentials are the potentials at which the direction of current flow will change (they will be addressed later). The current I_e can be either an injected input current, appropriate for representing sensory neurons and also the case where an experimenter is injecting current via electrodes, or it can be a postsynaptic current which results from the firing of a presynaptic neuron. Considering this circuit, the equations for the membrane potential should make sense. The central equation governing the membrane potential is derived directly from the behaviour

of a capacitor and is given in equation 2.1

$$C_m \frac{du}{dt} = I_e - (I_L + I_K + I_{Na}) \tag{2.1}$$

where u is the membrane potential and I_x are the three ionic currents through g_L, g_K and g_{Na} respectively. Note that, due to the reversal potentials, the ionic currents can be in either direction, and as such can actually end up adding to I_e. Thus the voltage u can rise even when $I_e = 0$. This is essential to AP generation.

Next, let us consider the equations for the three ionic currents which are as follows

$$I_L = g_L \times (u - E_L) \tag{2.2}$$

$$I_K = g_K \times n^4 \times (u - E_K) \tag{2.3}$$

$$I_{Na} = g_{Na} \times m^3 \times h \times (u - E_{Na}) \tag{2.4}$$

where g_x are the maximum conductances for each of the channels and E_x are the corresponding reversal potentials. These six parameters are constant for any given neuron, though they will likely differ somewhat between neurons. It was mentioned earlier that the HH model involves four DEs. The remaining three DEs govern the three variables m, n, and h. These three DEs have the form:

$$\frac{dx}{dt} = -\frac{1}{\tau(u)}[x - x_0(u)] \tag{2.5}$$

where the steady state value x_0 and time constant τ both depend on the membrane potential. The relationships between these quantities were determined experimentally by Hodgkin and Huxley and are best represented graphically as in Figure 2-4.

In these graphs the resting potential has been normalized to zero. Assuming the neuron has been at rest for some time, all three gating variables (m, n and h) will have reached their steady state values. From Figure 2-4 A we can see that if $u = 0$ then $n \approx 0.3$, meaning that it is at 30% activation. Thus, according to equation 2.3 the effective conductance for I_K will be $g_K \times (0.3)^4$. In terms of I_{Na}, we can see that m is almost zero and $h \approx 0.7$. However since I_{Na} depends on $m^3 \times h$ and $m \approx 0$, the cubic power will dominate and I_{Na} will be virtually zero.

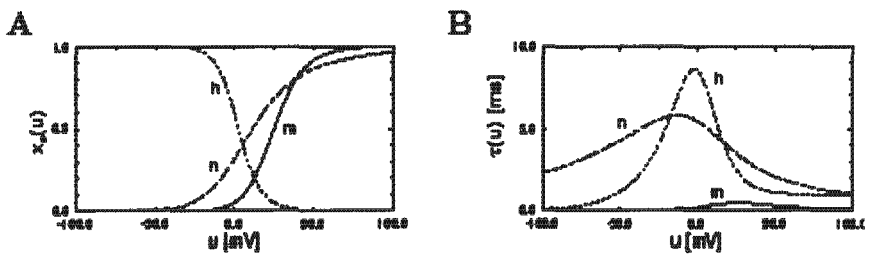

Figure 2-4: A shows steady state value ($x_0(u)$) and B shows time constant ($\tau(u)$) vs. voltage (u) for the variables m, n and h (reproduced from [58]).

This means that at rest I_K and I_L must cancel out, otherwise the neuron would not be at rest.

If a positive current Ie is injected, u will rise and might reach threshold. It must be pointed out that there is no fixed value for the threshold because it depends on the recent history of the gating variables. Let us assume for now that Ie is a short, strong stimulus that quickly raises u above threshold. We can see from Figure 2-4 B that n and h operate on similar time scales but m is considerably faster (it is often modelled as instantaneous). What this means is that m quickly reaches its new steady state value, which is nonzero, while n and h are slowly approaching theirs. Due to the value of E_{Na} (around 115mV) the current I_{Na} adds to Ie and as such further increases u. This in turn increases m, opening the channel further. This would continue unchecked were it not for the effect of h, which approaches zero as u increases. The fact that h has a much longer time constant than m allows a brief (about 5ms) inrush of current that increases u to a value of about 110 mV. This is the "upswing" of the action potential as shown in Figure 2-5. Around the same time that h finally shuts off I_{Na}, n (which operates on a similar time scale to h) will have reached a value close to unity so I_K becomes large. However because $E_K \approx -12mV$, I_K flows out of the cell. Thus once I_{Na} has stopped, I_K will act to quickly return u to the resting potential and beyond, causing the negative spike afterpotential (SAP).

2.3.2 Effects of Other Ion Channels

A huge variety of other ion channels, with their own characteristics, and involving ions such as Ca^{2+} and Mg^{2+}, have been identified in other neurons. Many of these channels have been

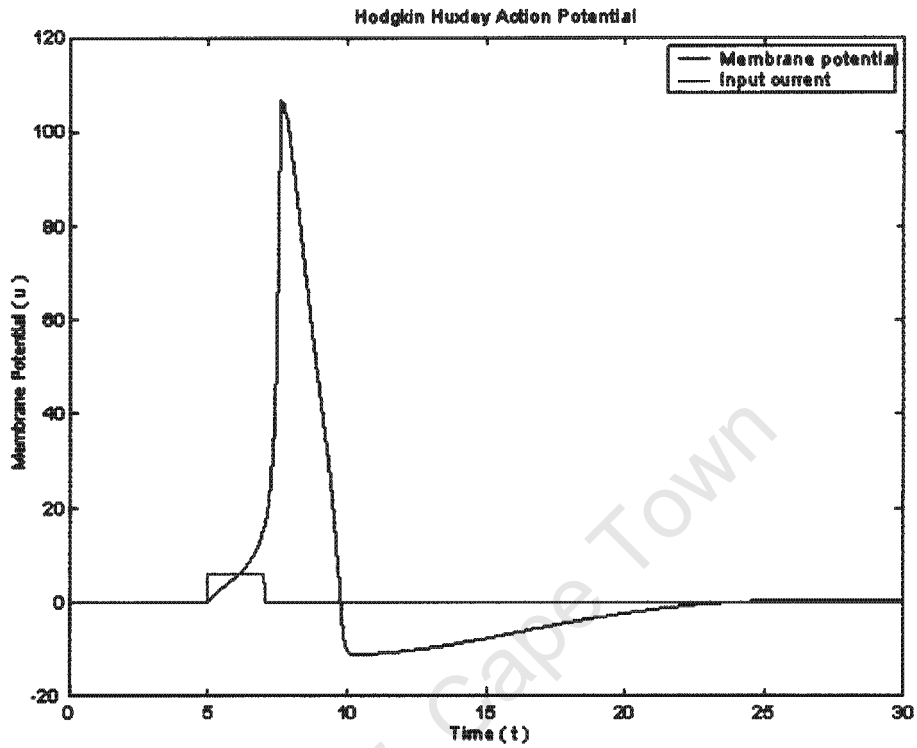

Figure 2-5: A simulated AP generated by the HH equations in response to a 2-second injected current pulse.

characterized by HH-like equations, and can be included to make conductance models of neurons such as mammalian pyramidal cells. One fairly common neural mechanism is called Firing Rate Adaptation, where a neuron's responsiveness to constant stimulation decreases over time as shown in Figure 2-6. This behaviour is the product of two additional ion channels involving Ca^{2+} [37].

The high threshold calcium current (I_{LL}) is an inward calcium current which only activates when the membrane potential is well above threshold. The effect of this is that calcium ions flow into the cell with each spike, building up over time. Being an imperfect insulator, the membrane allows Ca^{2+} to leak out slowly, so if the neuron is allowed time to recover, the calcium concentration will return to normal levels. The other half of the mechanism is a calcium dependent potassium current (I_{AHP}). Being a K^+ current, I_{AHP} is outwards and hyperpolariz-

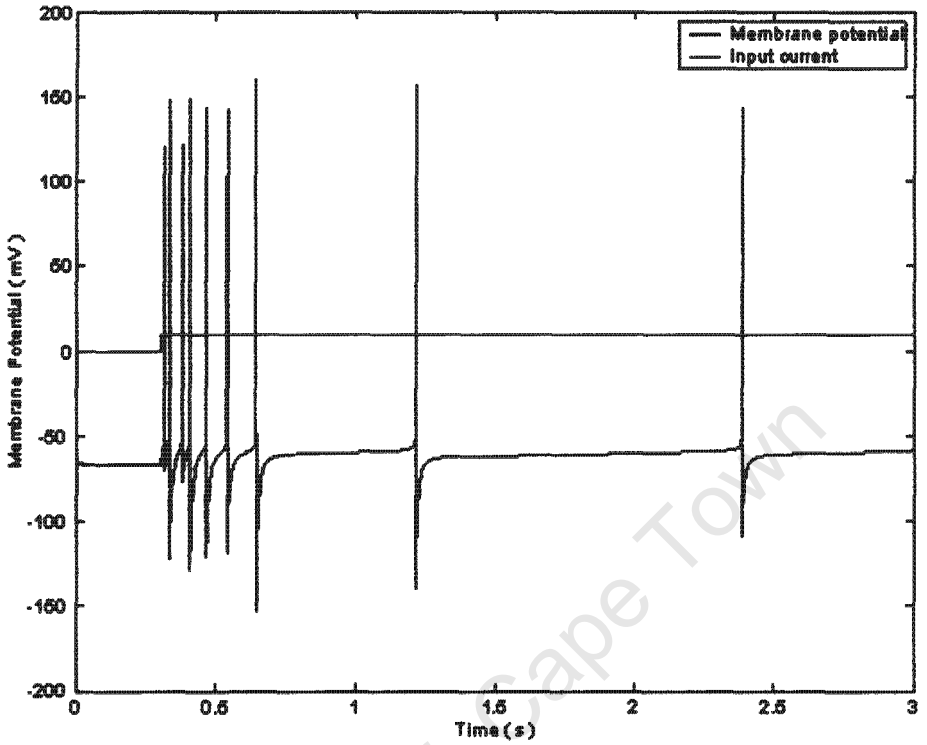

Figure 2-6: HH style model of mammalian Pyramidal Cell exhibiting Firing Rate Adaptation in response to a step current input (red). Note how the firing rate declines over time, with constant stimulation.

ing, but unlike I_K this current is dependent on intracellular calcium concentration, rather than voltage. As Ca^{2+} builds up I_{AHP} will increase, partially counteracting any excitatory input and reducing the excitability of the cell.

2.4 Threshold - Fire Models

This is a far simpler class of models which attempts to model the behaviour of the membrane potential without concern for the inner workings of the cell. In addition, only the subthreshold dynamics are modelled, and APs are represented by Dirac delta spikes, or simply recorded as a series of firing times. The descriptions of the following two models are based on [58, 37].

2.4.1 Spike Response Model

The spike response model (SRM) [58] defines the neuron's behaviour by means of its response to spikes, both its own and those of presynaptic neurons. The model includes a state variable which represents the membrane potential. At any point in time, the state of the neuron is determined by the combination of responses to all pre- and postsynaptic spikes. The responses to these spikes are characterized by functions called kernels. A presynaptic spike will induce an inhibitory or excitatory PSP, whose time course is defined by the function $\xi_{ij}(t)$, which can differ for each combination, i, j of pre- and postsynaptic neurons. Obviously this function must vanish for $t \leqslant 0$ and decay to zero for $t \rightarrow \infty$, to account for the leakiness of all neurons. When the neuron reaches the firing threshold, v, the neuron is said to fire. The membrane potential $u_i(t)$ is reset to U_{rest} (or possibly below) by means of a second kernel $\eta_i(t)$, which is a negative contribution that decays to zero for $t \rightarrow \infty$. Thus the state at any time t is:

$$u_i(t) = \sum_{t_i^{(f)} \in F_i} \eta_i(t - t_i^{(f)}) + \sum_{j \in \Gamma_i} \sum_{t_j^{(f)} \in F_j} \omega_{ij} \xi_{ij}(t - t_j^{(f)})$$

where F_i is the set of all firing times of this neuron, Γ_i is the set of presynaptic neurons and F_j is the set of firing times for each of these presynaptic neurons.

2.4.2 Leaky Integrate and Fire Model

In the leaky integrate and fire (LIF) [58] model, the cell membrane is modelled as a leaky integrator. The model is frequently presented in the framework of electrical circuits, as the leaky integration can be performed by a simple RC circuit as shown in Figure 2-7.

As a result, inputs in this model take the form of current pulses in response to presynaptic spikes. Like the SRM model, the LIF has a firing threshold v and a state variable $u(t)$. The neuron is said to fire when $u(t)$ crosses v from below, and the potential is mechanistically reset to U_{rest} by discharging the capacitor. The state of a LIF neuron progresses according to:

$$\tau_m \frac{du}{dt} = -u(t) + RI(t)$$

where $\tau_m = \frac{1}{RC}$ is the membrane time constant. In reality the input $I(t)$ is a combina-

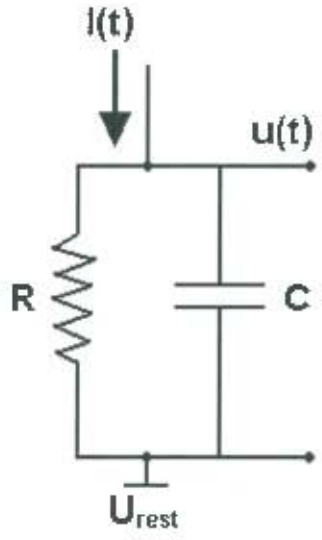

Figure 2-7: The leaky integrator for an LIF neuron in RC circuit form.

tion of postsynaptic currents from presynaptic neurons, but in the literature [58, 37] this is often replaced with an "injected" current which may or may not be constant. The membrane behaviour of an LIF neuron in response to constant current input is shown in Figure 2-8.

2.5 Rate Models

Rate models include such neurons as the sigmoidal gate, found in traditional non-spiking neural network (NN) theory. These models, while certainly useful in their own right, make the false assumption that neural information is encoded in mean firing rate alone. Therefore these models do not model individual spikes, but rather represent firing rate as an analog variable.

2.6 Discussion and Comparison

Neuron models are used in various fields, which impose different requirements. As a result, each of the models introduced above will be the optimal choice for a certain set of requirements. If one's goal is to further the understanding of actual neural behaviour, then conductance models

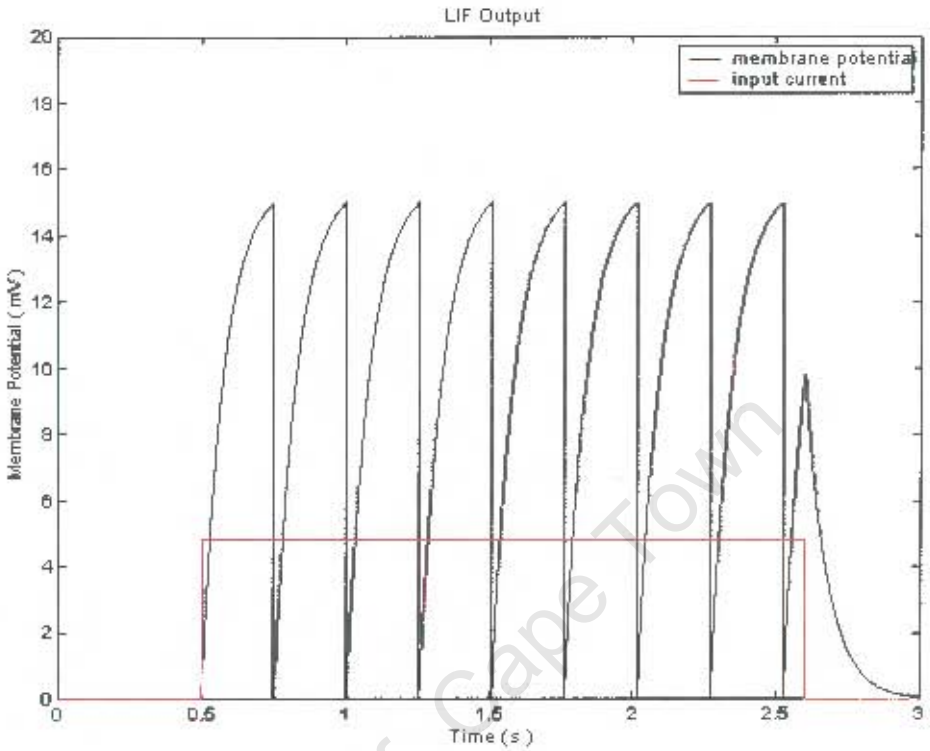

Figure 2-8: Membrane potential of an **LIF** neuron with $v_{rest} = 0$ and $v_{thresh} = 15mV$ in response to a current pulse.

are most suitable as they provide insight into the inner workings of nerve cells. However, the complexity of these models may be prohibitively high if the intention is to use them as computational elements. Rate models have been extensively studied, and networks of them have been found to be hugely powerful computational devices. However, the firing rate abstraction necessarily robs them of much of the potential possessed by real neurons, and renders them almost useless for the study of actual nervous systems. Threshold-fire models, also referred to as spiking neuron models, seem to offer a happy compromise. Being spiking neurons, they allow for the use of temporal features such as pulse codes which opens up a whole range of possibilities not offered by rate models. In fact spiking neuron models have been proven to have greater computational power than rate models [59]. The SRM model is not ideally suited to implementation or simulation because the task of summing contributions from many

kernels (one for each presynaptic spike) leads to excessive memory requirements, particularly in large networks. The LIF model, on the other hand, is ideally suited to implementation and simulation. Networks of LIF neurons can be created using analog, very large-scale integration (aVLSI) techniques [58], and the fact that the LIF equation is differential makes it very easy to simulate in discrete time steps with a program such as MatLab. Since the author has an engineering background, potential implementability is considered to be important. Therefore this thesis will make use of the LIF neuron model.

2.7 Noise in Neuron Models

Real neurons are intrinsically stochastic in nature [37, 58, 60, 76]. The reasons for this are numerous, but the net result is that neural spike trains are generally rather noisy in terms of interspike interval variability. Interestingly it has been shown that in many cases this noise is not only non-detrimental, but is actually beneficial [78]. Stochastisity in neurons helps with tasks such as phase locking [81] and also maintains diversity in the firing of populations of neurons. Much research remains to be done on the effects and benefits of noise in neural systems, but as that is not the focus of this work, the author will assume that all neurons and neuron models can include some noise. In the case of LIF neurons, this noise can be incorporated in several ways including noisy reset, noisy integration and noisy threshold [58]. The omnipresence of noise in both real and artificial systems serves as justification for this inclusion.

Chapter 3

Synapses

Synapses are the junctions between neurons through which information is passed. Synapses are almost always unidirectional [77], meaning that information travels in one direction, from the presynaptic neuron to the postsynaptic neuron.

3.1 Biological Background

Real synapses come in two distinct types, called electrical synapses (or gap junctions) and chemical synapses, which involve completely different mechanisms and behave in different ways. The vast majority of real synapses, including those involved in *Aplysia Californica's* withdrawal reflexes, are chemical. Thus all synapses referred to in this work are *chemical synapses*, the following description of which is based on [7, 77]. In addition, synapses are classified as excitatory or inhibitory, depending on whether presynaptic activity leads to hyperpolarization or depolarization of the postsynaptic neuron. The "sign" of the synapse depends on the nature of the neurotransmitter it employs and cannot change. All the synapses *from* a given presynaptic neuron will have the same sign, and so a neuron can also be referred to as excitatory or inhibitory based on the nature of its "output" synapses. The majority (about 80%) of neurons are excitatory.

The physical structure of a synapse involves processes from both pre- and postsynaptic neurons. A simplified diagram of a synapse (adapted from [1]) is shown in Figure 3-1. On the presynaptic side, there extends from the axon a mushroom-shaped protrusion called the

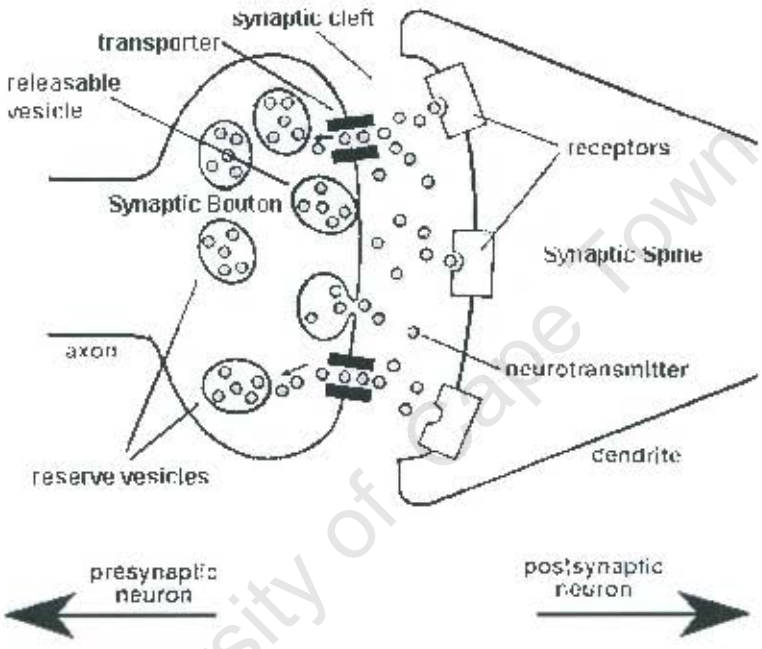

Figure 3-1: A simplified diagram of a chemical synapse (adapted from [1]) showing both pre- and postsynaptic processes.

synaptic bouton, which is a continuation of the cell membrane. On the postsynaptic neuron, a protrusion called the synaptic spine extends from the dendrite just opposite the bouton. The two are separated by a $20nm$ gap called the synaptic cleft. Within the bouton are tiny spheres ($35nm$ in diameter) filled with neurotransmitter, called vesicles. Some of the vesicles are docked against the presynaptic membrane, constituting the *docked vesicle pool*. The majority of the vesicles (those within the bouton but not in contact with the membrane) are the *reserve vesicle pool*. Vesicles always dock at a specific site, or sites, on the bouton surface called *active zones*. Directly opposite an active zone is a specialized area of postsynaptic membrane called a *postsynaptic density*.

When an AP arrives at the synaptic bouton it causes a momentary influx of Ca^{2+} and hence a briefly elevated calcium concentration. The elevated Ca^{2+} level initiates a process called exocytosis, whereby one or more vesicles may release their neurotransmitter into the synaptic cleft. Interestingly, this process is by no means deterministic. The release of transmitter vesicles in response to an AP is probabilistic in nature, meaning that synaptic outputs are stochastic and are not at all reliable. Different approaches to overcoming this problem are used. In the case of some peripheral circuits, where reliable transmission between a pair of neurons is required, reliability is accomplished by having many release sites in a single connection. This number can be over 1000 in the case of neuromuscular junctions. However in the vertebrate cortex there is insufficient space for so many redundant connections and transmission can be very unreliable. In this case one can only assume that averaging occurs via multiple parallel pathways.

3.2 Dynamic Synapses

Depending on the synapse in question, a presynaptic action potential can result in a postsynaptic potential (PSP) of different amplitudes. The average amplitude of the PSP at a specific synapse defines the "strength" of that synapse and depends on the number of readily releasable vesicles as well as the individual vesicle release probability [77]. The strength of a synapse however is by no means fixed, but rather is dynamic on a wide range of time scales, from milliseconds to years [60, 85]. The study of artificial neural networks (ANNs) has shown that the adjustment of synaptic strength can determine the functioning of a network and that the

correct adjustment for a specific task can be achieved with certain rules. Consistent with this is the finding that changes in synaptic strength are an important locus of learning and memory in animals [44]. As a parallel to the learning rules of ANNs there are many identified forms of synaptic plasticity at work in real neurons. In some cases we have a fair understanding of the underlying molecular mechanisms and in others not. However, many training algorithms for ANNs, such as those involving back-propagation, are not biologically feasible [54]. Another key difference is that real synaptic plasticity consists of physiologically distinct long- and short term modifications [12, 48, 63]. Long-term plasticity involves growth of extra connections, while short-term changes are thought to be due to changes in vesicle release probability, which in turn is the result of varied molecular mechanisms. Presented next is a brief description of some of the better-known forms of synaptic plasticity.

3.2.1 Hebbian LTP/LTD

LTP and LTD refer respectively to a long-term potentiation (increase) or depression (decrease) in synaptic strength. Different types of LTP/D exist, depending on what is required to induce them. Hebbian LTP/D results when presynaptic activity coincides with postsynaptic depolarization [25, 58]. LTP/D can be rapidly induced if the presynaptic stimulation is tetanic. Tetanic stimulation is basically a brief, high frequency burst of action potentials. Once induced, LTP/D can last for weeks, months or even a lifetime.

3.2.2 Use Dependent STP/STD

Short-term potentiation (STP) and depression (STD) are similar to LTP/D, but are much shorter in duration. In the neural context, short-term changes are generally taken to be those that last for milliseconds to hours. If stimulated with a train of pulses, a short-term depressing synapse will quickly lose strength. The exact time taken for this to occur depends on the synapse's characteristics. A short-term potentiating synapse will strengthen in response to the same input. In both cases the effects can occur within a single stimulus (train of pulses lasting seconds or less). Also, there is no postsynaptic condition, so the plasticity depends only on presynaptic activity. If left undisturbed, the synapse will quite quickly return to its original strength [66].

3.2.3 Paired Pulse Facilitation (Depression)

PPF(D) is a form of short-term plasticity where the strengthening (weakening) of the synapse depends on the specific timing between two pulses arriving at the synapse. A plot of delay versus alteration is roughly sigmoidal in shape, with peak facilitation (depression) usually occurring at an ISI around 5ms. The synapse responds quickly enough that the second of the two pulses is facilitated. If the delay is too long or too short the synapse will not be facilitated [26].

3.2.4 Spike Timing Dependent Plasticity

STDP is also similar to Hebbian LTP/D. The primary difference is that the direction of the modification (potentiation or depression) depends on the relative timing of pre- and postsynaptic spikes. Provided both spikes occur within a window of about 10ms, the synapse will be altered. If the presynaptic spike preceded the postsynaptic spike then the synapse will be potentiated. If however the presynaptic spike occurs just after the postsynaptic spike the synapse will be depressed [34].

Chapter 4

Learning and Memory

Learning refers to the ability of a system (typically an animal) to adjust its behaviour, or response to a specific stimulus, after some event alters the meaning of the stimulus or its context. Memory is the substrate for this modification. Being able to adapt is important because a stimulus, such as a loud noise, can have different significance depending on its context and history. An animal which was incapable of adapting its behaviour would quickly perish as the real world is a varied, dynamic and unpredictable one. All mobile life-forms are capable of modifying their behaviour to some degree and this plasticity is desirable in man-made systems, particularly autonomous ones.

4.1 Classification of Memory

Memory can be classified according to three primary criteria as presented in the following subsections, though it should be noted that lower life-forms lack explicit memory. The following is based on definitions of the respective terms found in [30].

4.1.1 Implicit or Explicit

This classification is based on the method of recall for the memory. Explicit or declarative memories are those which we actively recall, such as memory of facts or episodes from our lives. Implicit memory refers to things which are not actively recalled, such as the ability to play tennis or drive a car.

4.1.2 Associative or non-Associative

Associative memory involves learning or modifying associations between stimuli, while non-associative memory involves only a single stimulus.

4.1.3 Long Term or Short Term

This distinction is obviously made on the basis of how long the memory persists. Typically memories are considered short term if they last less than 30 seconds without rehearsing or refreshing, but in some cases memories lasting up to a few hours are still considered short term. There is a more reliable means of segregating long and short term memories based on the cellular mechanisms involved, which is discussed in Section 7.4.

4.2 Three Elementary Types of Learning

The following are three particularly well known types of simple learning which are exhibited by all but the simplest life-forms. All three of these are implicit.

4.2.1 Habituation

Habituation, the simplest of the three, is an elementary form of non-associative learning whereby an animal learns to ignore benign stimuli. Upon presentation of a stimulus with little behavioural significance the animal will make some response. If this stimulus is repeatedly presented and no punishment or reward follows, the animal's response will decline and eventually cease. Habituation is useful for filtering out unimportant information [3].

4.2.2 Sensitization

Sensitization (also non-associative) is a slightly more complicated process. The presentation of a strong noxious stimulus (often referred to as the unconditioned stimulus (US)) increases the animal's responsiveness to further (usually different) stimuli. This is useful for increasing the overall level of alertness in response to injury, fright or some perceived threat [27].

4.2.3 Classical Conditioning

Classical conditioning is more complex than the previous two types and is an associative process. In classical conditioning the animal forms an association between a benign stimulus called the conditioned stimulus (CS) and a behaviorally relevant one called the unconditioned stimulus (US). Initially the CS does not elicit a significant response, but the US elicits its natural response, called the unconditioned response (UR). If the CS is repeatedly presented just before the US, the animal will learn to associate them. Eventually the CS alone will elicit the same response, which is the UR [2].

Chapter 5

Model System: *Aplysia Californica*

Aplysia Californica or the Californian Sea Hare is a large sea snail of class Gastrapoda and phylum Mollusca and is depicted in Figure 5-1-B (fig. 5-1 A and B are adapted from [52]). *Aplysia* is shell-less and attains an average adult length of 25cm. *Aplysia* has been widely used as a lab animal for the study of neurobiology, particularly that of learning and memory. It possesses a fairly simple nervous system with approximately 20 000 neurons. *Aplysia* was used by Erik Kandel in his Nobel Prize-winning work on the physiological basis of learning and memory. *Aplysia* is a well-documented animal, but this chapter is based primarily on [18, 51, 52].

5.1 Invertebrates in Neuroscience

Invertebrates like *Aplysia* are well suited to neurological study for several reasons, including:

1. They possess much simpler nervous systems than vertebrates.
2. Many invertebrate neurons, including many of those in *Aplysia*, are relatively large and hence can be easily impaled with microelectrodes, which allows for intracellular recording.
3. Invertebrates possess distributed nervous systems composed of many local ganglia[1] which

[1] A ganglion is a cluster of neurons which, in invertebrates, is part of the central nervous system (CNS) and controls a subset of behaviour. Bundles of axons (connectives) connect the ganglion to sensory and motor systems, as well as to other ganglia.

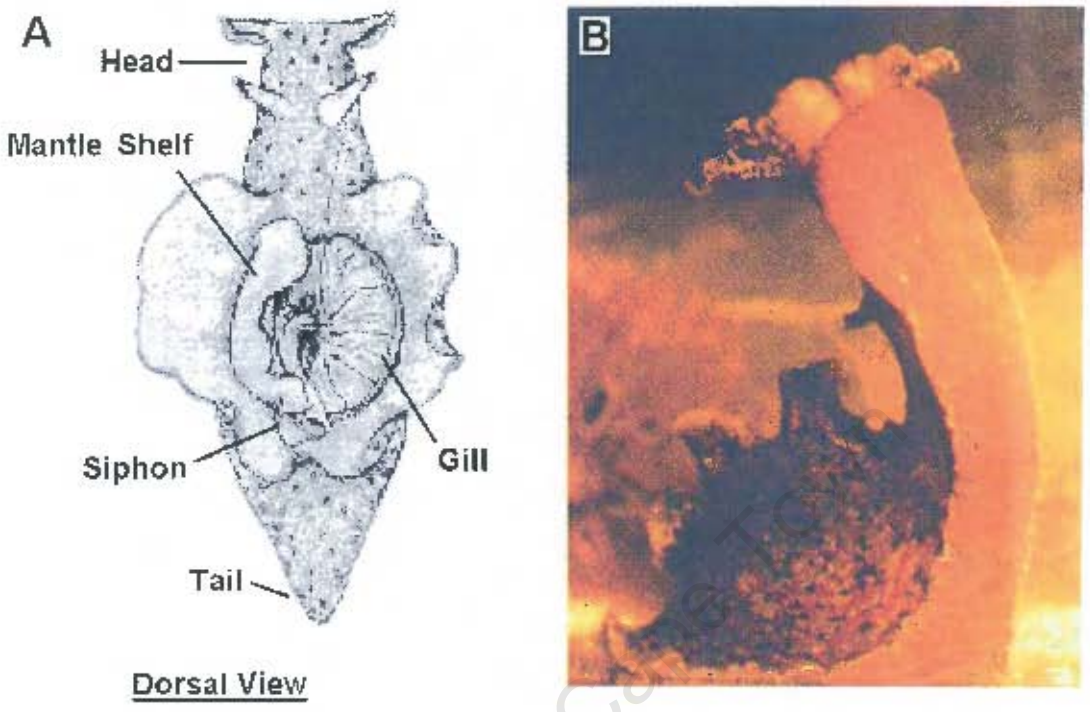

Figure 5-1: *Aplysia Californica* (adapted from [52]). A) anatomical sketch and B) photograph

control local behaviour. These ganglia and surrounding neurons can survive a surprisingly long time in reduced preparations.

Aplysia has become something of a standard for low-level neurological investigations and as a result is very well documented. In fact, much of its nervous system has been mapped to the point that individual neurons have been named and can be identified in all individuals of the species.

5.2 *Aplysia* Withdrawal Reflexes

Invertebrate reflexes have been popular for the investigation of learning at a simple level since it was found that the fundamental mechanisms of neural operation are conserved across phyla (see [52] for a review). *Aplysia* possesses several defensive reflexes which serve to withdraw exposed appendages from potential danger. Two particularly well-studied reflexes are gill and siphon

withdrawal and tail withdrawal [55]. Both of these reflexes exhibit forms of basic learning, including the three mentioned in the previous chapter and the underlying neural circuitry of these reflexes has been well defined.

5.3 The *Aplysia* Gill and Siphon Withdrawal Reflex

This work will focus primarily on the gill and siphon withdrawal reflex (GSWR) as it is more thoroughly documented in the literature than tail withdrawal. The GSWR serves to withdraw the delicate siphon and gill (see Figure 5-1-A) into the body in response to a possible threat, signalled by tactile stimulation of the siphon or mantle shelf. This reflex is mediated by the abdominal ganglion [21]. The single largest contribution to this reflex, contributing about $\frac{1}{3}$ of the observed response [6], is a monosynaptic pathway[2] from the sensory neurons (SNs) innervating the siphon skin to the gill motor neurons (MNs). In addition there is a polysynaptic pathway[3] which includes interneurons[4]. An additional component of this reflex is a connective from the pleural ganglia[5] which is activated by strong tail stimulation. This connective serves as an input pathway for the US in sensitization and conditioning. A simplified schematic of this pathway [52] is shown in Figure 5-2. An identified major locus of plasticity in this reflex is the monosynaptic connection between sensory and motor neurons.

[2] In its simplest form a monosynaptic pathway involves only two neurons and a single synapse between them. Information flows from the pre- to the postsynaptic neuron. In reality, monosynaptic pathways can involve more neurons in parallel with these two. Even if all the neurons in the first layer synapse onto all the neurons in the second layer, it is still considered monosynaptic.

[3] A polysynaptic pathway is one which is not monosynaptic.

[4] An interneuron is a neuron which is neither a sensory neuron nor a motor neuron and hence has no direct contact with the outside world.

[5] The left and right pleural ganglia are a pair of ganglia located near and controlling the tail.

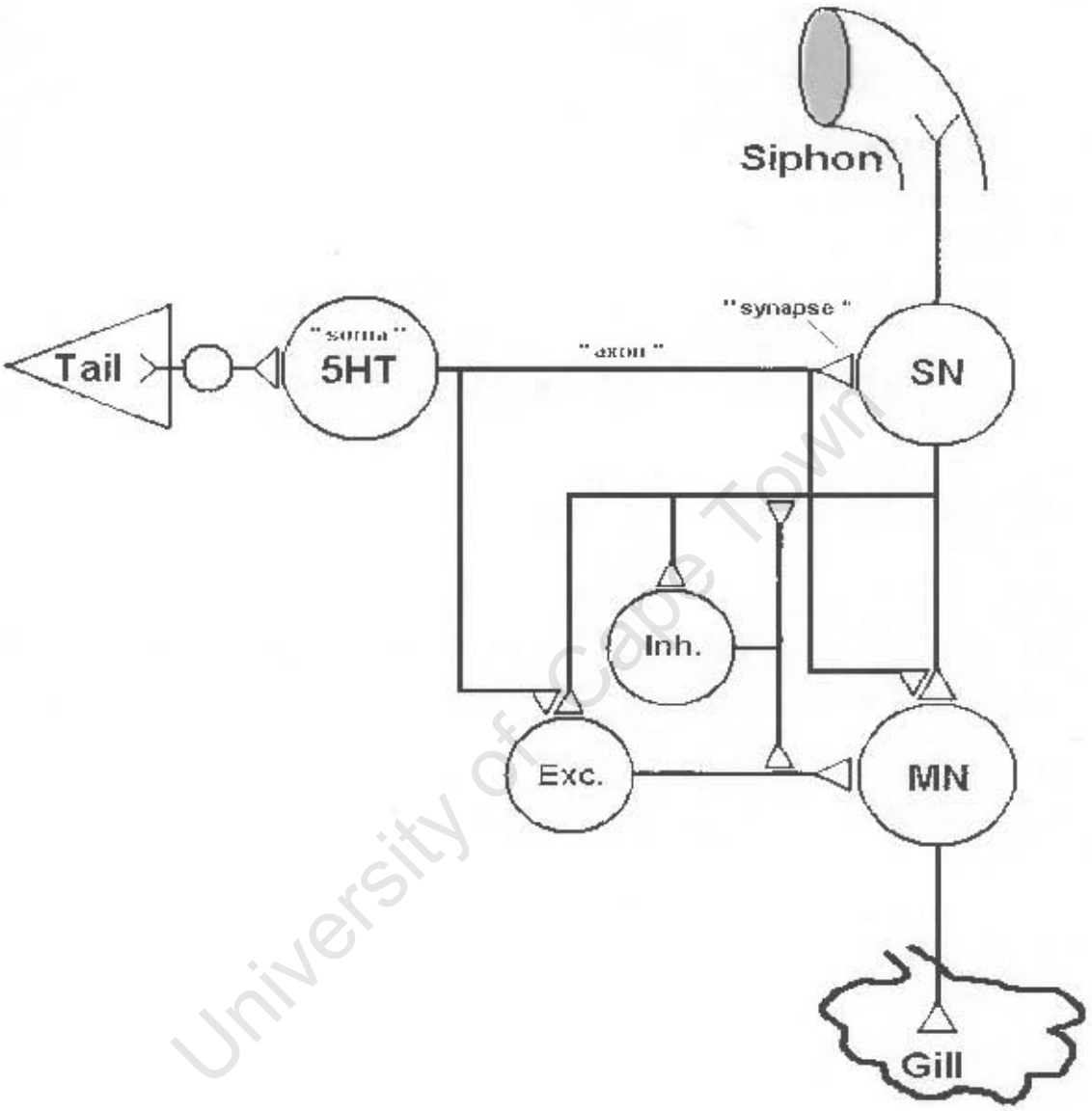

Figure 5-2: A simplified schematic of the neural circuit underlying the GSWR [52]. It includes: siphon sensory neuron (SN), gill motor neuron (MN), modulatory interneuron (5HT) as well as excitatory and inhibitory interneurons (Exc. and Inh. respectively).

Chapter 6

Behavioural Analysis of Plasticity in *Aplysia*'s GSWR

This chapter deals with behavioural, as opposed to cellular, experiments on *Aplysia*'s GSWR. These experiments generally involve whole *Aplysia*, and sometimes a semi-intact preparation where the tail, siphon and central nervous system are dissected from the body. In either case, input stimuli are presented to the appropriate body part and response is quantified in terms of the physical movement of the siphon. This is in contrast to cellular experiments where inputs usually take the form of currents injected into the cells via microelectrodes, and outputs are the measured PSPs at motor neurons. The results of these two types of experiment are qualitatively compatible, but are quantitatively different. This is due in part to the transformation performed by sensory and motor neurons.

6.1 Habituation

A typical habituation experiment as described in [19, 69, 71] proceeds along these lines: the siphon skin is briefly stimulated with a soft brush or a jet of water strong enough to elicit a significant withdrawal of the gill and siphon. Typically this is a water jet of < 1s duration. After somehow quantifying the withdrawal to use as a baseline (for comparison with later responses), the animal is repeatedly presented with the same stimulus at some regular interstimulus interval (ISI) and the withdrawal response is observed to decrease. Note that habituation is site

specific, meaning that the response will only habituate if the same spot on the skin is stimulated each time [80]. The maximum ISI which can produce habituation ranges from 1 - 5 minutes, depending on the individual animal, but typical experimental ISI's are 10 - 100 seconds.

One major inconsistency between experimental works is the quantification of the withdrawal. Some researchers measure the duration, while others try to estimate a percent reduction in area, and the techniques are seldom the same. However, regardless of the quantifying method and ISI used, the response always decays with an approximately exponential shape [70]. The choice of stimulus strength is quite significant as well, as it affects the time course of the withdrawal [69]. Lighter stimuli induce a withdrawal with a single, short-latency component whose duration and magnitude are proportional to intensity. At stronger stimulus intensities a second, longer-latency component contributes as well, leading to considerably longer withdrawal duration. Experiments tend to use stimuli that emphasize the short-latency component, as it corresponds more closely to known neural circuits. In addition, stronger stimuli are much slower to habituate [69].

A single training session, defined as an uninterrupted stimulus train with constant ISI, produced habituated responses as low as 5% - 45% of baseline[19, 69, 71]. The majority of this decrement occurred within the first 5 -10 stimuli (as can be seen in the data of [19, 69, 71]) and there would be little point in presenting more than 20 stimuli in a session. In absence of further presentations the response recovered to 75 - 85% of baseline in 10 - 20 minutes, but full recovery took up to two hours [69]. The effects became much longer lasting if multiple training sessions were employed. After the first training block (10 - 20 stimuli, ISI $\approx$ 30s) the animals were left for 1.5 - 24 hours and then presented with a second block. The response decrement over the first few stimuli was much more pronounced, and led to greater habituation by the end of the block. Four such blocks resulted in significantly greater habituation which was shown to last more than three weeks [20]. Interestingly, a massed training protocol where the same four blocks were presented with little or no time between them did not produce this long-term habituation [19, 20]. Spacing is a universal requirement for creating long-term memory (LTM) [8, 50].

6.2 Sensitization

A typical sensitization experiment as in [10, 36, 71] begins with a pretest, where the siphon is stimulated with a brush or water jet (the CS) and the response quantified to use as a baseline. After a 10 -15 minute delay a strong noxious stimulus (the sensitizing stimulus or US) is presented to another body part such as the neck or tail. The siphon is then stimulated again with the water jet and the response compared to the pretest. The sensitizing stimulus is typically a 1.5s, 50mA, 60Hz pulse train (shock) delivered to the tail by an electrode.

Training with a single shock produced sensitization lasting up to 1 hour but the effects of four shocks (ISI 2min - 2hrs) lasted up to 2 days [52]. Four trains presented 30 minutes apart, each consisting of four shocks with ISI = 30 seconds led to sensitization lasting four days, with facilitation peaking at approximately 200% of baseline. Repeating these blocks of 16 stimuli once per day for four days led to sensitization lasting several weeks, with a peak facilitation well over 500% of baseline [36]. Interestingly there is evidence that sensitization has a delayed onset, taking 20 - 30 min. before there is a noticeable response increment [21].

Dishabituation is an increase in a response which had previously been habituated. Initially it was thought that dishabituation reflected the same process as sensitization, but this was questioned on the grounds that they emerge at different times during the development of young *Aplysia* [71]. It has subsequently been found that dishabituation is a combination of the normal sensitization mechanism in parallel with a second mechanism which only affects depressed synapses [46].

6.3 Classical Conditioning

A typical classical conditioning experiment as in [4, 21, 43] begins with a presentation of the CS, which is a light touch or water jet to the siphon. The elicited weak withdrawal is used as the baseline. The US, which is a strong shock to the tail similar to that used in sensitization training, elicits a massive withdrawal of the gill and siphon. The animal is conditioned by repeatedly presenting the CS, followed about 0.5 seconds later by the US. Typically there will be 15 - 30 presentations with an ISI of about 5min.

Classical conditioning produces large enhancements and a single train of 30 presentations

can produce a 500% increase in withdrawal when the animal is tested with the CS alone, 24 hours later [21]. This observed facilitation obviously includes a contribution from non-associative sensitization, but this can be taken into account by presenting some animals with only the US, or with the US and CS unpaired. The US alone group exhibits no more than 200% facilitation so there is a major associative contribution. The associative component also exhibits site specificity, which means that the CS must be presented to the same spot on the siphon each time. If the animal is later tested with the CS on the opposite side of the siphon the response will only be partially facilitated by the sensitization effect [43].

It is unclear whether CC has distinct long-and short-term forms.

6.4 Combination of Effects

One of the issues complicating an analysis of these mechanisms is the fact that, with the exception of habituation, they cannot be induced alone. During sensitization experiments the test stimuli (CS) delivered to the siphon can lead to some habituation of the response. This is more significant with classical conditioning. As mentioned before the entire animal is sensitized by the US presentations and in addition it can habituate to the CS, which is presented regularly as well. This makes a quantitative analysis of classical conditioning, and to a lesser extent sensitization, quite difficult.

Chapter 7

Cellular Analysis of Plasticity in *Aplysia*'s GSWR

This chapter has several goals. Firstly, the neural circuit mediating the GSWR will be presented and its functioning and relationship to behaviour will be discussed. Next, the cellular basis of the observed learning will be discussed, with specific attention paid to the loci and mechanisms of this plasticity. This chapter is based on works involving cellular data from experiments on various reduced preparations of *Aplysia*. The basic types of preparation which are able to provide cellular data are as follows:

1. Semi-Intact Preparations: These typically include the pleural, pedal and abdominal ganglia as well as the actual tail and siphon tissue. Connectives between these body parts and ganglia are identified and kept intact. An advantage of this preparation is that the same tactile stimuli as those used in behavioural experiments can be delivered to the tail or siphon skin.

2. Isolated Ganglion: The ganglion is removed from the animal without any peripheral nerves or tissue. This facilitates direct access to all neural elements within the ganglion. Since tactile stimulation is impossible, stimuli must take the form of intracellularly injected currents.

3. Isolated Cell Culture: These typically include only a few cells, cultured rather than re-

moved from an animal. These preparations are useful as they allow for the examination of individual SN-MN synapses, which sheds light on the monosynaptic component of the reflex. Stimuli are intracellularly injected currents.

In all three cases the output is a measured excitatory postsynaptic potential (EPSP) in one of the gill motor neurons, rather than an observed withdrawal.

7.1 The Neural Circuit Mediating the GSWR

While the neural circuit mediating the GSWR is simple by neural standards, it is still fairly complicated. Also, there are likely to be contributions from as yet unidentified components, but the circuit described in this section accounts for most of the behaviour. The siphon tissue is innervated by a group of 24 sensory neurons called the LE cluster. The somata of these neurons are found in the abdominal ganglion [52] and can be uniquely identified. These neurons are the primary input stage for the CS (siphon tap). At the other end of the circuit, contraction of the gill muscles is controlled by a population of at least six gill motor neurons whose somata are also found in the abdominal ganglion. These neurons can also be uniquely identified and are called $L7$, $L9_1$, $L9_2$, LDG_1, LDG_2, and RDG. Each of these motor neurons controls a different component of the physical withdrawal by innervating different combinations of muscle fibres [29]. The two largest contributions to withdrawal come from $L7$ and LDG_1 [17].

Each of the 24 LE neurons synapses directly onto each of the motor neurons and also onto a population of interneurons. While estimates vary, the contribution from the direct (monosynaptic) pathway accounts for 30 - 50% of the observed gill withdrawal [17]. The remaining contributions come from less well delineated polysynaptic pathways, including disynaptic pathways via excitatory interneurons like L_{21} and L_{22} [17]. While the circuit described so far is sufficient for habituation, sensitization and classical conditioning also require an input pathway for the US. In behavioural experiments the US is presented to the tail or neck, so pathways from these locations must exist, but pathways from other body regions are likely to exist as well. Tail stimulation is by far the most common form of US, so the author will only consider this case.

Noxious stimulation of the tail (such as a strong electric shock) causes several things to occur.

Firstly there is strong withdrawal of the tail, mediated by the pleural and pedal ganglia, but in addition, two other things occur. Firstly there is activation of three classes [52] of modulatory interneurons in the pleural ganglia [79]. The serotonergic interneurons are most significant to this reflex [52]. Processes from these serotonergic neurons contact the presynaptic terminal of many of the synapses involved in this reflex, specifically the SN-MN synapses and those between the SNs and the excitatory interneurons. When stimulated, these neurons release serotonin[1] (5-HT), the role of which is discussed later in the sections on sensitization and classical conditioning. The second result of tail stimulation involves circuits from the tail-elicited siphon withdrawal reflex, and results in contraction of the gill in response to tail shock. This is significant to the mechanisms of classical conditioning discussed later.

7.2 Cellular Correlates of Behavioural Stimuli

The LE sensory neurons are laid out around the siphon in such a way that they have different but overlapping receptive fields. The significance of this is that a typical point stimulus will be in the receptive field of approximately eight of the 24 LE neurons [17]. Each of these neurons will fire approximately 1 - 15 spikes, depending on the strength of the siphon tap [35]. Thus each of the gill motor neurons are likely to receive between 8 and 120 spikes via the monosynaptic pathway (and more via the polysynaptic pathways) from a single presentation of the CS. The complex EPSP at each of the motor neurons is the combined response to all these spikes, scaled according to the present efficiency of the synapses they arrive through. In normal conditions the motor neuron would probably fire several times during the EPSP, but in order to record and quantify the EPSP one must prevent the motor neuron from firing. This is accomplished by hyperpolarizing the MN [19]. These complex EPSPs are the only input to the motor neurons and are proportional to the various components of withdrawal mediated by the respective motor neurons.

[1] Serotonin is a common modulatory neurotransmitter. Modulatory, in this sense, means that rather than directly resulting in postsynaptic currents, serotonin affects the efficiency of other molecular processes.

7.3 Complex and Monosynaptic EPSPs

As mentioned earlier in this chapter, the monosynaptic pathways from the LE sensory neurons to the gill motor neurons account for 30 - 50% of the response to siphon stimulation [17], with the remainder coming via polysynaptic pathways. A reliable cellular correlate of the observable withdrawal is the area of the complex EPSP in the gill motor neurons [33, 57], which is basically a superposition of the EPSP contributions from any active LE neurons along with contributions from the polysynaptic pathways in the reflex. Unfortunately when it comes to analyzing plasticity of the response, the complex EPSP does not supply information about changes in specific synapses. In order to model the synaptic plasticity underlying the behavioural modifications, one must reduce the system to a single locus of plasticity [6, 23, 29]. The obvious place to start is with the primary SN-MN synapses as these make the single largest contribution, can be most reliably identified and have been most extensively studied. Fortunately, the behaviour of this synapse can be independently observed by recording monosynaptic EPSPs at the motor neuron. Basically, the monosynaptic EPSP is the EPSP elicited by a single spike in a single sensory neuron, transmitted only via the monosynaptic pathway, and hence represents the postsynaptic effect of one spike at one synapse. In order to accomplish this there are two requirements:

Firstly a single LE cell must be made to fire a single spike. This can be reliably accomplished by stimulating the SN with intracellularly injected current [84]. The second requirement is to eliminate the contributions of the polysynaptic pathways. This can be accomplished in two ways. The most reliable approach is to physically reduce the circuit to a single LE cell and a single MN, for example L7, which is usually accomplished in cell culture [72]. The other approach is to perform the experiment in an environment with high levels of Ca^{2+} and Mg^{2+}, which has the effect of raising firing thresholds for all neurons and hence reducing the probability that the interneurons will fire [16, 29, 36]. Changes in the monosynaptic EPSP are the result of plasticity in the SN-MN synapses [23]. The remainder of this chapter will focus on the mechanisms of plasticity in the monosynaptic component of the GSWR.

7.4 Short-Term and Long-Term Memories

It has been quite conclusively shown that short- and long-term memories are represented by distinctly different mechanisms in the brain [48]. Evidence for this has been provided in part by clinical studies of humans [63], and also by cellular studies of animals like *Aplysia* [52]. In all cases it seems that repetition is the key for converting from short- to long-term memory. Short-term memory involves reversible modifications to existing structures, such as Ca^{2+} buildup or transmitter depletion [11]. Long-term memory, on the other hand, has been shown to require gene expression and protein synthesis [50], meaning that LTM involves structural changes to the neural circuit. Synapses are not usually formed or lost, but rather are strengthened or weakened by the growth or retraction of release sites within a synapse. The dependency of LTM on protein synthesis has been specifically shown for *Aplysia* [83].

7.5 The Cellular Mechanism of Habituation of the Monosynaptic EPSP

Cellular studies of habituation in *Aplysia* are generally inconsistent in their approach, but some example protocols can be found in [19, 24, 32]. Initially an AP in one of the LE sensory neurons will produce a fairly large PSP in the postsynaptic motor neurons. Repeated firing of the sensory neuron will result in a decreasing PSP. The time course of the PSP decrement is similar in shape to that of the behavioural decrement in whole-animal experiments. This response decrement is limited to the stimulated pathway, ruling out the possibility that the decrement is the result of deterioration due to isolation [19]. The observed habituation is independent of sensory adaptation or motor fatigue and the sensitivity of the postsynaptic neuron is unaffected [24]. The primary mechanism is homosynaptic depression - a reduction in the quantity of neurotransmitter released in response to an AP. The reduced release is due to a depletion of releasable vesicles at the active zones of the synapse, which in turn is due to insufficient vesicle mobilization [11]. Resting the neuron allows it to replenish the releasable vesicle pool from the storage pool, leading to recovery of the response.

Repeating the stimulation after rest leads to a greater decrement in EPSP amplitude and

conversion to long-term habituation. As expected (see 7.4), LTH requires protein and RNA[2] synthesis. Long-term habituation leads to a significant reduction in the number and size of active zones in the SN-MN synapse and in the number of transmitter vesicles associated with them [9].

7.6 The Cellular Mechanisms of Sensitization and Dishabituation of the Monosynaptic EPSP

7.6.1 Sensitization

There is little consistency among cellular studies of sensitization in *Aplysia*, but some example protocols can be found in [15, 39, 67]. Strong stimulation of the tail stimulates serotonergic interneurons[3] which contact the presynaptic terminal of SN-MN synapses. In response, the interneurons release serotonin (5-HT) into the synapse. As sensitization is not site specific, the axons of the facilitatory interneurons (FIN) contact all SN-MN synapses in this reflex, and probably others. The presence of 5-HT in the affected synapses acts to increase levels of cAMP[4], which in turn stimulates the cAMP-dependent protein kinase[5] (PKA). The increased PKA activity reduces two specific K^+ currents [52] which has the effect of broadening the AP generated by the sensory neuron [53]. This leads to increased Ca^{2+} influx during the AP, thereby increasing transmitter release. While the effects of 5-HT application do somewhat outlast its presence [62], the abovementioned mechanism still only accounts for short-term sensitization. According to [52], five tail shocks or five applications of 5-HT are sufficient to cause protein-synthesis-dependent long-term sensitization. Basically, the repeated applications lead to an increase in PKA activity which reaches high enough levels to activate the mitogen-activated protein kinase[6] (MAPK). These two enzymes then translocate to the nucleus and

[2]RNA is a nucleic acid involved in the transmission of genetic information from DNA. It is synthesized during the process of transcribing a gene into a protein or RNA sequence.

[3]A serotonergic interneuron is an interneuron which, when stimulated, releases serotonin.

[4]Cyclic adenosine monophosphate (cAMP) is a common second messenger regulating biochemical reactions dependent on hormones and neurotransmitters.

[5]cAMP-dependent protein kinase, or protein kinase A (PKA), refers to a class of enzymes whose degree of activity depends on the level of cAMP in the cell. Like other protein kinases, PKA modifies other proteins, generally resulting in a functional change in that protein. Most cellular pathways are regulated by kinases.

[6]Mitogen-activated protein kinase (MAPK) is a protein kinase which affects cell reponse to growth factors, as well as regulating activities such as gene expression, differentiation and mitosis (the normal process of cell

activate a transcriptional[7] cascade beginning with the transcription factor[8] CREB-1[9]. Finally, CREB-1 leads to the activation of some immediate response genes and then to growth of new connections.

Irrespective of the means of expression, animals that have received long-term sensitization training have up to twice as many varicosities, all of which show an increase in the number, size and vesicle component of active zones [10]. While these changes are induced and expressed presynaptically, some change in the postsynaptic neuron is required in order to accommodate these new release sites, most likely an upregulation of excitatory amino acid[10] (EAA) receptors [82].

7.6.2 Dishabituation

According to [46], broadening of the AP of a habituated synapse has little effect on transmitter release. This is because transmitter release in such synapses is limited by the available vesicle population rather than by AP duration. It is therefore not surprising that dishabituation of short-term habituated synapses involves an additional process. This process is likely to involve the mobilization of vesicles, which would have no effect on a synapse which was not habituated. Dishabituation of long-term habituation involves the re-growth of lost connections and is therefore the same as long-term sensitization of non-habituated synapses.

7.7 The Cellular Mechanisms of Classical Conditioning of the Monosynaptic EPSP

Some examples of protocols for cellular classical conditioning studies can be found in [4, 5, 41]. As with habituation and sensitization there is little consistency. Classical conditioning training involves the presentation of paired CS and US. Presentation of the US (tail shock) ob-

division/tissue growth).

[7] Transcription is the process whereby a DNA sequence is converted to a complementary RNA. It is the beginning of the process which eventually leads to the translation of genetic code into actual peptides or proteins.

[8] A transcription factor is a protein which regulates transcription.

[9] CREB-1 stands for cAMP Responsive Element Binding protein 1.

[10] Excitatory amino acids (EAAs) are a class of excitatory neurotransmitters. Many (but certainly not all) neurotransmitters are amino acids. EAA receptors are the receptor proteins that bind to these neurotransmitters.

viously causes sensitization of all SN-MN synapses in the GSWR. However, those synapses where the US is closely preceded by the CS undergo substantially greater facilitation [21]. The associative component of classical conditioning is a combination of two mechanisms, namely activity-dependent enhancement of presynaptic facilitation (ADPF) and postsynaptically induced long-term potentiation (Hebbian LTP) [5, 38, 73].

ADPF results from an interaction between elevated Ca^{2+} levels caused by the CS and the presence of 5-HT caused by the US. When the CS is presented the sensory neuron fires, leading to Ca^{2+} influx and hence to briefly elevated Ca^{2+} levels. When the US is presented the FIN releases 5-HT into the synapse, activating the PKA pathway as in sensitization. However if the CS is presented about 0.5 seconds before the US, then the PKA activation is significantly enhanced by the elevated Ca^{2+} level, leading to enhanced facilitation [5, 41].

Hebbian LTP occurs when presynaptic firing coincides with postsynaptic depolarization. As mentioned previously, presentation of the US elicits a strong withdrawal of the gill and siphon, and therefore depolarization of gill and siphon motor neurons. This depolarization of the motor neurons removes the Mg^{2+} block of NMDA-type glutamate-receptor-gated Ca^{2+} channels in the postsynaptic neuron. The removal of the Mg^{2+} blockade allows the channel to respond to the presynaptically released neurotransmitter (by opening). This allows Ca^{2+} to flood the postsynaptic cell. The elevated postsynaptic Ca^{2+} concentration then induces LTP [5].

Part II

Modelling

Chapter 8

Introduction to the Model

The first part of this thesis aimed to familiarize the non-neuroscientist with the basics of neuronal operation and with the functioning of the specific neural circuit under investigation. In fact part one can be viewed as an extended literature review. In Part II of this thesis the author will attempt to extract, from the broad and inconsistent experimental data within the literature, the nature of the synaptic plasticity at work in *Aplysia*'s GSWR and create a mathematical model describing this behaviour.

8.1 Scope of the Model

Despite the relative simplicity of *Aplysia*'s withdrawal reflexes, the GSWR is still too complex to model in its entirety. In order to set attainable goals, the author has decided to limit the scope of the model in two major ways:

1. The model will focus exclusively on the monosynaptic component of the reflex, in which the key site of plasticity is the SN-MN synapse.

2. The author will attempt only to model the short-term component of the plasticity.

In the monosynaptic GSWR circuit, the SN-MN synapse is the locus of plasticity underlying behavioural modification. While the plasticity (and hence this synapse) is the focus of the model, it will still be necessary to model the sensory and motor neurons to some degree so that the behaviour of the modelled synapse can be evaluated.

8.2 System breakdown

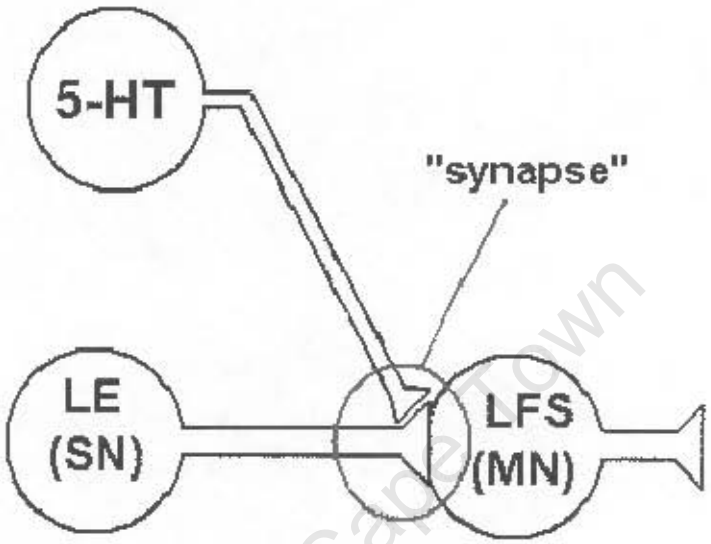

Figure 8-1: A sketch of the monosynaptic CSWR circuit as constructed in isolated cell culture. Shows LE sensory neuron (SN), LFS motor neuron (MN) and serotonergic interneuron (5-HT). The blue circle shows the synapse which includes parts of all three neurons.

The system in question consists of at least two neurons, namely one of the 24 LE[1] siphon sensory neurons and one of the LFS[2] class siphon motor neurons, as well as the synapse between them. In addition, there may be a third neuron, namely a serotonergic interneuron from the pleural ganglia, but in some experimental preparations this is omitted and the unconditioned stimulus (US) takes the form of exogenously applied serotonin. However, the question of delineating the synapse is somewhat difficult as a synapse does not exist as a discrete physical entity. A sketch of this arrangement can be found in Figure 8-1. Fortunately, from a functional point of view it is easy to separate this circuit into four "compartments", as shown in Figure

[1]The LE cluster is a population of 24 sensory neurons innervating the siphon skin. Their somata are all located in the abdominal ganglion.

[2]The LFS neurons are a group of siphon motor neurons that have been shown to make significant contributions to the CSWR [6].

8-2.

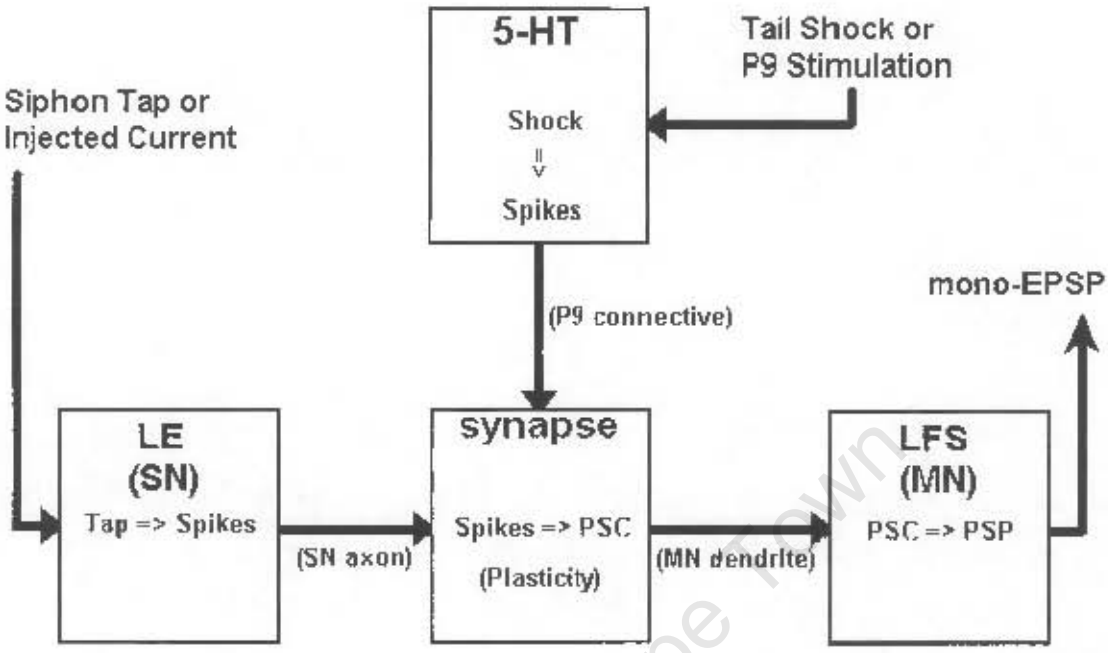

Figure 8-2: A block diagram showing the functional breakdown of the monosynaptic GSWR circuit with blocks representing each model "compartment".

The first compartment is the LE sensory neuron, including the majority of its axon. Its role is simply that of a transducer and serves to convert physical stimuli into trains of action potentials. These APs are generated at its axon hillock and propagate along the axon as stereotyped events. All the information in the spike train can be represented by a sequence of firing times.

The second compartment is the LFS motor neuron, including the majority of its dendrite. Its role is to convert inputs in the form of Postsynaptic Currents (PSCs) into outputs in the form of spike trains which in turn are converted, via the Neuromuscular Junction (NMJ), into physical muscle contractions.

The third compartment is the modulatory interneuron which fires in response to strong tail stimulation. Its role is to encode the strength and time of occurrence of the US, and present

this information to the synapse, where it will trigger 5-HT release.

The fourth (and for this work the most important) compartment is the synapse itself. This includes a portion of the presynaptic axon (from which sprouts the synaptic bouton) and the portion of the postsynaptic dendrite containing all the ion channels required to convert released neurotransmitter to postsynaptic current. Thus the input to the synapse is a set of firing times and the output is the monosynaptic EPSC.

8.3 Model Framework

Rather than using a dedicated neural simulation package, the author has chosen to use MatLab as the simulation platform. This choice was motivated in part by the author's familiarity with MatLab, and in part by its suitability for the task at hand. MatLab is a completely general package, affording the programmer full control and as such not imposing a specific structure on the model.

Chapter 9

Modelling the Sensory and Motor Neurons

In order to test the functioning of a model synapse, it is necessary to provide it with an input and view its output. In addition, this should be realised in a way that conforms to the data presented in the literature. Since the model to be developed is of the monosynaptic circuit, the relevant experiments are performed on reduced preparations. Regardless of whether LE spikes are elicited by touching the siphon skin or by intracellular current injection, the stimulus is controlled so as to produce a desired pattern of output spikes. In the literature where reduced preparations are used [31, 41, 65], the response is usually quantified in terms of the area under the monosynaptic EPSP, rather than in terms of physical withdrawal or MN spikes. Thus complete models are not required for the sensory and motor neurons.

9.1 LE Sensory Neuron

Detailed modelling of the workings of the LE neuron is not required for this project. Rather, it should be possible to create an LE spike train to match one used in a documented experiment. There is no need to model the membrane of the LE neuron, so instead a simple MatLab program was developed by the author which allows the user to specify any number of pretests[1], training

[1] A pretest is a single presentation of the CS, followed by a long delay, which is used to quantify the baseline response.

trials[2] and post tests[3]. This corresponds to the choice of training protocol. The only minor complication to an otherwise trivial model is that the LE neuron must encode the stimulus strength as well as its time of occurrence. Since APs are stereotyped, the stimulus strength is encoded by the number of spikes in a brief tetanus[4] which the LE neuron fires in response to each stimulus. A graph of the relationship between the strength of a siphon tap and number of spikes elicited is presented in [35] and is reproduced in Figure 9-1A. A good fit to the initial steep portion of this graph is obtained by the function[5]:

$$y = round(0.1661x^2 - 0.3308x + 2.2753) \tag{9.1}$$

where x is stimulus strength in g/mm^2 and y is limited to a maximum value of 13. The polynomial was found using regression. An example trace of membrane potential from a real LE neuron, also from [35], is included in Figure 9-1B. One can see that the firing rate is initially higher and declines over time, but this would be quite difficult to model. Instead the author's model uses an average firing rate of 50Hz.

Those experiments which use electrical rather than tactile stimulation generally elicit a tetanus of 5 to 40 spikes duration at a frequency between 20 and 50Hz. Such stimuli have constant frequency, so this model more closely resembles these cases.

9.2 LPS Motor Neuron

In the literature, the vast majority of experiments involving the monosynaptic component of the GSWR use the amplitude of, or area under, the monosynaptic EPSP as the measured output. However, in many cases the EPSP could exceed the firing threshold and should therefore elicit a spike. This must be prevented because a postsynaptic AP would mask a portion of the EPSP. Fortunately the motor neuron can easily be prevented from firing by sufficiently hyperpolarizing it by means of injected current. This allows the EPSP to be recorded, as shown in Figure 9-1C

[2] Different training protocols are used to elicit different types of plasticity.

[3] A post test is a single presentation of the CS, usually after a long delay, used to quantify the status of the synapse after some period of recovery.

[4] A tetanus is a brief bout of high frequency firing, usually in response to a single stimulus.

[5] *Round* is a psuedo-function which rounds off its argument to the nearest integer.

Parameter	Value
C_m	$1.2\mu F$
R_m	$65.6M\Omega$
U_{rest}	$45.1mV$

Table 9.1: Paramaters for a model LFS motor neuron [49]

(also taken from [35]). Needless to say, the hyperpolarized level must be used as a baseline for calculating the amplitude or area of the EPSP.

In order to replicate these experiments, the model motor neuron must also be prevented from spiking while converting the PSC to a PSP. As discussed in section 2.6, the Leaky Integrate-and-Fire (LIF) model is a good balance between realism and simplicity. As such, the motor neuron was modelled as a leaky integrator with the firing mechanism removed or, rather, not included. The only significant variables for an LIF neuron that will be prevented from firing are the membrane capacitance (C_m), the membrane resistance (R_m) and the resting potential (U_{rest}). In order to make quantitative comparisons between model behaviour and experimental data, these three variables would need to have realistic values. Empirically obtained values for these variables were found in [49], and are reproduced in Table 9.1.

9.3 The US Pathway

In addition to modelling the SN, MN and synapse, it is also necessary to allow for the input of the US. In reduced preparations this is performed in one of two ways. The first possibility is to leave one or both of the pedal nerves (P9) connected to the abdominal ganglion, and either electrically stimulate the P9 nerves themselves [65] or leave the tail attached and stimulate it [4]. In this case, the peak $5-HT$ concentration varies linearly with stimulus intensity, as shown in Figure 9-2 (adapted from [62]).

The second possibility, which is most commonly used in isolated cell culture, is to use exogenous application of a $5-HT$ solution, typically with a concentration[6] of around $50\mu M$ [13]. The reader may have noticed that the concentration of applied $5-HT$ is about 1000 times greater than in response to tail stimulation. The reason for this difference is that the

[6] concentration in Micro Mol

applied $5-HT$ has to pass through diffusion barriers and contend with active $5-HT$ transport mechanisms, so only a small percentage of the applied $5-HT$ will penetrate the synapse and bind to serotonin receptors.

For the purposes of this model, the author has chosen to implement the former case. Ascertaining the nature of the $5-HT$ release in response to P9 stimulation will be part of a later chapter, so for now only the relative strength and time of occurrence of P9 activity comprise the US.

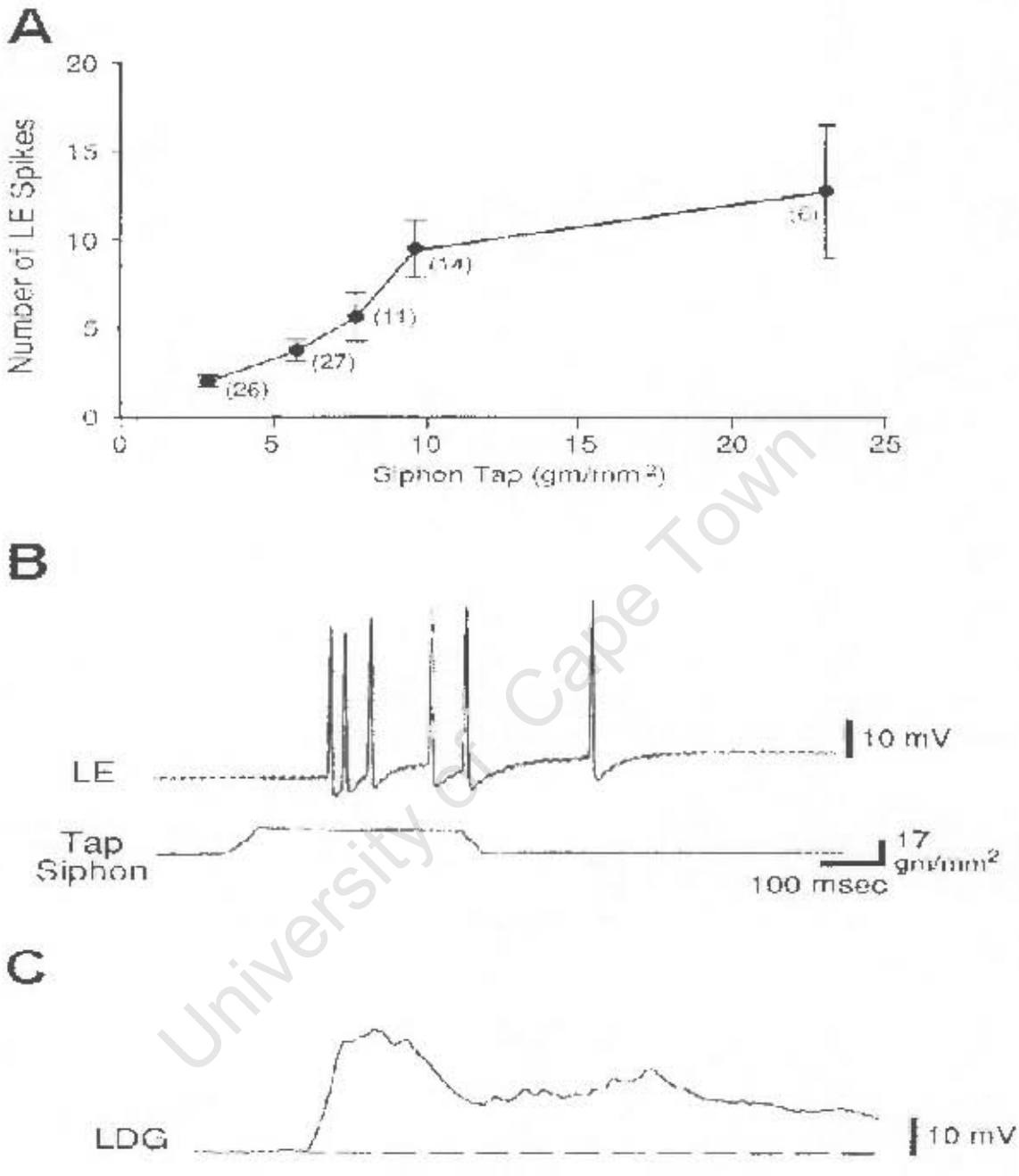

Figure 9-1: A) Number of spikes in an LE sensory neuron as a function of tap strength. Numbers in brackets are the number of instances on which the reading is based. Bars show standard deviation. B) A recording from a real LE neuron in response to siphon tap as indicated on graph. C) EPSP recorded from the LFS motor neuron in response to the spike train in B). All three were reproduced from [35].

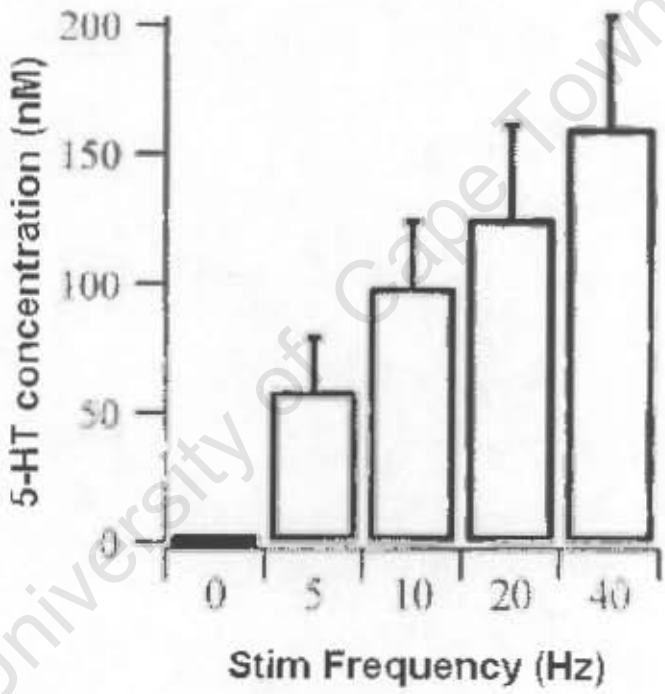

Figure 9-2: A graph of maximum 5-HT concentration versus tail shock frequency. Tail shock is a 2s train of 5ms, 15V pulses (adapted from [62]).

Chapter 10

Modelling the Synapse

The original aim of this thesis was to model the synaptic plasticity underlying certain behavioural modifications in *Aplysia's* GSWR. Preliminary investigation, reported in Chapter 7, has shown that the single largest contribution to this plasticity originates from the primary sensorimotor synapses in the circuit. The author's decision to model only the protein-synthesis-independent, short-term plasticity provides a further simplification of the original aim. While the basic mechanisms reported in the literature have already been presented, a deeper investigation into the details of these mechanisms and their interactions will be necessary in order to model the synapse with a reasonable degree of accuracy. Before modelling the dynamics of each separate form of plasticity, it will be necessary to determine how they assert their influence on the PSP.

10.1 PSP and Plasticity

As discussed previously, the effects of synaptic plasticity are best observed as changes in the area under the EPSP. In the literature [6, 33, 84], EPSPs are generally referred to as being either complex or monosynaptic. While the shape of a complex EPSP is quite unpredictable, due to the many contributions from various synapses, the shape of a monosynaptic EPSP is quite consistent (see Figure 10-1, taken from [4]). The shape of the EPSP depends on two factors, namely the membrane time constant and the PSC. Before beginning to look at the plasticity, it is necessary to model the time course of the PSC in response to an AP.

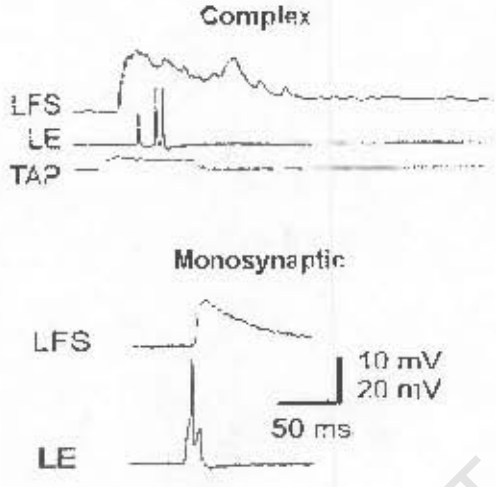

Figure 10-1: Examples of complex and monosynaptic EPSPs elicited in an LFS motor neuron in response to the LE activity shown (reproduced from [4]).

A good approximation of the shape of a real monosynaptic EPSP (such as that in Figure 10-1) can be achieved if the PSC is a decaying exponential like the one shown in Figure 10-2. The PSC is described by its initial value at the time of spike occurrence (called PSC_0) and its time constant of decay (T_{PSC}). For this slightly idealized case, the EPSP area varies linearly with the peak amplitude. The amplitude, and hence area, is the product of the time-to-peak (TTP) and rate-of-rise (ROR) of the EPSP, as illustrated in Figure 10-3. These two in turn are dependent on T_{PSC} and PSC_0 respectively.

For the sake of realism it is desirable to know how the PSC varies with plasticity. According to [45], these two properties (TTP and ROR) are affected differently by different types of plasticity. Specifically [45] shows that for depression to 70%, the relative contributions are 16% TTP and 84% ROR, while for facilitation to 175% the contributions are 63% TTP and 37% ROR. For the sake of simplicity the author will neglect the smaller of the above contributions. Thus in this model habituation will affect ROR via PSC_0 and sensitization will affect TTP via T_{PSC}.

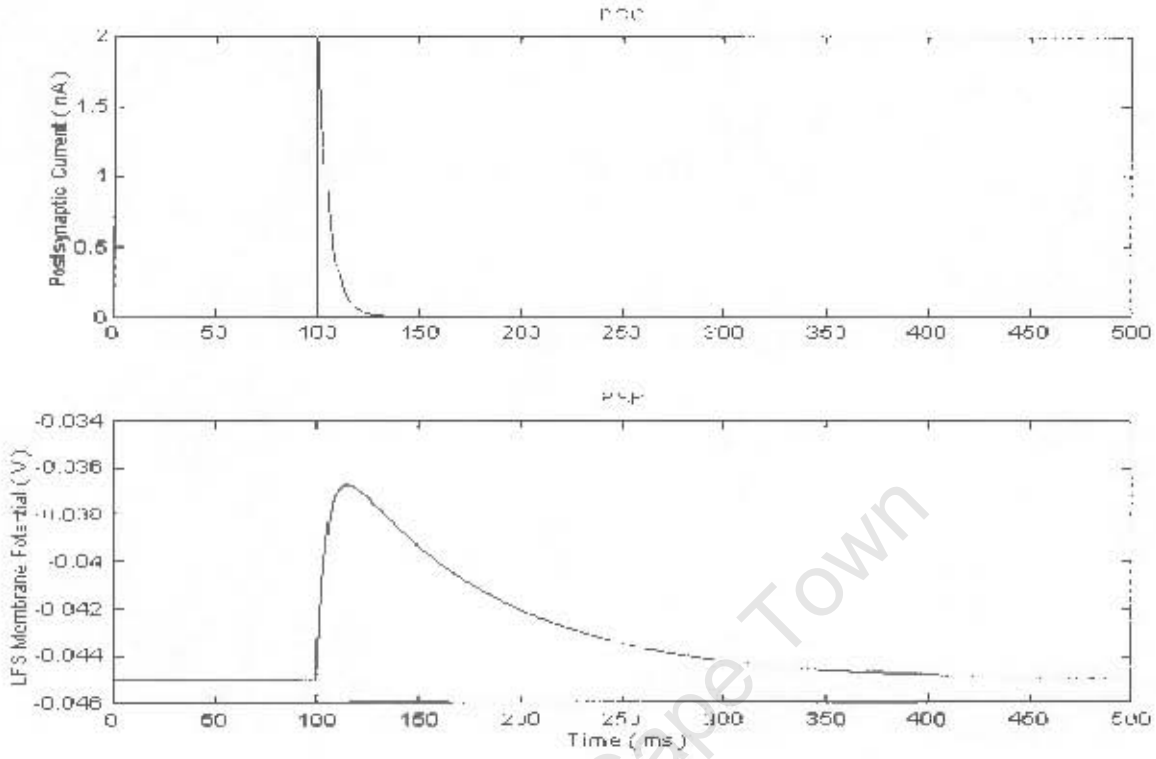

Figure 10-2: PSC (top) produced by the synapse model and resulting PSP (bottom) from the LFS model.

10.2 Synaptic Stochasticity

It was mentioned in Section 3.1 that the release of neurotransmitter during an AP is probabilistic in nature. The probability of an individual docked vesicle undergoing exocytosis on arrival of a spike is approximately 0.05 [77]. However, this unreliability can be compensated for by increasing the number of releasable vesicles. The SN/MN synapses in this circuit contain over 2000 vesicles in total [9], of which about 30% are releasable [11]. This means that on average over 30 vesicles should undergo exocytosis in response to each SN spike. Random fluctuations in the number of released transmitter quanta will contribute to the variability in EPSP amplitude, but this model will neglect these fluctuations in the interests of simplicity. The release of transmitter will therefore be modelled as being deterministic and release probability will not feature in the model. If it becomes necessary to include the effects of stochastisity at a later

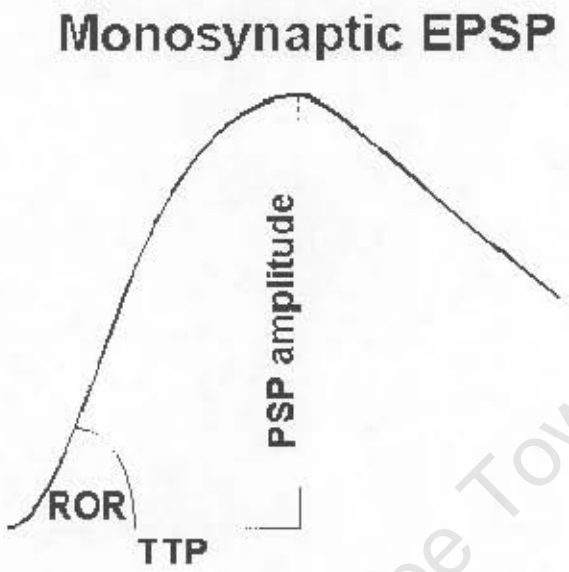

Figure 10-3: Effects of rate-of-rise (ROR) and time-to-peak (TTP) on the amplitude of a monosynaptic EPSP.

stage it would be fairly trivial to do so. A possible method would be to include a white noise component, with appropriate variance, in the PSC.

10.3 Basic Structure of Model Synapse

Having examined the shape of the EPSP and determined a suitable structure for the PSC, the next step of the model is to create a "blank" synapse, into which the mechanisms of plasticity can be inserted. Plasticity aside, the role of this synapse model is to convert a presynaptic firing time into a postsynaptic current. The procedure for accomplishing this is as follows:

$$If\ (t = t_{spike})\ then\ PSC = PSC + PSC_0 \tag{10.1}$$

The meaning of the pseudocode above is that whenever a presynaptic action potential occurs ($t = t_{spike}$) the PSC is stepped up by an amount PSC_0. The current then dies away according to:

$$\frac{dPSC}{dt} = (-PSC)/T_{PSC} \tag{10.2}$$

Where $T_{PSC} \approx 5ms$, corresponding to the TTP for a baseline EPSP [15]. A value of $PSC_0 = 2nA$ was estimated by the author, as this value produced an EPSP of plausable amplitude in the motor neuron. A comparison between an EPSP generated by the model and a real EPSP is shown in Figure 10-4. It is the shape and order of magnitude which are significant.

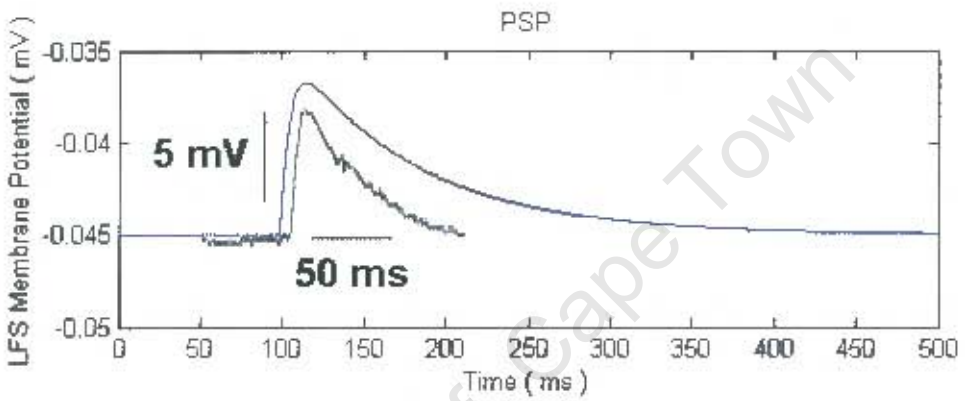

Figure 10-4: A graph showing the similarity in shape of a real LFS EPSP (adapted from [5]) (black) and a simulated LFS EPSP from the model (blue).

In order to allow for the later inclusion of plasticity, variables called Hab and $Sens$ are introduced. These variables are used to scale PSC_0 and T_{PSC} respectively, and both have initial values of unity. However, Hab is limited to the range $0 \longrightarrow 1$ while $Sens \geqslant 1$. So, for example, $Hab = 0.7$ and $Sens = 1$ corresponds to habituation to 70% of control, while $Hab = 1$ and $Sens = 1.5$ corresponds to sensitization to 150% of control. It may become necessary to include another variable to account for some part of classical conditioning, but that will be decided later.

How these variables change in response to synaptic activity is the subject of the remainder of this chapter and is the essence of this model.

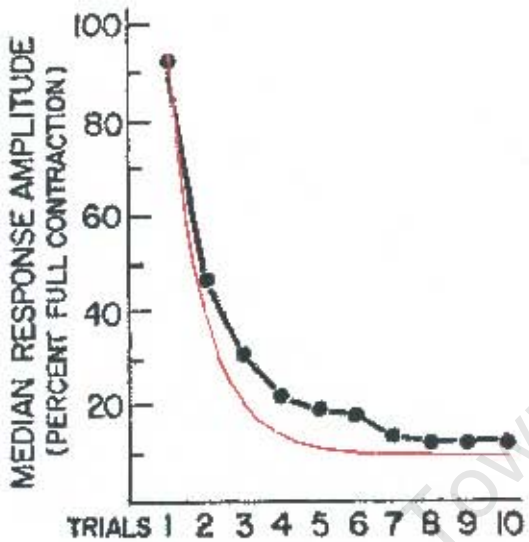

Figure 10-5: Typical habituation data (adapted from [20]) (black) and the negative exponential that approximates it (red). The equation for the red curve is: $y = 90(e^{-x}/0.4) + 10$, where x is trial number and y is response amplitude (percent of control).

10.4 Habituation

Habituation of the GSWR in *Aplysia* was originally described in [69], and has been attributed to homosynaptic depression in the form of reduced transmitter release [24]. This in turn is thought to be due to depletion of the releasable vesicle pool [11]. This standard depletion model is quite widely accepted and accounts for the exponential-like decay of efficiency with repeated stimulation [70]. A typical habituation time course (adapted from [20]) and the exponential that approximates it are shown in Figure 10-5. Note that the exponential is a function of the number of presentations, rather than of time. The spontaneous recovery from habituation with rest follows a similar exponential-like time course, an example of which (taken from [69]) is shown in Figure 10-6. So, as a first approximation, habituation could be modelled as follows:

$$\frac{dHab}{dt} = [(Hab_0 - Hab) - I_{Hab}]/T_{Hab} \tag{10.3}$$

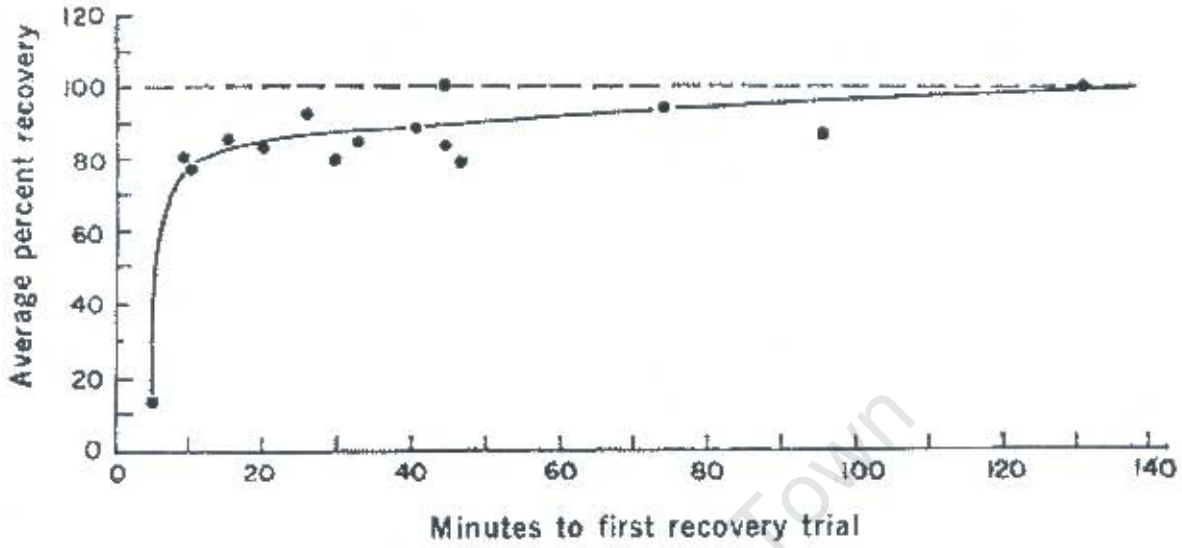

Figure 10-6: Spontaneous recovery from habituation (reproduced from [69]). Animals were habituated and then allowed to recover for different periods before being presented with a single stimulus to test for recovery. Each point is an average of three separate tests, except the last which is based on two.

Where Hab is a variable in the range $0 < Hab < 1$, $Hab_0 = 1$ and I_{Hab} is a pulse train, corresponding to presynaptic spikes, which provides the drive to habituate the synapse. The response of this model to a training session consisting of 10 trials with ISI = 10s, and appropriate values for I_{Hab} and T_{Hab}, is shown in Figure 10-7A. While at first glance this may appear to be a fairly good approximation, the problem arises when one attempts to train the same synapse with a different ISI.

In *Aplysia*, habituation occurs with similar dynamics across a wide range of ISIs - from 1 to 100 seconds [16] and more. Unfortunately, when the model described by 10.3 is stimulated with an ISI of 100s (a tenfold increase) the increased recovery time between each trial allows for full recovery and hence no buildup of habituation, as seen in Figure 10-7B. A further problem arises when an ISI of 1s is used. With so little time to recover between each spike, the variable Hab is driven below zero. This is not acceptable as real synapses can never change sign through learning (see Section 3.1).

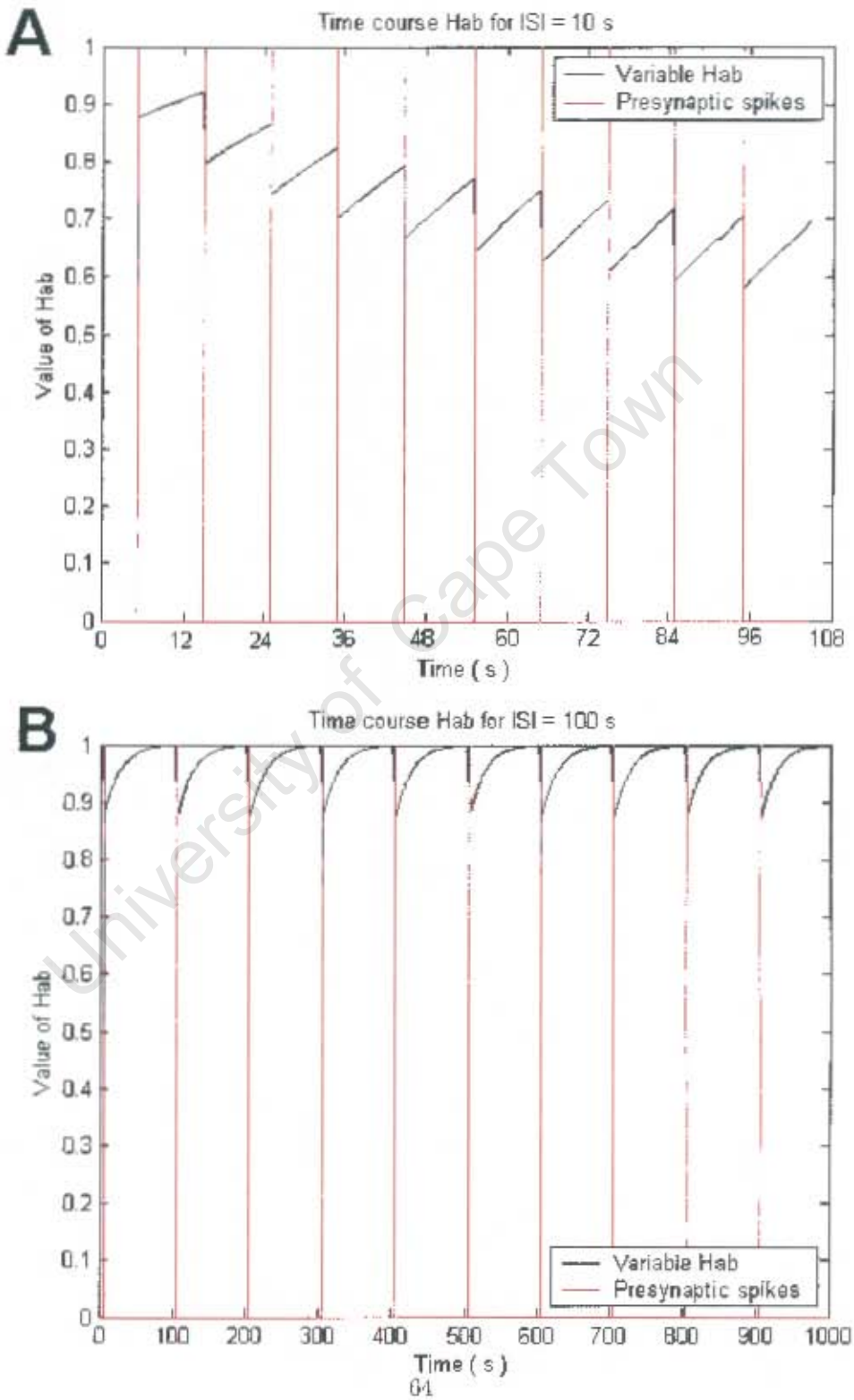

Figure 10-7: Time course of the variable Hab (first approximation model) in response to 10 stimuli. A) ISI = 10 seconds B) ISI = 100 seconds. As can be seen, the degree of habituation is too dependent on ISI.

In order to solve the latter problem, some mechanism is required that will prevent Hab from going below zero. One possibility would be to multiply the equation for $\frac{dHab}{dt}$ by Hab so that $\frac{dHab}{dt} \Longrightarrow 0$ as $Hab \Longrightarrow 0$. The problem with this approach is that as more time is spent driving Hab towards zero (even once it is indistinguishable from zero), more time is required for recovery. A more promising approach is to use an entirely different method, and create the exponential-like decay by multiplying Hab by some number less than one for each presynaptic spike.

$$If\ (t = t_{spike})\ then\ (Hab = Hab \cdot \Delta H) \tag{10.4}$$
$$\text{where: } \Delta H \in \mathbb{R}; 0 < \Delta H < 1$$

The meaning of the pseudocode in 10.4 is that for each presynaptic action potential ($t = t_{spike}$), the variable Hab is multiplied by some real number (ΔH) which is in the range zero to one. In the absence of any recovery function, this will produce a negative exponential which approaches a limit of zero with a steepness determined by ΔH. Recovery can take the same form as in the prior model, namely:

$$\frac{dHab}{dt} = (Hab_0 - Hab)/T_{Hab} \tag{10.5}$$

Where T_{Hab} is the time constant of recovery and $Hab_0 = 1$. Now Hab will tend to some value, $Hab_{min} \geqslant 0$, dependent on the two free variables ΔH and T_{hab}. This will occur when the decrement with each spike is exactly balanced by the recovery between them. For constant ΔH, T_{Hab} and ISI, and assuming that $\frac{dHab}{dt}$ remains constant during recovery, the steady state value of Hab is given by:

$$Hab_{steady} \approx \frac{ISI}{(T_{Hab} \cdot (1 - \Delta H) + ISI)} \tag{10.6}$$

In order to proceed with the model, it is necessary to determine the nature of ΔH and T_{Hab}. While it would be convenient to assume that they are constants, this is unfortunately not the case. In fact, [16] shows that there are some unexpected effects of ISI on the time course of

habituation. The following subsection is based on that research.

10.4.1 Effects of ISI

In [16], Byrne investigates the effect of training ISI on certain aspects of habituation and finds that "These data are inconsistent with a classical depletion model for synaptic depression and indicate that either a single complex function of time and ISI or multiple functions underlie synaptic depression and its recovery at the sensory neuron synapse." His findings show that three properties, namely the maximal depression attained, the median depression of the second of two EPSPs and the rate of recovery, are non-linearly dependent on ISI. The relationships between these quantities and ISI are well summarized in three graphs in Byrne's paper, which are reproduced here, along with extracts from their original text, in Figure 10-8.

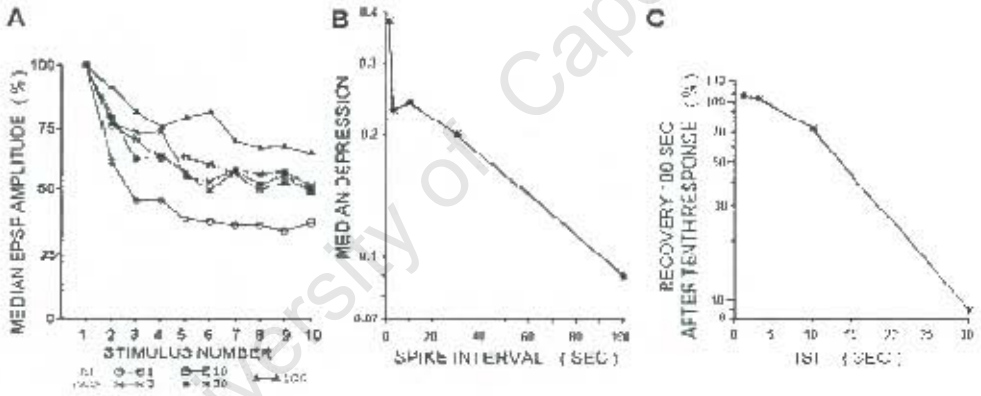

Figure 10-8: Effects of ISI on habituation, adapted from [16]. The following are extracts from the original captions. A) "EPSP depression versus stimulus number. Group data from 62 cells in 37 different experiments. At least 12 cells were examined at each ISI with the amplitude of the first EPSP scored as 100%." B) "Relationship between spike interval and second of two EPSPs. Depression is defined as $1 - \frac{EPSP_2}{EPSP_1}$ where $EPSP_1$ is the size of the first EPSP and $EPSP_2$ the size of the second EPSP." C) "Relative recovery 100s after 10th EPSP. One hundred seconds after a train of 10 EPSPs at ISIs of either 1, 3, 10, or 30s, an 11th EPSP was elicited. Percent recovery is defined as $100 \times \frac{EPSP_{11} - EPSP_{10}}{EPSP_1 - EPSP_{10}}$."

Examining this data, some qualitative conclusions about the effect of ISI can be drawn:

1. The maximum depression attainable with a given ISI is non-linearly dependent on said ISI, with a flat region in the vicinity of 3 to 30s ISI.

2. The mean depression of the second of two EPSPs shares a similar non-linear dependence on ISI, also with a flat region between 3 and 30s ISI.

3. The relative recovery after 100s is inversely related to ISI. However, since recovery after 100s is inversely proportional to the time constant of recovery, this time constant is directly, but still non-linearly, related to ISI.

Ideally this model would reproduce these relationships exactly, but unfortunately that is unlikely to be possible for several reasons. Minor complications arise from needing to find functions which fit the data in Figure 10-8 and from the fact that these graphs include so few data points. The real problem however is in determining the relationship between the quantities in the data (maximum depression, depression of the second of two EPSPs and recovery after 100 seconds) and the variables ΔH and T_{Hab}. While recovery after 100 seconds depends only on T_{Hab}, the other two quantities are dependent on both ΔH and T_{Hab}. After some preliminary work attempting to find functions for ΔH and T_{Hab} that fit the data, it is the author's opinion that such functions, if found, would be impractically complicated. For this reason and in the interests of model simplicity, the following simplifications will be made:

1. The maximum attainable depression will be identical for all ISIs. A value of $Hab_{\max} \approx 0.5$ will be used, as this is approximately the value for ISI = 3 to 30 seconds [16].

2. The rate of depression (as a function of stimulus number, not time) will be identical for all ISIs.

3. Rate of recovery is inversely proportional to ISI. No attempt will be made to reproduce the nonlinear relationship in the data.

These are clearly significant simplifications which make the model less accurate and realistic, but the author feels they are warranted. Considering that a 100 fold increase in ISI (from 1 to 100 seconds) leads to a mere 30% change in $Hab_{\max}$, the first two simplifications seem reasonable. The recovery data presented by Byrne is problematic, as it shows recovery after 100 seconds. The problem is that 100 seconds is a habituating ISI, so the stimulus used to measure the recovery will also cause habituation. Further, Byrne has not presented recovery

data for a 100-second training ISI. These problems with the data mean that accurate and realistic modelling of the dependence of recovery on ISI is not possible, so instead the model will only reproduce the key qualitative aspect, which is that recovery is slower for longer training ISIs. This serves as justification for the third simplification.

In light of these simplifications, the requirements can be met if $\Delta H = \alpha$ and $T_{Hab} = \beta \cdot ISI$, where α and β are constants. In addition to influencing $Hab_{\max}$, ΔH also affects the "sharpness" of the exponential so a value of $\alpha = 0.85$ was chosen (by trial and error) such that Hab has almost reached steady state within 10 stimuli. Next, a value of $\beta = 5.25$ was found (also by trial and error) to produce the correct $Hab_{\max}$. So, the next two equations for the model are:

$$\Delta H = 0.85 \tag{10.7}$$

$$T_{Hab} = (5.25 \cdot ISI)s^{-1} \tag{10.8}$$

10.4.2 Implementation Details

In order to implement the model described by equations 10.4 to 10.7 in MatLab, a few issues must still be cleared up. The first is how to determine what a suitable training trial is and when to apply the changes from said trial. The answer to this comes from the observation that the response to the first of a series of training stimuli is not decremented at all. This is obviously because the experimenter uses a long delay between pretests and the onset of training. The implication of this is that it is actually the gap between spikes, rather than the spikes themselves, that constitutes a training trial. So, whenever a spike occurs, $Hab = Hab \cdot \Delta H$ and this new value of Hab is used to calculate the amplitude of the EPSP in response to that spike. However, if the interval since the last spike is sufficiently long (as for the first training spike) then no decrement should occur. It is therefore necessary to actively impose a "maximum decrementing ISI" ($ISI_{\max}$). There is also the issue of "minimum decrementing ISI". It has already been mentioned that LE neurons fire a brief tetanus in response to tactile stimulation and we would certainly not want the synapse to habituate to each individual spike in the tetanus. For this reason it is also necessary to impose a "minimum decrementing ISI" ($ISI_{\min}$), below which no habituation is performed. The $1s$ ISI used in [16] is the shortest the author has observed in the

literature, so this seems to be a reasonable value for $ISI_{\min}$.

Another issue is what ISI to use in determining T_{Hab}. Basing recovery on only the most recent ISI is not appropriate, as that would allow, for example, a single short ISI to override the effects of a whole training session with long ISI. Thus it is necessary to determine the average training ISI, which will be called ISI_{mean}. Only decrementing ISIs should be included in this average. Now equation 10.4 can be updated as follows:

$$\begin{aligned} &if\ (t = t_{spike})\ and\ (ISI_{\min} \leqslant ISI \leqslant ISI_{max})\ then\{ \\ &Hab - Hab \cdot \Delta H \\ &ISI_{mean} = ISI_{mean} \cdot (\frac{\Lambda - 1}{\Lambda}) + ISI \cdot (\frac{1}{\Lambda})\ \} \end{aligned} \tag{10.9}$$

Where ISI is the time since the last spike, $ISI_{\min} = 1s$ and $ISI_{\max} = 120s$ are the minimum and maximum decrementing ISIs respectively and $\Lambda = 10$ is a user-definable constant determining the relative weight of the most recent ISI. The choice of $ISI_{\max}$ was rather arbitrary, but seems reasonable considering the ISIs observed in the literature.

10.4.3 Output of the Habituation Model

The equations presented above are the author's description of the habituation exhibited by the primary SN-MN synapses in the *Aplysia* GSWR. An evaluation of this and other forms of plasticity can be found in Chapter 11, but the preliminary results are promising. The response of the model to input trains consisting of 10 spikes with various ISIs is shown in Figure 10-9.

10.5 Sensitization and Dishabituation

The mechanism of short-term behavioural sensitization of the GSWR in *Aplysia* was first described in [22] and was shown to be the result of presynaptic facilitation which in turn is the result of serotonin activated cyclic AMP[1] (cAMP) [15]. A few years later it was found that cAMP exerts its influence by reducing a specific K^+ conductance, leading to increased Ca^{2+} in-

[1] Cyclic adenosine monophosphate, or cAMP is a common second messenger for communication within a cell.

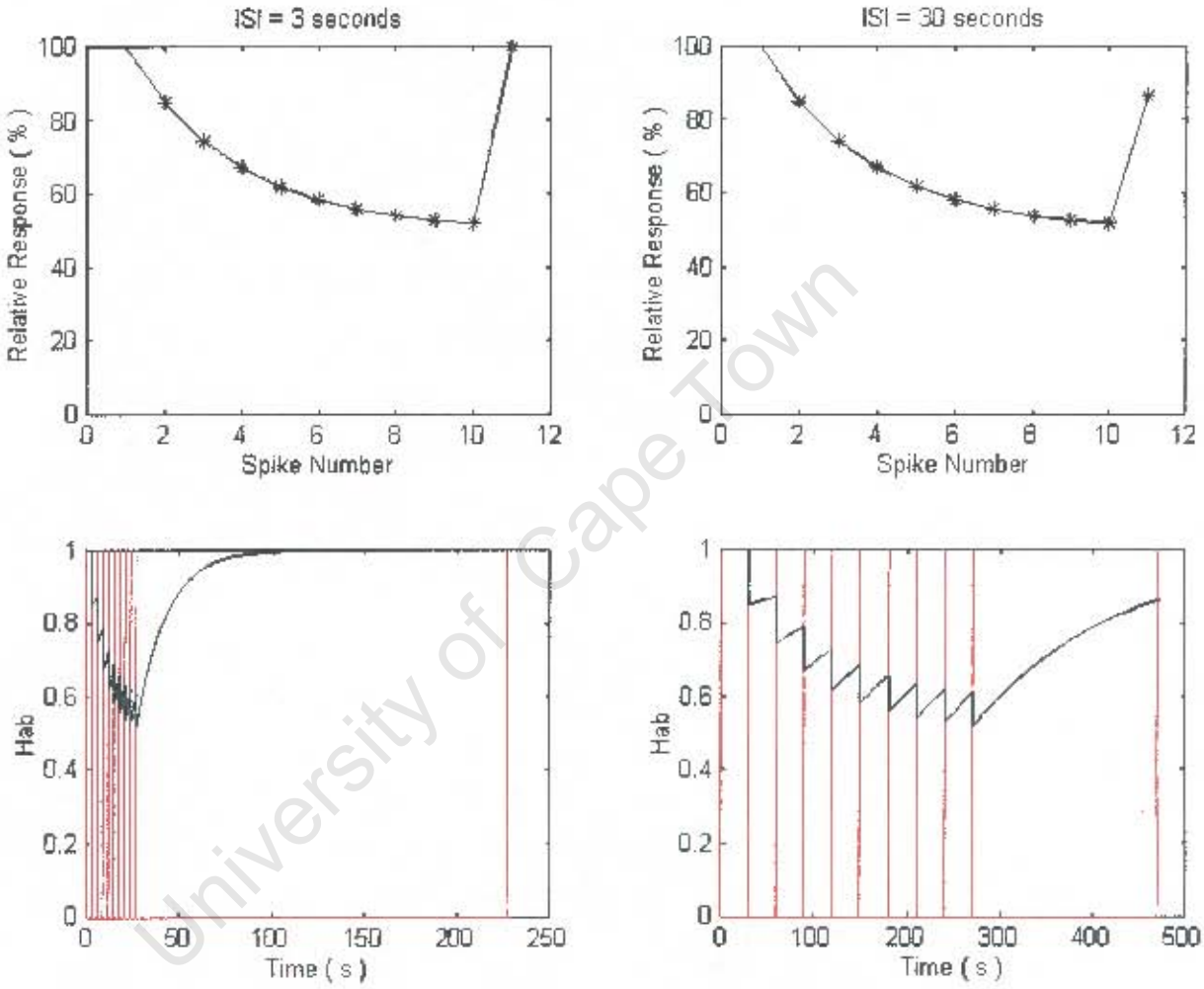

Figure 10-9: Response of the habituation model to ten training spikes at an ISI of 3 (left) or 30 (right) seconds. The top two plots show only the relative response to each spike. Note that the delay between spike 10 (the last training spike) and spike 11 (the post test) is 200 seconds. The bottom two plots show the actual time course of the variable Hab (black) and the times of the presynaptic spikes (red).

flux during the AP [53], which in turn leads to spike broadening. This change in the duration of the AP allows for more transmitter to be released. Initially it was thought that dishabituation, being facilitation of a depressed synapse, shared the same mechanism and was merely a special case of sensitization. This was disproved by [46] which showed that when transmitter-release levels are depressed, prolongation of the AP does not lead to a significant change in transmitter release. Further proof for a second, spike-broadening independent process was provided by [71], which showed that sensitization and dishabituation emerge at different times during the development of *Aplysia*. Both of these processes however are triggered by the presence of serotonin in the synapse [39]. Before the mechanisms of sensitization and dishabituation can be modelled, it will be necessary to model the 5-HT dynamics.

10.5.1 Serotonin in the Synapse

The nature of serotonin release in response to tail nerve stimulation was first investigated in [62], in which the US took the form of a 2-second train of pulses delivered to P9 (the pedal tail nerve). Stimulus intensity was controlled by varying the frequency of this spike train over the range 0 to 40Hz. It was found that 40Hz stimulation resulted in a peak 5-HT concentration of approximately 160nM and that this peak was reached within 4-6 seconds. The authors of [62] also found that it takes approximately 40 seconds for the concentration to return to baseline.

The buildup of serotonin in the synapse is likely to be the result of a 5-HT "current" flowing into the synapse (I_{5HT}). In the absence of information about the nature of this current, the author will model it as a square current pulse, whose duration corresponds to the time-to-peak of the 5-HT concentration (see Figure 10-10). The net outward 5-HT current is likely to be proportional to the concentration, so the return to baseline will probably have the shape of a negative exponential. The serotonin concentration in the synapse can therefore be approximated by the following equations:

$$\begin{aligned} if\ (t &= t_{US\ onset})\ then\{ \\ I_{5HT}(x)]_t^{t+I_{5HT}D} &= I_{5HT\,\max} \cdot P9_{stim\ strength}\} \end{aligned} \tag{10.10}$$

$$\frac{d5HT}{dt} = I_{5HT} - \frac{5HT}{T_{5HT}} \tag{10.11}$$

Where $t_{P9\ stimulus\ onset}$ = time of US onset, $I_{5HT}D$ = duration of serotonin current pulse (5s in this case), $I_{5HT\ max}$ = serotonin current required to reach maximum concentration of 160nM ($\pm 40nM.s^{-1}$ in this case), $P9_{stim\ strength}$ = relative strength of US on the range $0 \Rightarrow 1$ and T_{5HT} is a time constant governing the rate of decay of the serotonin concentration ($T_{5HT} = 8$s in this case). The time course of 5-HT concentration as determined by this model (for maximal US strength) is shown in Figure 10-10.

10.5.2 Dishabituation

The spike-broadening independent process of dishabituation is believed to involve vesicle mobilization [46]. Considering that short-term habituation results from a depletion of readily releasable vesicles [11], it makes sense for dishabituation to be applied to the same variable as habituation, namely *Hab*. While little is known about the exact time course of recovery with dishabituation, it is known that the majority of recovery has occurred within 90 seconds of US presentation, but can continue for up to 10 minutes [61]. Unfortunately, as mentioned in the previous subsection, the 5-HT concentration returns to baseline within about 40 seconds. This means that serotonin can not act directly on the depleted vesicle pool, nor on the variable *Hab* in this model, as its effect significantly outlasts its presence. This prolongation of activity is undoubtedly due to cAMP or some cAMP-activated process but, for the purposes of this model, it is only the resulting delay that matters. Also, the exact mechanism of this process is not currently known. To include this process in the model an intermediary variable called *Dishab*, whose time course parallels that of dishabituation, will be included. This variable will depend on 5-HT concentration as follows:

$$\frac{dDishab}{dt} = [5HT - Dishab]/T_{Intermediate} \tag{10.12}$$

Where $5HT$ is the variable representing serotonin concentration and $T_{Intermediate}$ is a time constant ($T_{Intermediate} = 7s$) chosen by trial and error so that the majority of the area under *Dishab* comes within 90 seconds of 5-HT onset, as illustrated in Figure 10-10. The next step is

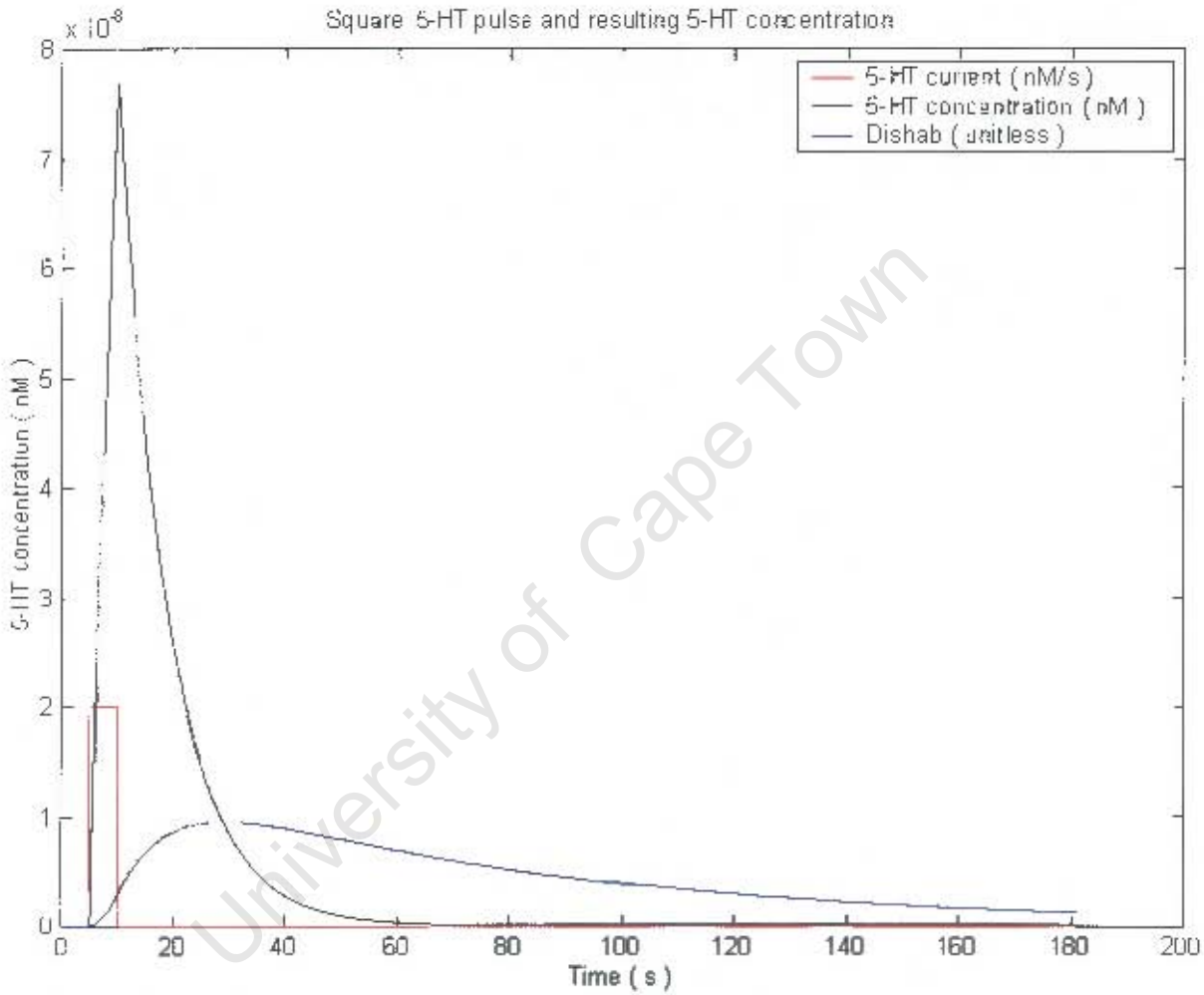

Figure 10-10: I_{5HT} pulse caused by a single US presentation at maximum strength (red) and the resulting time course of $5HT$ concentration (black) as determined by the model. Also shown is the time course of the intermediate variable *Dishab* (blue), which drives dishabituation as described in section 10.5.2.

to modify the previously presented equation for the recovery of Hab (equation 10.5) to include the dishabituating effect of serotonin. This is accomplished as follows:

$$\frac{dHab}{dt} = (Hab_0 - Hab)/T_{Hab} + \frac{Dishab}{T_{Dishab}} \tag{10.13}$$

Where $Dishab$ is the previously discussed intermediary variable and T_{Dishab} is a time constant ($T_{Dishab} = 0.8\mu s$) chosen so that Hab recovers within a realistic time frame. Recovery from habituation with and without a dishabituating stimulus is shown in Figure 10-11. For $Dishab = 0$ this equation obviously reduces to its previous form.

10.5.3 Sensitization

As already discussed, sensitization exerts its influence primarily through spike broadening [53]. In keeping with this, and the findings of [45], it was stated at the beginning of this chapter that sensitization would be applied to the time-to-peak of the EPSP via the variable T_{PSC}. While the mechanism underlying sensitization is quite well understood and has been discussed previously, it will be necessary to ascertain the time course of sensitization onset in order to model it.

It turns out that the onset of sensitization is quite different for monosynaptic versus complex EPSPs. Experiments involving complex EPSPs or intact *Aplysia*, such as [61], show that sensitization only begins to set in between 10 and 20 minutes after US presentation. In this same work it is found that a stronger tail shock leads to lower sensitization or, for sufficiently strong stimulation, to inhibition. A good review of this data is presented in [33], which goes on to compare behavioural sensitization to that of the complex and monosynaptic EPSP. It was previously mentioned that the complex EPSP closely parallels the observed withdrawal. It is therefore not surprising that the modifications to complex EPSP and to the behaviour display the same time course of onset and dependency on stimulus strength. Fortunately (for the sake of model simplicity) the monosynaptic EPSP behaves in a more straightforward manner. Specifically, the monosynaptic EPSP is significantly facilitated within 30 seconds of 5-HT application (the cellular analog of tail shock) and also shows stronger facilitation for stronger tail shocks. Thus it can be concluded that both the delayed onset and inverse effect of stronger stimuli are the result of competing inhibitory processes which are not present in the

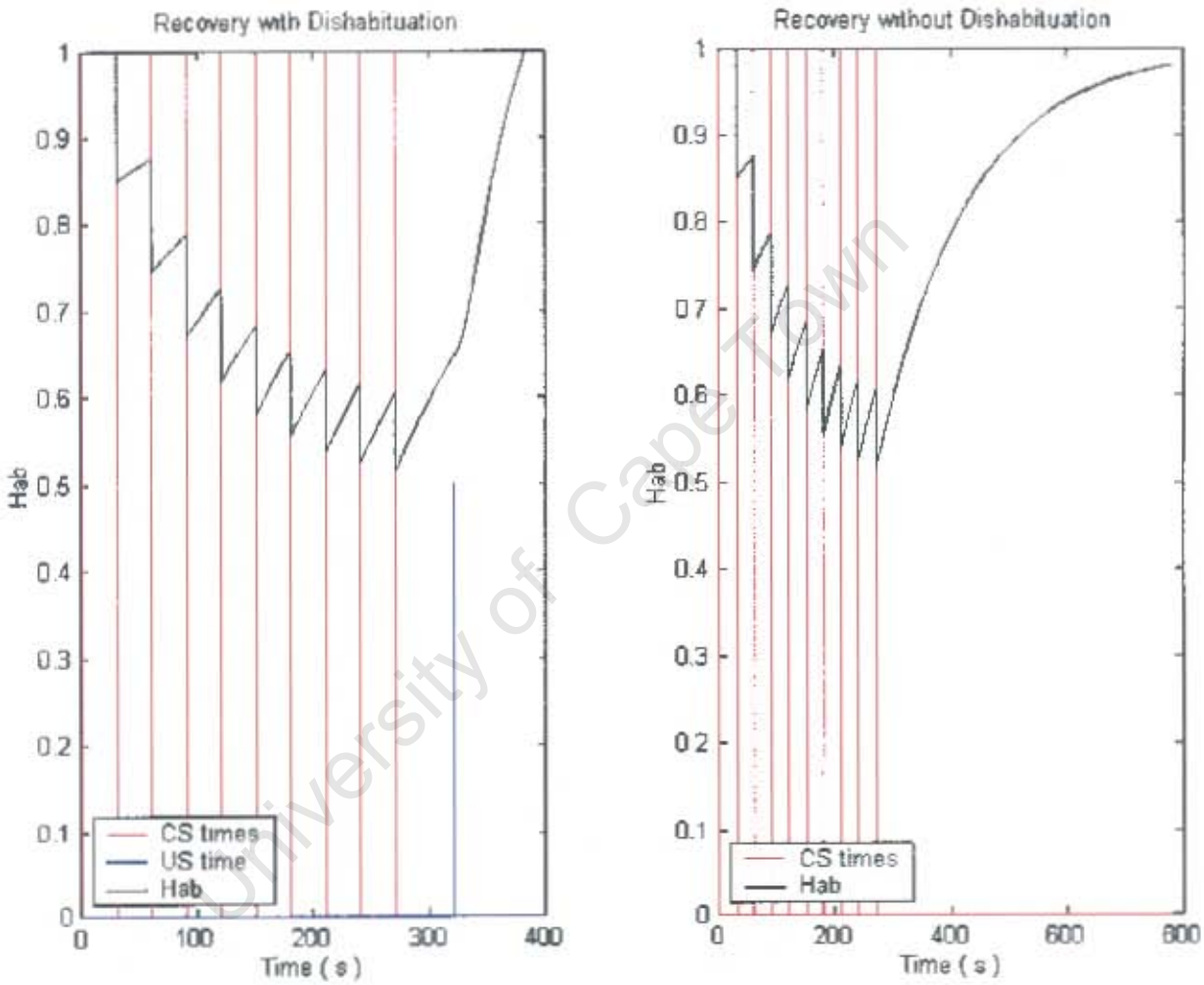

Figure 10-11: Recovery from habituation with (left) and without (right) a dishabituating stimulus. The US had a relative strength of 0.5 and its time of occurence is shown in blue.

monosynaptic component of the reflex.

Little is known about the exact time course of sensitization onset, probably due to a lack of "high resolution" experimental data. Instead, experiments in the literature [33, 84] generally use only a few post-tests which are too far separated in time to provide detailed information about sensitization onset. While there are undoubtedly good reasons for this from an experimental point of view (probably to do with not habituating the synapse), it does limit the precision with which sensitization can be modelled. In particular, the difficulty is in determining the time taken for sensitization to reach its maximum value. Other factors which must be included in the model are the rate of recovery and the maximum sensitization attainable from a single US presentation.

Serotonin leads to spike broadening through cAMP-dependent Protein Kinase [53], so sensitization is unlikely to be immediate. Instead, its peak occurs somewhere in the vicinity of 30 to 90 seconds post stimulus. For the sake of simplicity, the author has chosen to use the 5-HT concentration to directly drive the sensitization, rather than utilizing an intermediate variable as in the case of dishabituation. While this is not entirely accurate from a biological standpoint, it produces peak sensitization approximately 35 seconds after stimulus presentation, corresponding to the time taken for the 5-HT concentration to return to near baseline. Assuming that the recovery from sensitization is roughly exponential in shape, we have the following equation for the variable $Sens$:

$$\frac{dSens}{dt} = [5HT \cdot R_{Sens} + (Sens_0 - Sens)]/T_{Sens} \tag{10.14}$$

Where $5HT$ is the serotonin concentration, $Sens_0 = 1$ is the resting value of $Sens$, R_{Sens} is a constant governing the degree of sensitization produced by a given quantity of serotonin and T_{Sens} is a time constant of recovery. The next step in creating the model is to find values of R_{Sens} and T_{Sens} which provide a good fit to the experimental data.

In [62] it is stated that "exogenous application of 10–50μM 5-HT produce maximal effects on tail SN plasticity under our current experimental conditions.". In [33], exogenous application of 50μM 5-HT leads to facilitation to 275% of baseline at the 30 second post-test, which is the maximum facilitation reported in that work. Therefore it seems reasonable to assume that this is the maximum facilitation attainable by a single, brief 5-HT application. So, for the purposes

of this model, the author will select values of R_{Sens} and T_{Sens} which produce a good fit to the data of [33], for maximum strength US. Using a trial and error procedure, the following values were found: $R_{Sens} = 0.42 \times 10^9$ and $T_{Sens} = 350s$. A graph of the sensitization produced by this model in response to a maximum strength US is shown in Figure 10-12(top).

As mentioned earlier, the process of spike broadening underlying sensitization of this reflex has little effect on transmitter release when the synapse is already depressed [46]. Thus it is necessary to modify the sensitization model to reflect this. In the real synapse this ineffectiveness is due to a lack of releasable vesicles, but the model developed thus far does not explicitly represent the transmitter pool. Instead, this reduced sensitivity to spike broadening while depressed will be accounted for by modifying the model as follows:

$$\frac{dSens}{dt} = [Hab^n \cdot (5HT \cdot R_{Sens}) + (Sens_0 - Sens)]/T_{Sens} \tag{10.15}$$

Where Hab^n is the variable representing habituation, raised to the n'th power. The choice of n determines the "steepness" of the cutoff, and a value of $n = 10$ was chosen by the author. This choice was estimated, as the author was unable to find any specific data in the literature describing the relationship between the degree of depression and the effectiveness of sensitization. The effect of a sensitizing stimulus for depressed and for rested model synapses is shown in Figure 10-12.

10.6 Classical Conditioning

Classical conditioning of this reflex was first reported in [21], and was attributed to activity-dependent amplification of presynaptic facilitation (ADPF) in [41]. Later experimental work revealed the involvement of a second process, namely Hebbian long-term potentiation (H-LTP) [5, 38, 64]. Both of these mechanisms have been introduced in Chapter 7.7. From a functional point of view, both of these processes are fairly straightforward. There are however two significant complications. The first of these lies in determining how the two mechanisms interact, while the second lies in separating the long- and short-term forms of classical conditioning. Unfortunately, while attempting to answer the first of these questions, papers which seemed to contradict each other were discovered in the literature. This is the subject of the following

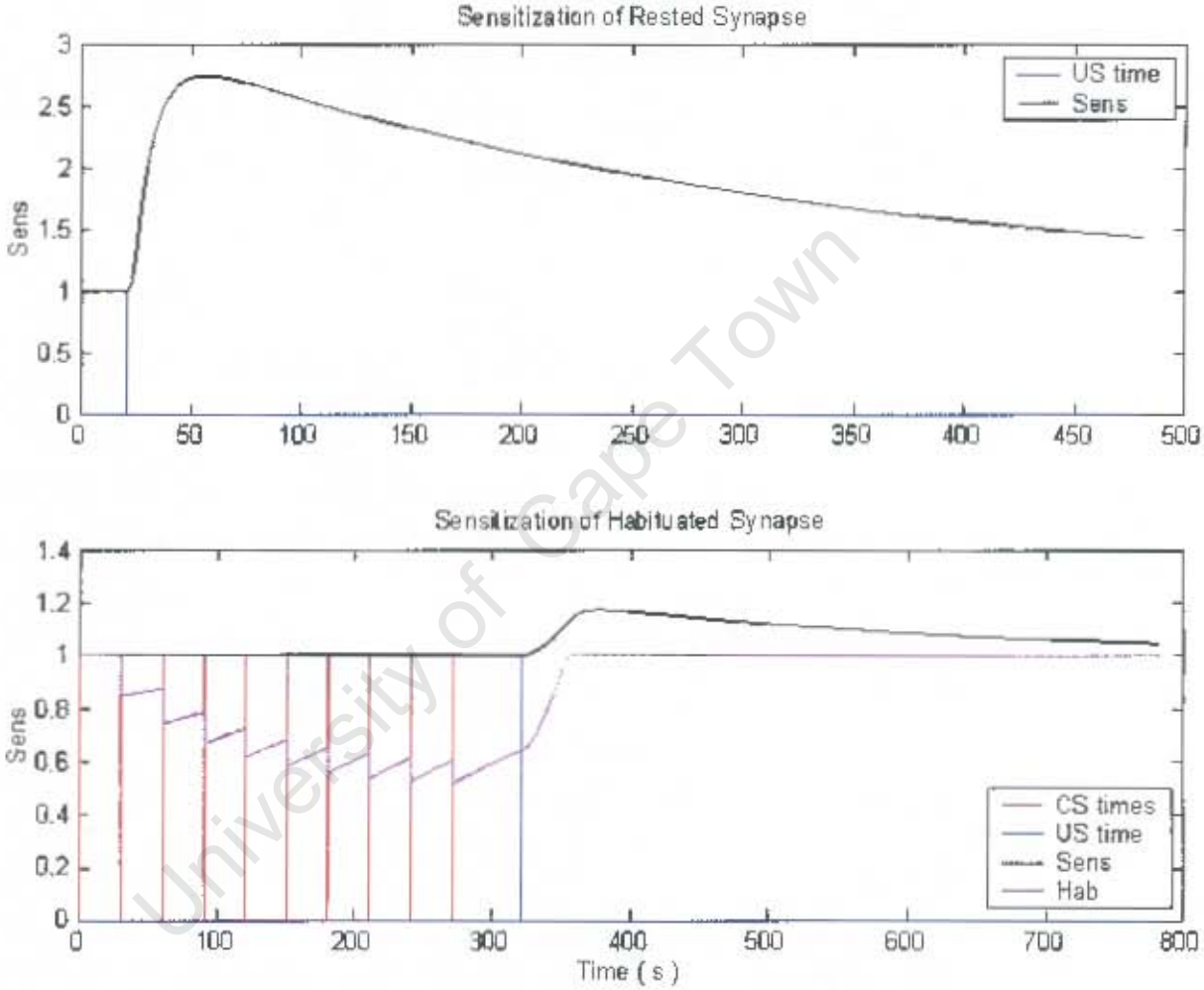

Figure 10-12: Time course of the variable *Sens* in response to maximum strength US as generated by the model, for undepressed (top) and depressed (bottom) synapses. Note the reduced effectiveness of the sensitizing stimulus when the synapse is depressed (bottom).

subsection.

10.6.1 Unravelling the Mechanism of Classical Conditioning

The Contradiction

In a recent work [5] it is reported that "conditioning of the siphon-withdrawal reflex is blocked by bath application of either the PKA[2] inhibitor KT5720 or the NMDA receptor[3] antagonist APV". The significance of this is that PKA is required for ADPF, while NMDA receptors play a critical role in H-LTP. Thus the finding that either of these substances block CC altogether implies that the two mechanisms cannot function independently.

In contradiction to this, [38] reports that H-LTP was elicited in a reduced preparation which involved no possible source of 5-HT. Further contradiction comes from [31], which uses an isolated cell culture and produces ADPF despite the fact that the postsynaptic motor neuron is hyperpolarised below -80mV for the purposes of recording. This is significant because postsynaptic depolarization is one of the requirements for H-LTP, so hyperpolarization blocks this mechanism.

Two Forms of Classical Conditioning

A possible explanation for these inconsistencies was provided by [74]. In this work the authors report two forms of activity-dependent enhancement, both of which last over 24 hours. The first of these, henceforth Form-1, is induced by a single pairing of 5-HT with a brief tetanus (20Hz, 2 seconds) and is similar in magnitude and duration to that produced by four applications of 5-HT alone, showing little decrement over 24 hours. The other, Form-2, is induced by multiple pairings of 5-HT and tetanus. The single most important difference between the two forms is that the associative component of Form-2 is blocked by postsynaptic hyperpolarization (which is known to block H-LTP), while Form-1 is not. Further information about the mechanisms of classical conditioning can be inferred from the experimental data presented. This data has been extracted from the graphs in [74] and is summarised in table 10.1.

[2]Protein Kinase A (PKA) is activated by cAMP and is involved in presynaptic facilitation.

[3]NMDA receptors are a specific type of glutamate receptor which have the role of detecting coincident pre- and postsynaptic activity. Thus they are vital to the process of H-LTP.

Training Stimulus	30 min Test	24 hr Test	24 hr Test (L7 hyp)
1× Tetanus	100% (assumed)	100%	100% (assumed)
1 × 5-*HT*	Unknown	105%	100%
1× Pairing	150% (assumed)	150%	150%
4× Tetanus	100%	105%	105% (assumed)
4 × 5-*HT*	150%	150%	150%
4× Pairing	150%	185%	150%

Table 10.1: Effects of repetition and of L7 hyperpolarization on the onset of facilitation

The first thing to observe from this data is that, as mentioned, only Form-2 conditioning is blocked by L7 hyperpolarization. The next point is that at 30 minutes post training, the facilitation produced by 4 × 5-*HT* and by 4× Pairing are identical, and that the further associative enhancement only kicks in over the next 24 hours. In addition, hyperpolarization of L7 during training reduces the 24 hour post-test for 4× Pairing to the same level as for 4 × 5-*HT*. This strongly suggests that the further 35% enhancement is attributable to H-LTP.

It seems reasonable to assume that the enhancement produced by 1× Pairing is presynaptic (as it is not affected by L7 hyperpolarization) and therefore that full facilitation is present at 30 minutes post training, as for 4 × 5-*HT*. It also seems reasonable to assume that 1× Pairing is unlikely to produce more facilitation than 4× Pairing at the 30-minute post-test. Thus in the absence of data, a value of 150% for the 1× Pairing 30-minute post-test will be assumed.

An Hypothesis

In light of this assumption, and the abovementioned observations, the following seems a reasonable explanation: The facilitation observed at the 30-minute post-test is produced by presynaptic mechanisms involving cAMP. This presynaptic facilitation has a maximum of 150% for the 5-HT concentration used, which can be achieved by four applications of serotonin. However, while pairing these applications with tetanus does not produce greater presynaptic facilitation, it does increase the efficiency of the serotonin, allowing a single pairing to have the same effect as four applications of 5-HT alone. For a single pairing, postsynaptic mechanisms are not recruited so no further facilitation occurs. In the case of multiple pairings, however, there is a further associative enhancement due to H-LTP which sets in over the next 24 hours and is blocked by L7 hyperpolarization during training.

Evaluation of the Hypothesis

Having developed this theory based on [74] alone, a good test of its validity will be how well it explains the inconsistencies mentioned at the beginning of this subsection. In [5] it was reported that postsynaptic application of the NMDA receptor antagonist APV (which blocks H-LTP) blocks the associative enhancement. However, this work uses a training protocol consisting of three sets of four pairings each, and is hence comparable to Form-2 conditioning, which does require H-LTP. Another observation is that this work also shows facilitation to 150% of control for the first set of pairings. On the other hand, [31] produces an associative enhancement despite postsynaptic hyperpolarization, but this work uses a training protocol involving only a single presentation of the stimulus, as in Form-1, so this is also consistent with the theory.

In [38], H-LTP is induced in a preparation involving no serotonin and hence no ADPF. While this does not directly contradict the proposed theory, having made no prediction as to whether H-LTP can exist alone, there is an inconsistency in terms of onset of LTP. This work shows peak facilitation at the 10-minute post-test, in the absence of ADPF, while [74] shows no sign of H-LTP at the 30-minute post-test. A possible explanation for this is that the rate of onset, as well as the magnitude, of H-LTP could depend on the nature of the training. Specifically, the requirement for postsynaptic depolarization is unlikely to be binary. In [38], the US is "strong postsynaptic depolarization", while in both [5] and [74] the postsynaptic neuron is "naturally" depolarized by presynaptic activity. While the degree of depolarization in [38] is not reported, it could well have been significantly stronger than in either of the other works. In fact, this theory helps explain the fact that [5] does not show any significant associative enhancement when ADPF is blocked. In control experiments, the first presentation of the training stimulus leads to significant facilitation of the synapse. Thus, the following siphon tap will lead to greater postsynaptic depolarization which in turn will facilitate the induction of H-LTP. When ADPF is blocked, there is no initial facilitation so subsequent presentations do not lead to greater postsynaptic depolarization. Rather the postsynaptic response declines, as a result of habituation to the CS. So while H-LTP can be induced alone, it interacts with ADPF indirectly through the latter's ability to enhance the postsynaptic depolarization required for the former.

In Conclusion

While the theory presented above is unlikely to be entirely correct, it does seem to explain some of the peculiarities of classical conditioning. The distinction between Form-1 and Form-2 conditioning is also useful, as it had not been possible to define long- and short-term forms of classical conditioning. While both forms last over 24 hours, Form-1 is likely to be shorter lasting than Form-2, as it does not involve LTP. There is also a similar dependence on the number of training presentations, and a difference in the underlying mechanism. Since the scope of this work has been limited to the short-term component of plasticity, the model of classical conditioning will be restricted to Form-1, and hence will only incorporate ADPF.

10.6.2 Modelling Form-1 Classical Conditioning

The mechanism of ADPF has been fairly well understood for some time [41] [see [73] for review], and was described in Chapter 7.7. To recap briefly, CS presentation (siphon tap or SN stimulation) results in temporarily elevated Ca^{2-} in the presynaptic terminal. If the US is presented just after the CS, the elevated Ca^{2+} level interacts with the serotonin so as to enhance cAMP synthesis, leading to greater activation of PKA and hence greater facilitation. Thus the first step in modelling this process is to characterize the Ca^{2+} buildup resulting from a tetanus.

According to [56] the Ca^{2+} concentration builds up during the tetanus, reaching its peak just after the tetanus ends. The Ca^{2+} concentration then decays back to baseline with a double exponential time course and time constant, T_{Ca}, of about 30 seconds. There must, however, be a maximum attainable concentration, Ca_{Max}. With continued tetanic stimulation the Ca^{2+} concentration will approach this limit. The numeric value of this maximum concentration is not significant to this model, so $Ca_{Max} = 1$ will be used, and $0 \leqslant Ca \leqslant 1$. Classical conditioning is maximal when the CS precedes the US by approximately 500ms [42]. While the real mechanism may include some intermediate messenger through which Ca^{2+} and 5-HT interact, this model will assume that they interact directly.

Let us assume that the calcium concentration exerts its effect on cAMP synthesis only at the time of 5-HT release. While this is unlikely to be the case in reality, it does simplify the model. Then the model calcium concentration must be at a maximum approximately half a second after the onset of the tetanus.

The first step is to model the calcium current, I_{Ca}. To avoid excessive complexity, some simplifying assumptions will be made:

1. Each AP results in a square pulse with magnitude $I_{Ca}M$, which will be determined later, and duration $I_{Ca}D$. In [68], the authors investigate the duration of calcium current in neurons taken from chick embryos and find that, for slow APs, the Ca^{2+} current begins 0.4ms after the AP peak and ends just after the potential returns to baseline. It is likely that I_{Ca} in *Aplysia* will have a similar time course due to the general conservation of neuronal mechanisms. Based on the traces of LE neuron APs presented in [45] the time from peak to baseline is estimated at 2.5ms. Thus $I_{Ca}D = 2.5$ms.

2. Current pulses will never overlap. It is impossible to elicit a second AP before the first is over and I_{Ca} pulses do not outlast the AP. In the model a tetanus is a 50Hz spike train, so the shortest ISI possible is 20ms.

In light of these assumptions, we can define the calcium current as follows:

$$\begin{aligned} if\ (t &= t_{spike})\ then\ \{ \\ I_{Ca}(x)]_t^{t+I_{Ca}D} &= I_{Ca}M\ \} \end{aligned} \tag{10.16}$$

Where t_{spike} are the firing times of the presynaptic neuron. A value of $I_{Ca}M \quad 10\mu M.s^{-1}$ was chosen. The calcium concentration at any given time is dependent on the calcium current and is given by:

$$\frac{dCa}{dt} = [I_{Ca}\frac{Ca_{Max} - Ca}{Ca_{Max}} - 2 \cdot Ca]/T_{Ca} \tag{10.17}$$

Where I_{Ca} is given by the previous equation, $T_{Ca} = 30s$ is the time constant mentioned previously and Ca is the variable representing the Ca^{2+} concentration. The calcium concentration resulting from a brief tetanus is shown in Figure 10-13.

Brief application of 5-HT alone or tetanic stimulation alone both lead to a similar degree of short-lasting facilitation, to about 130% and 125% of control respectively [31]. Pairing the stimuli produces facilitation with a peak magnitude roughly equal to the sum of the two

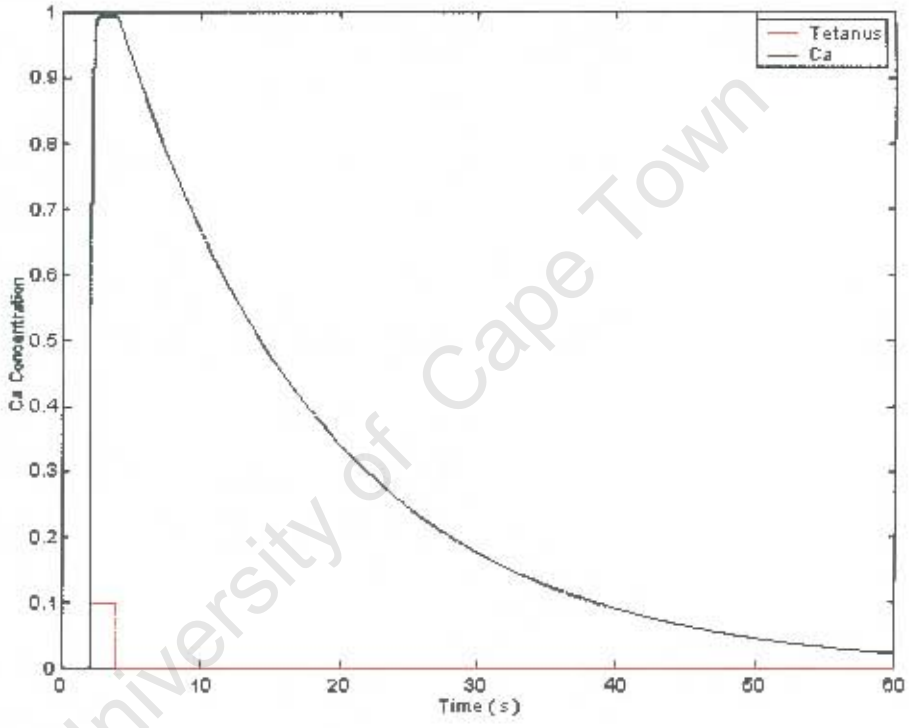

Figure 10-13: Relative Ca^{2+} concentration (black) resulting from a 2 second, 50 Hz tetanus (red) as determined by the model.

components [13] but much longer lasting. However, post-tetanic potentiation is not within the scope of this work so the important feature to model is the extended duration of facilitation. The data of [74] (reproduced in 10.1) suggests that there is no significant decrement in the facilitation over 24 hours. On the other hand, [31] claims that the associative facilitation shows no significant decrement over 20 minutes, while [13] reports that a pairing produced "larger facilitation that lasted $\succ$ 30 min". It is difficult to draw conclusions from such varied results, particularly considering that all three works used the same preparation, consisting of an L7 motor neuron co-cultured with two pleural ganglion mechanoreceptor neurons. All three works use a 20Hz, 2s tetanus as the CS, and exogenous 5-HT application ($10\mu M$ in [31] and $50\mu M$ in the other two works) as the US and all three use a protocol with a single pairing. The only apparent difference in the protocols is that [74] has a 3-minute delay between wash-in and wash-out of serotonin, while [13] and [31] use delays of $<$ 60s and 30s respectively. According to [62] the serotonin concentration resulting from strong tail nerve stimulation returns to baseline within about 40s of the end of stimulation, so the exposure durations used by [13] and [31] are more realistic than that of [74]. If these three works are anything to go by, it seems that the duration of the associative facilitation is related to the duration of 5-HT application. In this model, serotonin is released in response to P9 stimulation and dissipates within 60 seconds, a similar time course to that in [13]. To avoid excessive complexity, the author has chosen not to model the proposed relationship between duration of serotonin presence and duration of facilitation. Instead, the modelled ADPF will have similar duration to that reported in [13].

Because this model does not include PTP, the only differences between sensitization and conditioning are the requirement of the latter on presynaptic Ca^{2+}, and the difference in duration. Equation 10.10 characterises the serotonin concentration resulting from the US. Let us introduce another variable which will represent the combined presence of calcium and serotonin as follows:

$$\begin{aligned} if\ (t &= t_{US\ onset})\ then\{ \\ I_{5HT\_Ca}(x)\big|_t^{t+I_{5HTD}} &= I_{5HT\max} \cdot P9_{stim\ strength} \cdot Ca\} \end{aligned} \tag{10.18}$$

$$\frac{d5HT\_Ca}{dt} = I_{5HT\_Ca} - \frac{5HT\_Ca}{T_{5HT}} \tag{10.19}$$

Where $5HT\_Ca$ represents the serotonin concentration scaled by the relative Ca^{2+} concentration (variable Ca) at the time of US presentation. The other variables are the same as in equation 10.10. Next, we introduce a variable called CC, representing the associative enhancement of ADPF, which is governed by equations of the same form as for sensitization (equation 10.15) except driven by $5HT\_Ca$ as follows:

$$\frac{dCC}{dt} = [Hab^n \cdot (5HT\_Ca \cdot R_{Sens}) + (CC_0 - CC) \cdot T_{Sens}/T_{CC}]/T_{Sens} \tag{10.20}$$

Where $CC_0 = 1$ is the steady state value of CC, T_{CC} is a time constant controlling the rate of recovery from conditioning and the other variables are the same as those in 10.15. Note that the onset of CC is scaled by T_{Sens} but the rate of recovery depends on T_{CC}, the value of which is estimated from [13] to be 60 minutes ($T_{CC} = 3600$ seconds). The next question is what to do with the variable CC. ADPF is an extension to the mechanism of sensitization, so rather than allowing CC to directly affect the PSC it will be act via $Sens$. A simple but effective solution is to use CC as the steady state value of $Sens$, namely $Sens_0$. We do this by adapting equation 10.15 as follows:

$$\frac{dSens}{dt} = [Hab^n \cdot (5HT \cdot R_{Sens}) + (CC - Sens)]/T_{Sens} \tag{10.21}$$

Where the only modification was to replace $Sens_0 = 1$ with the new variable CC, so that $Sens \geqslant CC$. Thus if, at the time of US onset, $Ca = 0.5$ then $Sens$ will initially be larger than CC, but as $Sens$ begins to decay (faster than CC does) it only goes as far as its new baseline, namely CC. This rather confusing situation is illustrated in Figure 10-14. In most classical conditioning scenarios, the presynaptic calcium concentration will be very close to maximum when the US occurs. In these cases, I_{5HT_Ca} will be virtually identical to I_{5HT} and as a result $Sens$ will not be noticeably larger than CC. This will result in $Sens$ simply tracking the time course of CC. The time course of modelled facilitation resulting from paired and unpaired presentation of the CS and US is shown in Figure 10-15. The CS is a 1s, 50Hz tetanus which is followed (0.5s later for paired training or 60s later for unpaired training) by a US of 25%

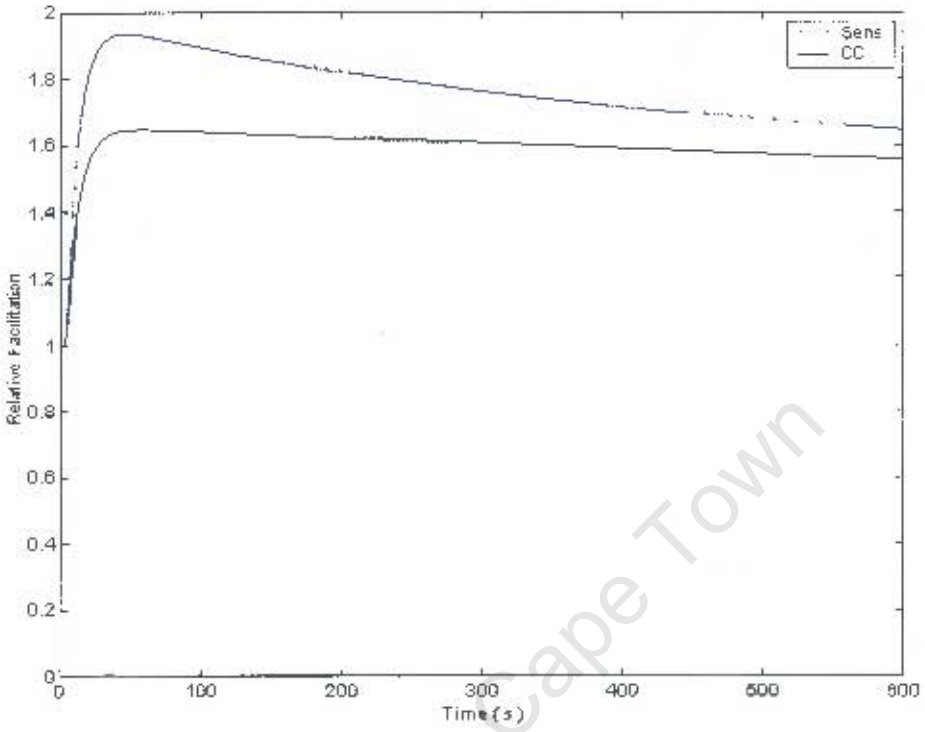

Figure 10-14: Time course of variables $Sens$ (blue) and CC (black) in response to paired stimulation at $t = 0$. The tetanus used was unusually short so that, at the time of US onset, $Ca \approx 0.6$.

strength, as described in section 9.3.

10.7 The complete synapse model

The model developed over the course of this chapter is reproduced here in its entirety. The equations describing the model can be grouped into two classes. The first of these is the group of DEs which govern the evolution of the variables. They are:

$$\frac{dCa}{dt} = [I_{Ca}\frac{Ca_{Max} - Ca}{Ca_{Max}} - 2 \cdot Ca]/T_{Ca} \tag{10.17}$$

$$\frac{d5HT\_Ca}{dt} = I_{5HT\_Ca} - \frac{5HT\_Ca}{T_{5HT}} \tag{10.19}$$

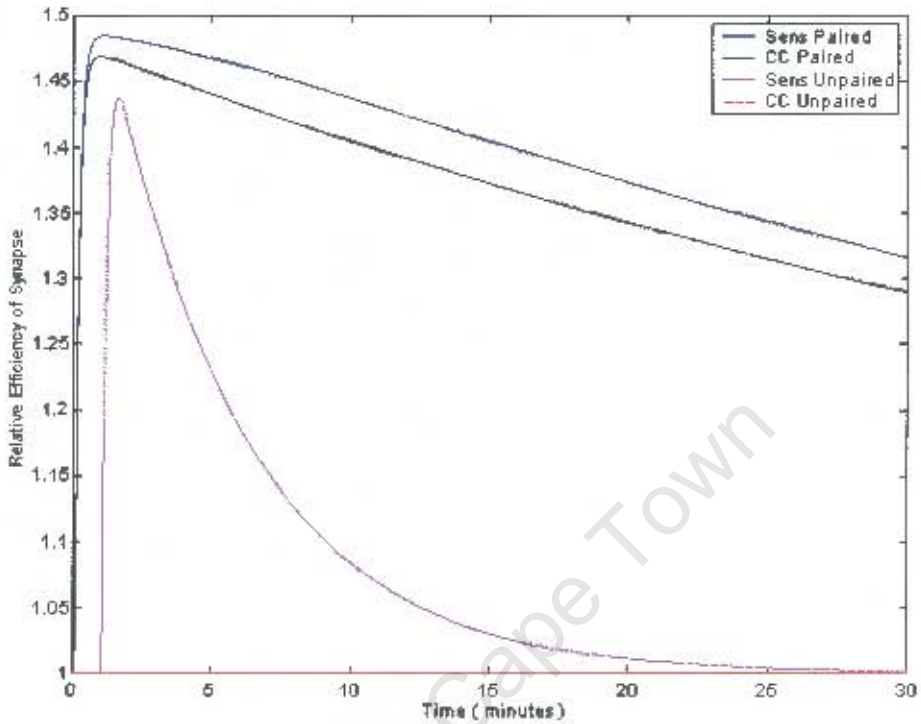

Figure 10-15: Paired training results in the variable CC (black) being driven nearly as high as $Sens$ (blue) and then prolonging the duration of $Sens$. Unpaired training, where the US follows the CS by 60s, results in CC (red) never leaving baseline. While $Sens$ (magenta) is initially almost as high as for paired training, it dies away much faster.

$$\frac{d5HT}{dt} = I_{5HT} - \frac{5HT}{T_{5HT}} \tag{10.11}$$

$$\frac{dDishab}{dt} - [5HT - Dishab]/T_{Intermediate} \tag{10.12}$$

$$\frac{dHab}{dt} = (Hab_0 - Hab)/T_{Hab} + \frac{Dishab}{T_{Dishab}} \tag{10.13}$$

$$where \quad : \quad T_{Hab} = 5.25 \cdot ISI_{mean} \tag{10.8}$$

$$\frac{dSens}{dt} = [Hab^n \cdot (5HT \cdot R_{Sens}) + (CC - Sens)]/T_{Sens} \tag{10.21}$$

$$\frac{dCC}{dt} = [Hab^n \cdot (5HT\_Ca \cdot R_{Sens}) + (CC_0 - CC) \cdot T_{Sens}/T_{CC}]/T_{Sens} \tag{10.20}$$

$$\frac{dPSC}{dt} = (-PSC)/(T_{PSC} \cdot Sens) \tag{10.22}$$

The second group describes the response of the model to CS and US spikes. These "equations" are in the form of pseudocode statements. If the condition or conditions of the *if* () *then* statements are met, then the lines of code within the brackets { } are executed once in sequence. These equations are the source of discontinuities in the time courses of the variables

$$\begin{aligned} if\ (t &= t_{US\ onset})\ then\{ \\ I_{5HT}(x)|_t^{t+I_{5HT}D} &= I_{5HT\,\max} \cdot P9_{stim\ strength} \qquad (10.10) \\ I_{5HT\_Ca}(x)|_t^{t+I_{5HT}D} &= I_{5HT\,\max} \cdot P9_{stim\ strength} \cdot Ca\} \qquad (10.18) \end{aligned}$$

$$\begin{aligned} &if\ (t = t_{spike})\ and\ (ISI_{\min} \leqslant ISI \leqslant ISI_{\max})\ then\{ \qquad (10.9) \\ &Hab = Hab \cdot \Delta H \\ &ISI_{mean} = ISI_{mean} \cdot (\frac{\Lambda - 1}{\Lambda}) + ISI \cdot (\frac{1}{\Lambda})\ \ \} \end{aligned}$$

$$\begin{aligned} if\ (t &= t_{spike})\ then\ \{ \\ PSC &= PSC + PSC_0 \cdot Hab \qquad (10.23) \\ I_{Ca}(x)|_t^{t+I_{Ca}D} &= I_{Ca}M\ \} \qquad (10.16) \end{aligned}$$

The various constants which feature in these equations are presented in Table 10.2. The

Variable	Value	Variable	Value
ΔH	0.85	n	10
Λ	10	PSC_0	2nA
$Ca_{\max}$	1	R_{Sens}	$0.42 \times 10^9 \Omega$
CC_0	1	T_{5HT}	8s
$Duration_{5HT}$	5s	T_{Ca}	30s
Hab_0	1	T_{CC}	3600s
$I_{5HT_{\max}}$	$40nM.s^{-1}$	T_{Dishab}	$0.8\mu s$
$I_{Ca}D$	2.5ms	$T_{Intermediate}$	7s
$I_{Ca}M$	10	T_{PSC}	5ms
$ISI_{\max}$	120s	T_{Sens}	350s
$ISI_{\min}$	1s		

Table 10.2: Values for the constants in the synapse model

equations presented here, combined with the simple model neurons as described in chapter 9 constitute the author's model of the GSWR. The MatLab code written by the author to implement these equations is included in Appendix A. An evaluation of its accuracy and realism is presented in the following chapter.

Chapter 11

Model Evaluation

It is the aim of this chapter to evaluate the validity of the author's model. However, a rigorous verification is not possible for two primary reasons. The first is the lack of a benchmark with which to compare the model. The experimental data in the literature is inconsistent in its detail, meaning that there is no single ideal case. The second reason is that models in neuroscience are never complete. This issue was discussed in the context of neuron models in Chapter 2. Probably the two best known neuron models are the Hodgkin Huxley (HH) equations and the Leaky Integrate-and-Fire (LIF) model, and even the former is an approximation. While the HH model comes relatively close to reality, producing fairly realistic membrane behaviour, the far simpler LIF model is still considered a valid approximation to neural functioning.

The author's synapse model lies somewhere between the HH and LIF models on a scale of complexity. While not directly modelling ion channel dynamics (as the HH model does) it does not simplify to the same degree as the LIF model. Thus this model will be considered valid if it reproduces the broadscale features of the real synapse. This evaluation is split into four sections; one for each of the three forms of plasticity it includes, and a fourth dealing with the model as a whole.

11.1 Evaluating Habituation

In Section 10.4 it was decided that the progression of habituation (as a function of stimulus number) should be independent of ISI. It was also decided that the rate of recovery should be

dependent on ISI, but in a simple, linear fasion. Figure 11-1 shows the response of the model to habituation training consisting of ten trials at an ISI of 3, 10, 30 or 100s. As can be seen, habituation tends to a limit of 50% of $EPSP_1$ for all ISIs used. This value is approximately that reported in [16] for ISIs of 3, 10 and 30s. Also evident from these plots is the slower recovery of synapses trained with longer ISIs. Spontaneous recovery from habituation is shown in Figure 11-2 (left), and has a time course similar to that reported in [69].

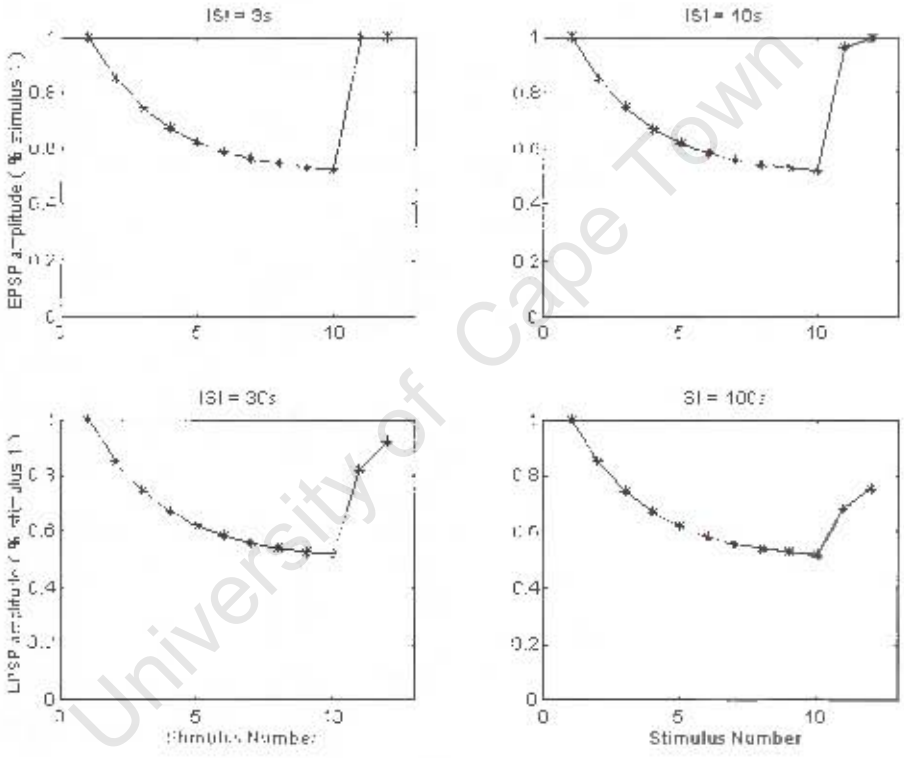

Figure 11-1: Habituation and recovery for training ISIs of 3, 10, 30 and 100s. The two post tests (stimuli 11 and 12) are at an ISI of 125s. CS strength = $4g.mm^{-2}$.

This model's main flaw is that, due to the imposition of a minimum and maximum decrementing ISI, there is a sudden jump from full habituation to zero habituation as the ISI crosses these limits. This behaviour is obviously unrealistic and undesirable. While there is certainly room for improvement, it is the author's opinion that this habituation model does reproduce many of the broadscale features exhibited by habituation of the real synapse.

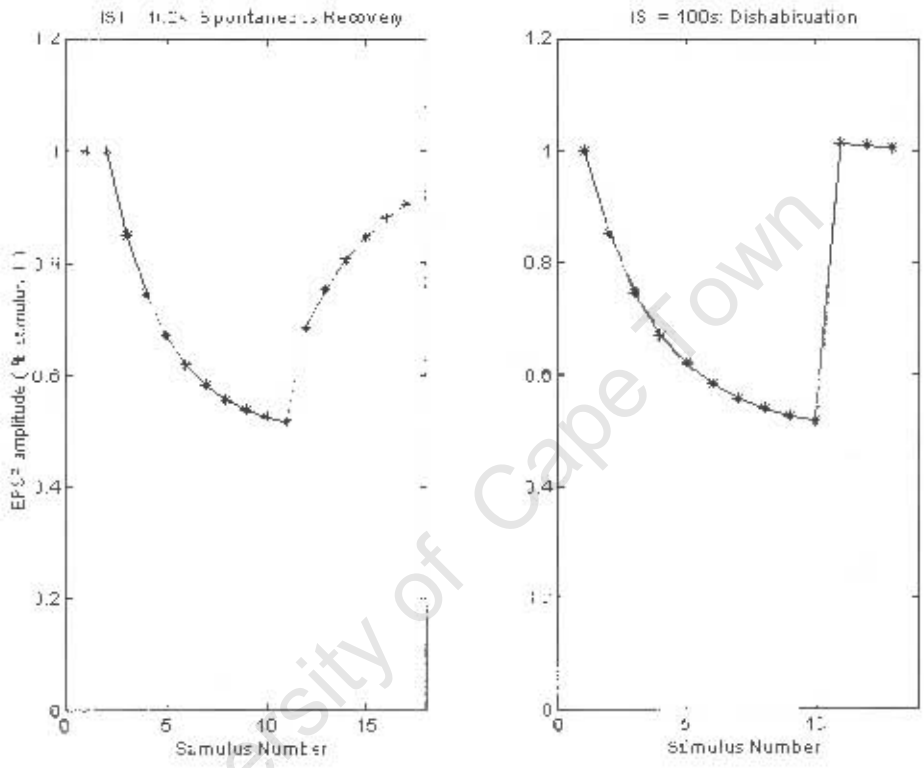

Figure 11-2: Spontaneous recovery from habituation (10 stimuli) with rest (left) and dishabituation (right). Training ISI = 100s and the post tests are at an ISI of 125s in both cases. The US is presented 5s after stimulus 10 (right). CS strength = $4g.mm^{-2}$, US strength = 50%.

11.2 Evaluation of Dishabituation and Sensitization

The effect of a dishabituating stimulus is shown in Figure 11-2 (right), and Figure 11-3 (left) for stimuli of 50% and 25% strength respectively. The response quickly returns to baseline, but is not significantly facilitated. As mentioned in Section 10.5.2, little is known about the specific time course of dishabituation, but comparison with Figure 11-4 (A) (taken from [67]) suggests that the model is quite accurate.

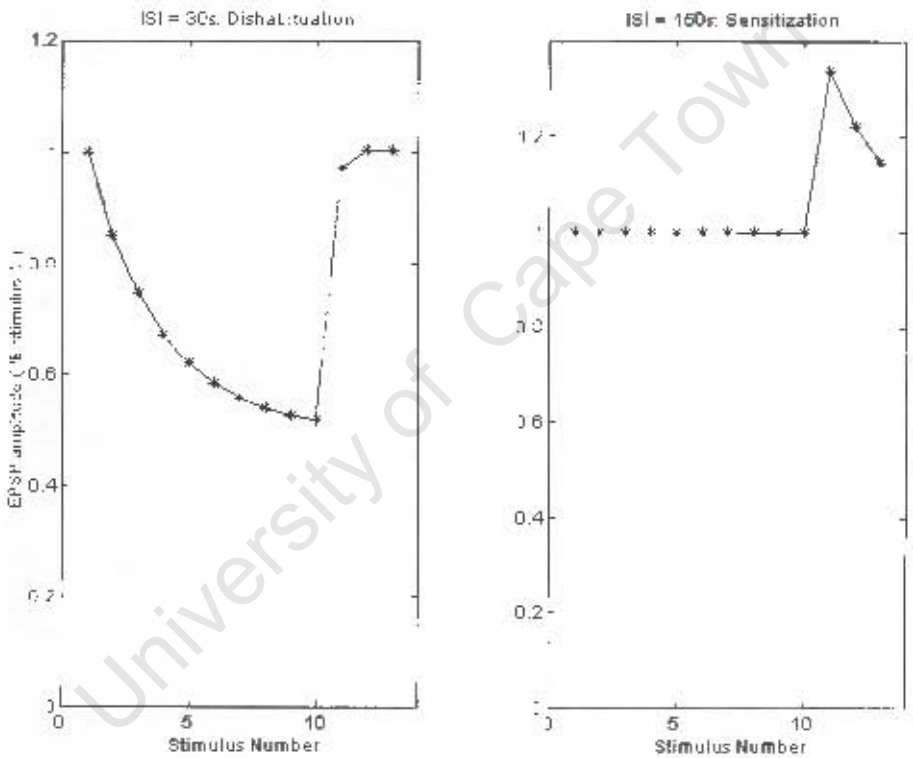

Figure 11-3: Habituation with a 30s ISI followed by a 25% strength dishabituating US, presented 5s after stimulus 10 (left). Ten stimuli at a non-decrementing ISI of 150s followed by a 25% strength dishabituating US, presented 5s after stimulus 10 (right). ISI for the three post tests is 125s in both cases.

The response of the model to sensitization is illustrated in Figure 11-3 (right). Again there is the problem of a lack of specific data about the time course of sensitization, but if the model output is compared with 11-4 (B) (taken from [67]), the similarity is immediately evident.

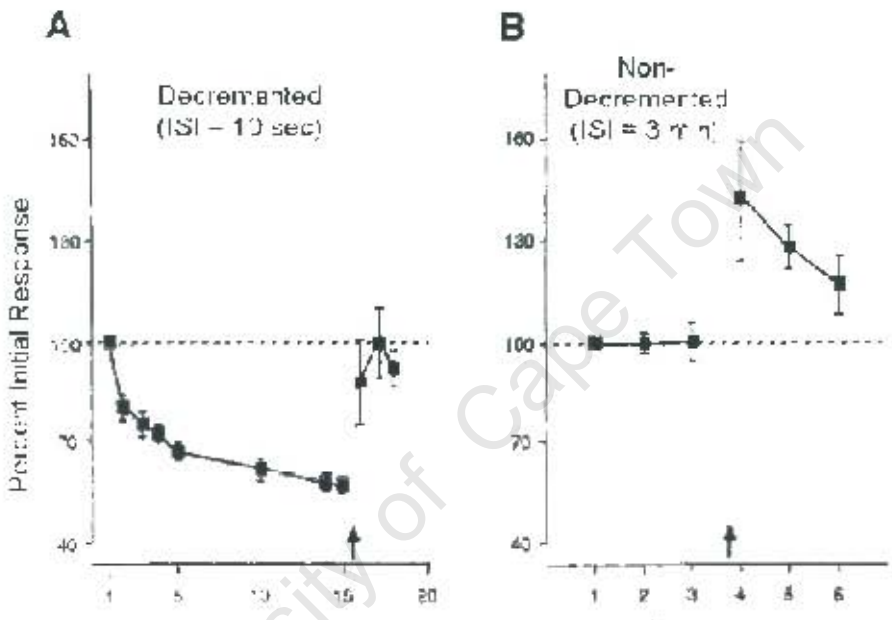

Figure 11-4: Cellular analog of dishabituation (A) and sensitization (B), taken from [67]. The time of US presentation is indicated by the arrows.

In Section 8.1, it was decided that this model would seek to reproduce only the short-term forms of the plasticity under investigation. Since a requirement for conversion to long-term memory is repetition, the author has thus far assumed only a single presentation of the US. The effect of repeated sensitizing stimuli on the model must now be investigated. To this end, Figure 11-5 (left) shows the effect of three US presentations in short succession. As can be seen, the facilitation builds up over the three stimuli. However, this accumulation is not representative of long-term sensitization, as the duration of facilitation is not significantly affected. To more accurately reproduce the protein-synthesis-independent process of short-term sensitization, it would be necessary to impose some limit on the value of *Sens*, representing the maximal effect of spike broadening on transmitter release. Apart from this problem, the model reproduces the broadscale, qualitative features of dishabituation and short-term sensitization with a satisfactory degree of realism.

11.3 Evaluation of Classical Conditioning

In keeping with the decision to model only short-term plasticity, it was decided in Section 10.6 that only "Form-1" conditioning would be included in this model. Thus the actual process being modelled is ADPF. It was also decided in Section 10.6 that the effect of pairing the CS and US should primarily be to increase the duration (rather than the magnitude) of facilitation. Figure 11-6 shows the time course of facilitation resulting from a single US presentation, either unpaired (left) or paired (right) with the CS. As can be seen, the duration of facilitation is substantially greater for paired stimuli. Figure 11-7 shows the effect of the relative timing between CS and US on conditioning. There is a reasonable degree of temporal specificity, particularly for delays shorter than the optimum of 0.5s. For longer delays however (Figure 11-7, bottom right) the degree of specificity depends on the duration of the CS. The modelled Ca^{2+} concentration reaches near maximum within 0.5s of CS onset. If, however, a long CS is used, the Ca^{2+} concentration will be near maximum from 0.5s after CS onset until just after CS offset. Conditioning will be near maximum if the US is presented at any point in this window, reducing the temporal specificity. Fortunately, the output trains produced by real LE neurons [35] and the model LE neurons presented in Section 9.1, in response to a single CS are both

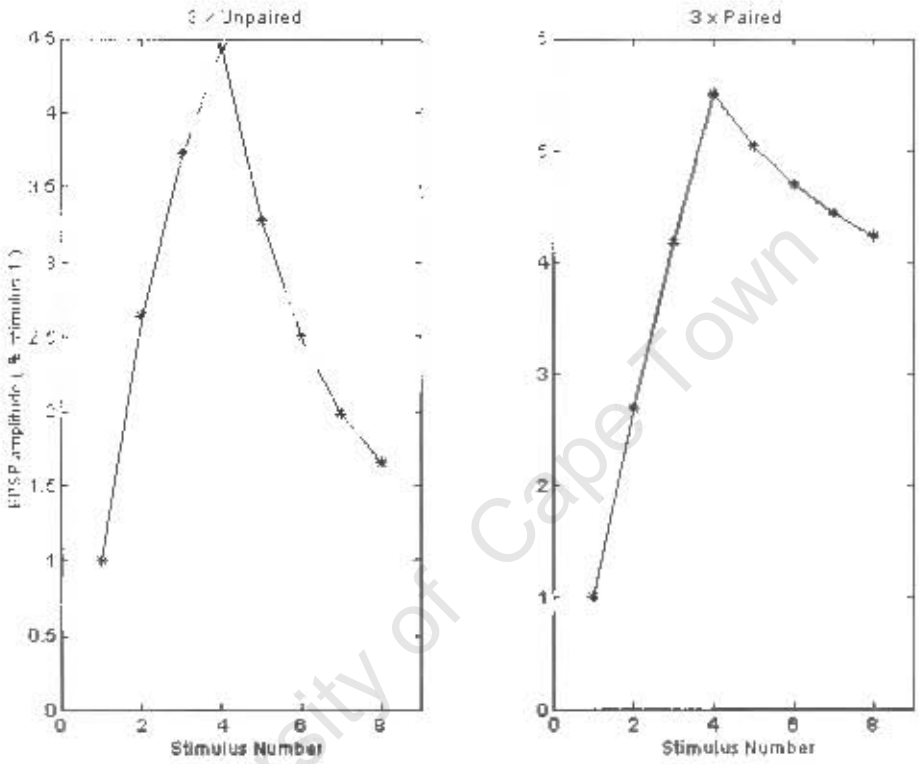

Figure 11-5: Multiple presentations of either unpaired (left) or paired (right) CS and US. An ISI of 125s was used throughout in both cases. The protocol consisted of 3 training trials followed by 5 post tests. For unpaired training (sensitization) the US was presented 60s after the CS. For paired training (conditioning) the US followed 0.5s after the CS. CS strength = $4g.mm^{-2}$ and US strength = 100% in both cases.

less than 1s in duration.

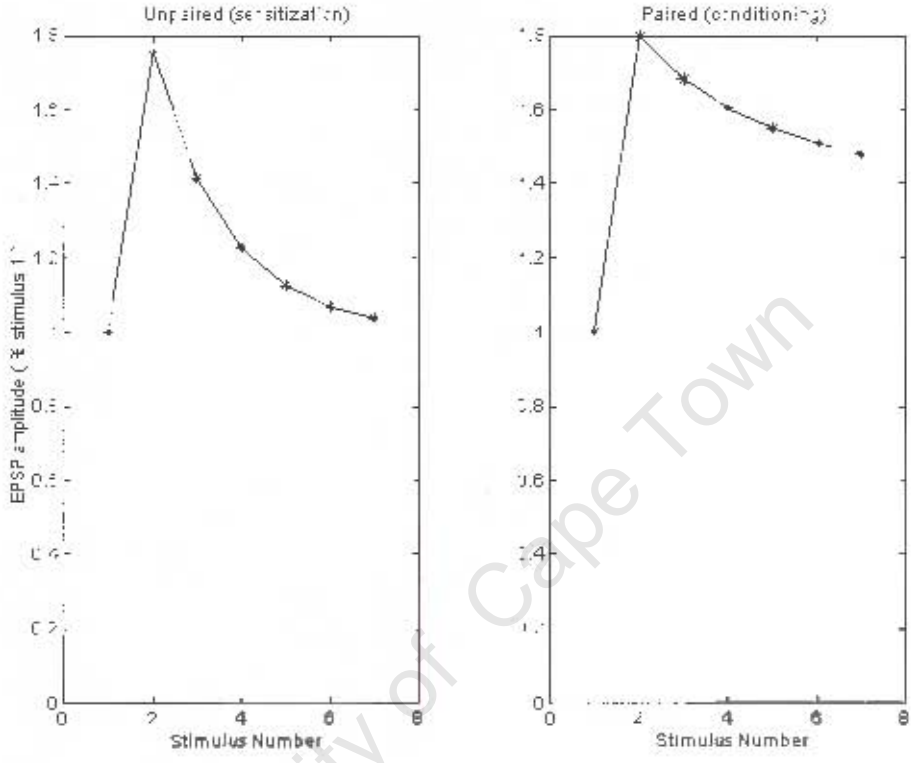

Figure 11-6: Time course of facilitation resulting from a single presentation of US, either unpaired (left) or paired (right) with the CS. ISI = 180s and CS strength = $4g.mm^{-2}$. The US is presented either 90s (unpaired) or 0.5s (paired) after the first CS and is 50% strength in both cases.

Figure 11-5 (right) shows the effect of multiple CS/US pairings. As discussed in Section 10.6, Form-1 conditioning is by definition the product of a single pairing. Therefore the fact that facilitation builds up with repeated pairings is undesirable in this model.

It is the author's opinion that, while being significantly limited in its scope, the model of classical conditioning presented in this work reproduces well the associative facilitation resulting from a single CS/US pairing.

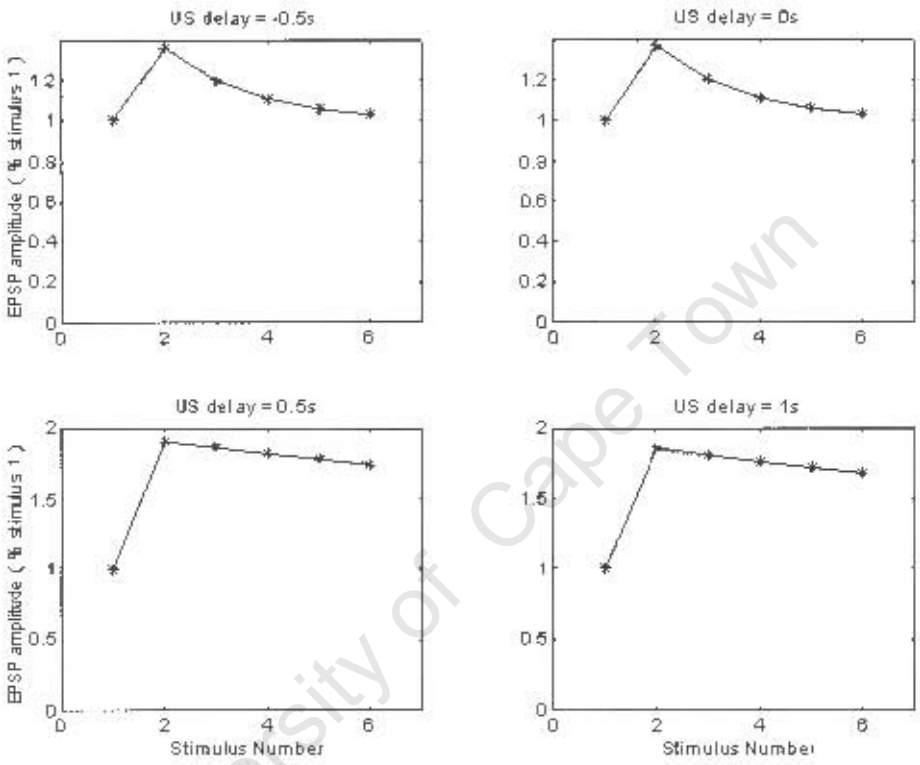

Figure 11-7: Effect of CS/US timing on conditioning. Cases shown are: US precedes CS by 0.5s (delay = -0.5); US presented at same time as CS (delay = 0s); US follows 0.5s after CS (delay = 0.5s); US follows 1s after CS (delay - 1s). Training is followed by 5 post tests. ISI = 180s, CS strength = $10g.mm^{-2}$ and US strength = 50% in all cases.

11.4 Evaluating the Complete Synapse Model

The simple models used for the LE and LFS neurons are sufficient for reproducing experiments involving reduced preparations of the monosynaptic GSWR, in which the output is a measured EPSP in the motor neuron and the input is chosen to produce a specific LE spike train. More detailed models of these two neurons would almost certainly be compatible with the synapse model in this work. The US pathway is not modelled with much realism, and is better suited to representing exogenous $5-HT$ application than release in response to tail stimulation.

The emphasis of this work is on the SN-MN synapse and the plasticity which it exhibits, so the model synapse is the most significant component. The basic role of the synapse is converting presynaptic spikes into PSCs. The structure of this PSC (discussed in Section 10.3), when integrated by the model motor neuron, results in a PSP that closely resembles that of a real LFS EPSP (Figure 10-4). The decision to apply habituation and sensitization to different components of the PSC (Section 10.1) adds to the realism of the model, but is mostly cosmetic as both $PSC_0 \cdot Hab$ and $T_{PSC} \cdot Sens$ linearly affect the EPSP area, except for $Sens \ll 0$. It was decided in Section 10.1 that habituation would be applied to rate-of-rise (ROR) of the PSP, while sensitization would be applied to time-to-peak (TTP). Figure 11-8 shows three representative PSPs for sensitized, habituated and control synapses, in which the effects on ROR and TTP can be seen.

The models of habituation, dishabituation, sensitization and classical conditioning have been discussed independently in the previous three sections. However, the interactions between these processes must also be considered. Figure 11-9 (left) shows habituation of a sensitized synapse. The onset of habituation is somewhat steeper, as it is accentuated by sensitization wearing off. When the habituating stimulus stops and is replaced by a non-decrementing ISI, the response recovers to above baseline, as the sensitization time constant is the longer of the two. This would not have been possible if a single variable had been used to represent the combined effects of both processes. The author was unable to find experimental data with a similar protocol, but this is likely to be correct, as the mechanisms of habituation and sensitization are independent (see Sections 7.5 and 7.6). A similar situation occurs when habituation is preceded by conditioning, as shown in Figure 11-9 (right). The interaction between the separate mechanisms does not seem to introduce any unexpected behaviour. As a result of using separate variables for habituation,

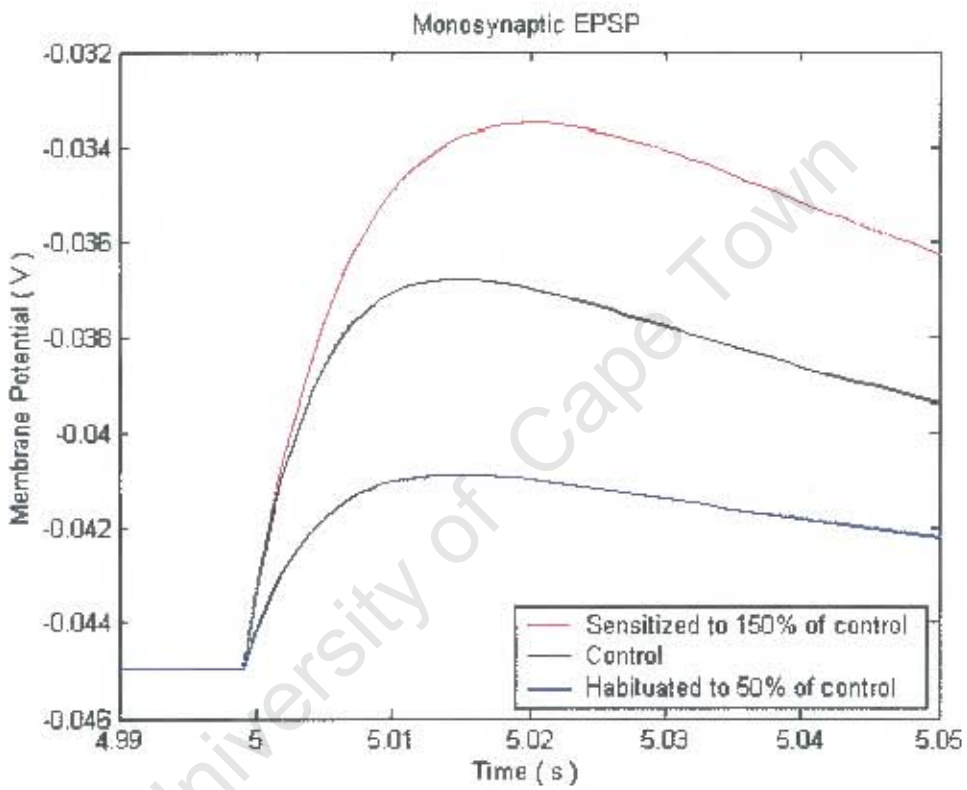

Figure 11-8: PSPs as produced by the model in response to a single presynaptic spike, for rested (black), sensitized (red) or habituated (blue) synapses. Note the longer TTP for the sensitized case and the lesser ROR for the habituated case.

sensitization and conditioning, the synapse can exhibit fairly rich behaviour. This is because the synapse efficiency depends in a complex way on several underlying processes. Thus more information is stored in the synapse than is represented by its efficiency alone.

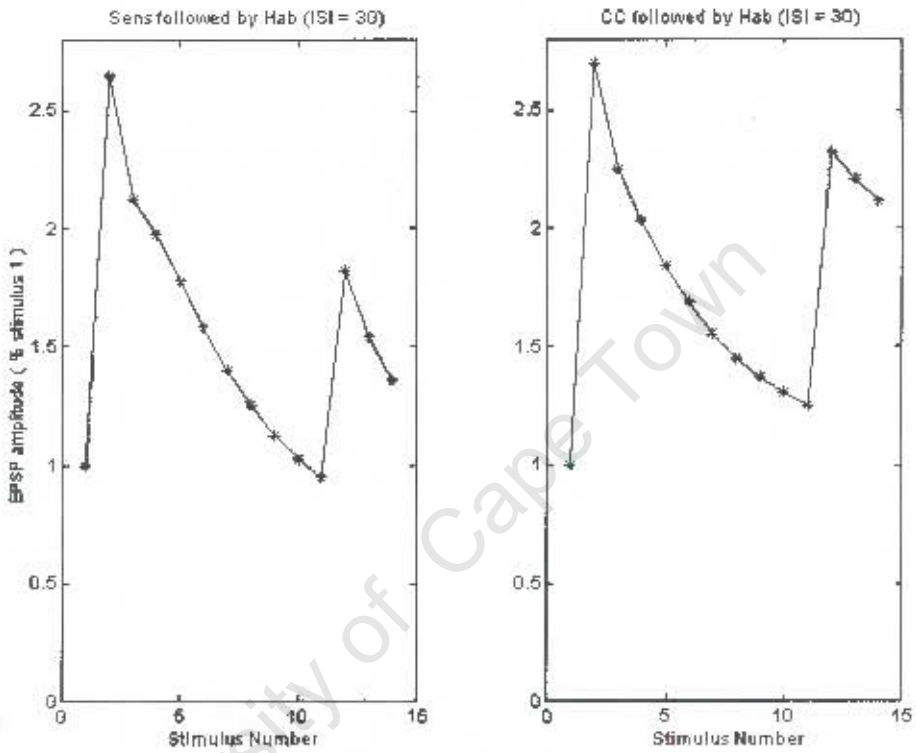

Figure 11-9: Habituation of a synapse that has received either sensitization (left) or conditioning (right). In the case of sensitization, the pretest is followed 60s later by the US. In the case of conditioning, the US is presented 0.5s after the pretest. Habituation training begins 125s after the pretest in both cases and a 30s ISI is used. The three post tests are presented with an ISI of 125s. CS strength $= 4g.mm^{-2}$, US strength $= 100\%$.

Chapter 12

Conclusions

Having completed the synapse model and evaluated its behaviour, some specific conclusions can be drawn.

- The model is a definite success, and reproduces quite accurately the short term components of habituation, sensitization and classical conditioning.
- While adding to the complexity of the model, the decision to maintain separate variables for each of the three processes was definitely correct. Not only is it biophysically accurate, it also allows the synapse to exhibit rich behaviour which could not be predicted from a knowledge of the present synaptic efficiency and incoming stimulus alone.
- The decision to model the shape of the PSP was perhaps unnecessary. While it does add to the realism of the model, it is unlikely to have a significant behavioural effect because the duration of the PSP is very short compared to the time scale of behavioural stimuli. Similarly, applying habituation and sensitization to different aspects of the PSC was not necessary as both have the same effect on PSP area.
- In terms of balancing realism and simplicity, the model in its present state leans quite heavily towards realism. The author had originally hoped for a simpler model, but in retrospect the present model is an indespensible stepping stone.
- Where this model will really be of use is in ascertaining which features of the real synapse, and of the mechanisms of plasticity, are behaviorally significant.

Chapter 13

Recommendations for Future Work

Further work on this project could progress in three possible directions:

1. The present model has been significantly limited in its scope. The first major simplification was choosing to model only the short term component of plasticity, while the second was choosing to model only the monosynaptic component of the reflex. Thus one avenue of future work would be to expand the present model to include long term plasticity and/or include the contributions of polysynaptic pathways in the reflex.

2. The present model, while being quite realistic, is still hugely simplified. A possible direction for future work would be to improve on the realism of the model and more accurately model the processes underlying the various forms of plasticity. For example, the dynamics of cAMP and PKA, as well as the interactions between cAMP and Ca^{2+}, could be directly modelled. Also, the probabilistic process of transmitter release could be modelled, possibly even at the level of individual vesicles.

3. The present model is unfortunately far too complicated to run in real time (without a very powerful simulation platform). Before the synapse model could be used as a processing element in a real time spiking neural network, it will be necessary to simplify it quite drastically. Ideally the key properties of the synapse would be encapsulated in a model which could be implemented in hardware, such as analog VLSI.

Bibliography

[1] The brain: Understanding neurobiology. http://science.education.nih.gov/supplements/nih2/addiction/guide/lesson2-2.htm, 2005.

[2] M. Allaby, editor. *"Conditioning" A Dictionary of Zoology.* Oxford University Press, New York, 1999.

[3] M. Allaby, editor. *"Habituation" A Dictionary of Zoology.* Oxford University Press, New York, 1999.

[4] I. Antonov, I. Antonova, E. R. Kandel, and R. D. Hawkins. The contribution of activity-dependent synaptic plasticity to classical conditioning in aplysia. *J. Neuroscience*, 21:6413–6422, 2001.

[5] I. Antonov, I. Antonova, E. R. Kandel, and R. D. Hawkins. Activity-dependent presynaptic facilitation and hebbian LTP are both required and interact during classical conditioning in aplysia. *Neuron*, 37:135–147, 2003.

[6] I. Antonov, E. R. Kandel, and R. D. Hawkins. The contribution of facilitation of monosynaptic PSPs to dishabituation and sensitization of the aplysia siphon Withdrawal reflex. *J. Neuroscience*, 19:10438–10450, 1999.

[7] M. A. Arbib, editor. *The Handbook of Brain Theory and Neural Networks.* MIT Press, Cambridge, Massachusetts, 2003.

[8] C. H. Bailey, D. Bartsch, and E. R. Kandel. Toward a molecular definition of long-term memory storage. *PNAS*, 93:13445–13452, 1996.

[9] C. H. Bailey and M. Chen. Morphological basis of long-term habituation and sensitization in aplysia. *Science*, 220:91–93, 1983.

[10] C. H. Bailey and M. Chen. Long-term sensitization in aplysia increases the number of presynaptic contacts onto the identified gill motor neuron l7. *PNAS*, 85:9356–9359, 1988.

[11] C. H. Bailey and M. Chen. Morphological basis of short-term habituation in aplysia. *J. Neuroscience*, 8:2452–2459, 1988.

[12] R. Balakrishnan. Learning from a sea snail: Eric kandel. *Resonance*, June:86–90, 2001.

[13] J.-X. Bao, E. R. Kandel, and R. D. Hawkins. Involvement of presynaptic and postsynaptic mechanisms in a cellular analog of classical conditioning at aplysia sensory-motor neuron synapses in isolated cell culture. *J. Neuroscience*, 18:458–466, 1998.

[14] S. Blackburn, editor. *The Oxford Dictionary of Philosophy "brain"*. Oxford University Press, New York, 1996.

[15] M. Brunelli, V. Castellucci, and E. R. Kandel. Synaptic facilitation and behavioral sensitization in aplysia: Possible role of serotonin and cyclic AMP. *Science*, 194:1178–1181, 1976.

[16] J. H. Byrne. Analysis of synaptic depression contributing to habituation of gill-withdrawal reflex in aplysia californica. *J. Neurophysiology*, 48:431–438, 1982.

[17] J. H. Byrne, V. F. Castellucci, and E. R. Kandel. Contribution of individual mechanoreceptor sensory neurons to defensive gill-withdrawal reflex in aplysia. *J. Neurophysiology*, 41:418–431, 1978.

[18] J. H. Byrne and T. Crow. Invertebrate models of learning: Aplysia and hermissenda. In M. A. Arbib, editor, *The Handbook of Brain Theory and Neural Networks*, pages 581–585. MIT Press, Cambridge, Massachusetts, 2003.

[19] T. J. Carew and E. R. Kandel. Acquisition and retention of long-term habituation in aplysia: Correlation of behavioral and cellular processes. *Science*, 182:1158–1160, 1973.

[20] T. J. Carew, H. M. Pinsker, and E. R. Kandel. Long-term habituation of a defensive withdrawal reflex in aplysia. *Science*, 175:451–454, 1972.

[21] T. J. Carew, E. T. Walters, and E. R. Kandel. Classical conditioning in a simple withdrawal reflex in aplysia californica. *J. Neuroscience*, 1:1426–1437, 1981.

[22] V. Castellucci and E. R. Kandel. Presynaptic facilitation as a mechanism for behavioral sensitization in aplysia. *Science*, 194:1176–1178, 1976.

[23] V. Castellucci, H. Pinsker, I. Kupfermann, and E. R. Kandel. Neuronal mechanisms of habituation and dishabituation of the gill-withdrawal reflex in aplysia. *Science*, 167:1745–1748, 1970.

[24] V. F. Castellucci and E. R. Kandel. A quantal analysis of the synaptic depression underlying habituation of the gill-withdrawal reflex in aplysia. *PNAS*, 71:5004–5008, 1974.

[25] G. Chechik, D. Horn, and E. Ruppin. Hebbian learning and neuronal regulation. In M. A. Arbib, editor, *The Handbook of Brain Theory and Neural Networks*, pages 511–514. MIT Press, Cambridge, Massachusetts, 2003.

[26] G. Chen, N. C. Harata, and R. W. Tsien. Paired-pulse depression of unitary quantal amplitude at single hippocampal synapses. *PNAS*, 101:1063–1068, 2004.

[27] L. J. Cleary, W. L. Lee, and J. H. Byrne. Cellular correlates of long-term sensitization in aplysia. *J. Neuroscience*, 18:5988–5998, 1998.

[28] D. Cofer. Neuron basics. www.mindcreators.com/NeuronBasics.htm, 2002.

[29] T. E. Cohen, S. W. Kaplan, E. R. Kandel, and R. D. Hawkins. A simplified preparation for relating cellular events to behavior: Mechanisms contributing to habituation, dishabituation, and sensitization of the aplysia gill-withdrawal reflex. *J. Neuroscience*, 17:2886–2899, 1997.

[30] A. M. Colman. *Oxford Dictionary of Psychology.* Oxford University Press, New York, 2003.

[31] L. S. Eliot, R. D. Hawkins, E. R. Kandel, and S. Schacher. Pairing-specific, activity-dependent presynaptic facilitation at aplysia sensory-motor neuron synapses in isolated cell culture. *J. Neuroscience*, 14:368–383, 1994.

[32] Y. Ezzeddine and D. L. Glanzman. Prolonged habituation of the gill-withdrawal reflex in aplysia depends on protein synthesis, protein phosphatase activity, and postsynaptic glutamate receptors. *J. Neuroscience*, 23:9585–9594, 2003.

[33] K. Fitzgerald, W. G. Wright, E. A. Marcus, and T. J. Carew. Multiple forms of non-associative plasticity in aplysia: A behavioral, cellular and pharmacological analysis. *Philisophical Transactions: Biological Sciences*, 329:171–178, 1990.

[34] Y. Fregnac. Hebbian synaptic plasticity. In M. A. Arbib, editor, *The Handbook of Brain Theory and Neural Networks*, pages 515–522. MIT Press, Cambridge, Massachusetts, 2003.

[35] L. Frost, S. W. Kaplan, T. E. Cohen, V. Henzi, E. R. Kandel, and R. D. Hawkins. A simplified preparation for relating cellular events to behavior: Contribution of LE and unidentified siphon sensory neurons to mediation ad habituation of the aplysia gill- and siphon- withdrawal reflex. *J. Neuroscience*, 17:2900–2913, 1997.

[36] W. N. Frost, V. F. Castellucci, R. D. Hawkins, and E. R. Kandel. Monosynaptic connections made by the sensory neurons of the gill- and siphon- withdrawal reflex in aplysia participate in the storage of long-term memory for sensitization. *PNAS*, 82:8266–8269, 1985.

[37] W. Gerstner and W. M. Kistler. *Spiking Neuron Models. Single Neruons, Populations, Plasticity.* Cambridge University Press, New York, 2002.

[38] D. L. Glanzman. The cellular basis of classical conditioning in aplysia californica - it's less simple than you think. *Trends Neuroscience*, 18:30–36, 1995.

[39] D. L. Glanzman, S. L. Mackey, R. D. Hawkins, A. M. Dyke, P. E. Lloyd, and E. R. Kandel. Depletion of serotonin in the nervous system of aplysia reduces the behavioral enhancement of gill withdrawal as well as the heterosynaptic facilitatio produced by tail shock. *J. Neuroscience*, 9:4200–4213, 1989.

[40] L. J. Graham and R. T. Kado. Biophysical mosaic of the neuron. In M. A. Arbib, editor, *The Handbook of Brain Theory and Neural Networks*, chapter III, pages 170 – 175. MIT Press, Cambridge, Massachusetts, 2003.

[41] R. D. Hawkins, T. W. Abrams, T. J. Carew, and E. R. Kandel. A cellular mechanism of classical conditioning in aplysia: Activity-dependent amplification of presynaptic facilitation. *Science*, 219:400–405, 1983.

[42] R. D. Hawkins, T. J. Carew, and E. R. Kandel. Effects of interstimulus interval and contingency on classical conditioning of the aplysia siphon withdrawal reflex. *J. Neuroscience*, 6:1695–1701, 1986.

[43] R. D. Hawkins, N. Lalevic, G. A. Clack, and E. R. Kandel. Classical conditioning of the aplysia siphon-withdrawal reflec exhibits response specificity. *PNAS*, 86:7620–7624, 1989.

[44] R. S. Hine and E. Martin, editors. *"synaptic Plasticity", Oxford Dictionary of Biology.* Oxford University Press, New York, 2004.

[45] B. Hochner, M. Klein, S. Schaceher, and E. R. Kandel. Action-potential duration and the modulation of transmitter release from the sensory neruons of aplysia in presynaptic facilitation and behavioral sensitization. *PNAS*, 83:8410–8414, 1986.

[46] B. Hochner, M. Klein, S. Schacher, and E. R. Kandel. Additional component in the cellular mechanism of presynaptic facilitation contributes to behavioral dishabituation in aplysia. *PNAS*, 83:8794–8798, 1986.

[47] A. L. Hodgkin and A. F. Huxley. A quantitative description of membrane current and its application to conduction and excitation in nerve. *J. Physiology*, 117:500–544, 1952.

[48] L. M. Igaz, M. R. M. Vianna, J. H. Medina, and I. Izquierdo. Two time periods of hippocampal mRNA synthesis are required for memory consolidation of fear-motivated learning. *J. Neuroscience*, 22:6781–6789, 2002.

[49] J. J. R. Lieb and W. N. Frost. Realistic simulation of the aplysia siphon-withdrawal reflex circuit: Roles of circuit elements in producing motor output. *J. Neurophysiology*, 77:1249–1268, 1997.

[50] S. A. Josselyn, C. Shi, W. A. Carlezon, R. L. Neve, E. J. Nestler, and M. Davis. Long-term memory is facilitated by cAMP response element-binding protein overexpression in the amygdala. *J. Neuroscience*, 21:2404–2412, 2001.

[51] E. R. Kandel. *Cellular Basis of Behavior.* Freeman, San Francisco, CA, 1976.

[52] E. R. Kandel. Nobel lecture: The molecular biology of memory storage: A dialog between genes and synapses. *Bioscience Reports*, 21:565–611, 2001.

[53] M. Klein and E. R. Kandel. Mechanism of calcium current modulation underlying presynaptic facilitation and behavioral sensitization in aplysia. *PNAS*, 77:6912–6916, 1980.

[54] K. Klemm, S. Bornholdt, and H. G. Schuster. Beyond hebb: Exclusive-or and biological learning. *Physical Review Letters*, 84:3013–3016, 2000.

[55] F. B. Krasne and D. L. Glanzman. What can we learn from invertebrate learning. *Annu. Rev. Psychology*, 46:584–624, 1995.

[56] R. Kretz, E. Shapiro, and E. R. Kandel. Post-tetanic potentiation at an identified synapse in aplysia is correlated with a ca2+ -activated k+ current in the presynaptic neuron: Evidence for ca2+ accumulation. *PNAS*, 79:5430–5434, 1982.

[57] I. Kupfermann, V. Castellucci, H. Pinsker, and E. Kandel. Neuronal correlates of habituation and dishabituation of the gill-withdrawal reflex in aplysia. *Science*, 167:1743–1745, 1970.

[58] W. Maas and C. M. Bishop, editors. *Pulsed Neural Networks.* MIT Press, Cambridge, Massachusetts, 1999.

[59] W. Maass. Networks of spiking neurons: The third generation of neural network models. *Neural Networks*, 10:1659–1671, 1997.

[60] W. Maass and A. M. Zador. Dynamic stochastic synapses as computational units. *Neural Computation*, 11:903–917, 1999.

[61] E. A. Marcus, T. G. Nolen, C. H. Rankin, and T. J. Carew. Behavioral dissociation of dishabituation, sensitization and inhibition in aplysia. *Science*, 241:210–213, 1988.

[62] S. Marinesco and T. J. Carew. Serotonin release evoked by tail nerve stimulation in the CNS of aplysia: Characterization and relationship to heterosynaptic plasticity. *J. Neuroscience*, 22:2299–2312, 2002.

[63] J. L. McGaugh. Memory–a century of consolidation. *Science*, 287:248–251, 2000.

[64] G. G. Murphy and D. L. Glanzman. Mediation of classical conditioning in aplysia californica by long-term potentiation of sensorimotor synapses. *Science*, 278:467–452, 1997.

[65] G. G. Murphy and D. L. Glanzman. Cellular analog of differential classical conditioning in aplysia: Disruption by the NMDA receptor antagonist DL-2-amino-5-phosphonovalerate. *J. Neuroscience*, 19:10595–10602, 1999.

[66] F. Nadim and Y. Manor. The role of short-term synaptic dynamics in motor control. *Current Opinion in Neurobiology*, 10:683–690, 2000.

[67] T. G. Nolen and T. J. Carew. The cellular analog of sensitization in aplysia emerges at the same time in development as behavioral sensitization. *J. Neuroscience*, 8:212–222, 1988.

[68] J. M. Pattillo, D. E. Artim, J. E. S. Jr, and S. D. Meriney. Variations in onset of action potential broadening: Effects on calcium current studied in chick cilary ganglion neurones. *J. Physiology*, 514.3:719–728, 1999.

[69] H. Pinsker, I. Kupfermann, V. Castellucci, and E. Kandel. Habituation and dishabituation of the gill-withdrawal reflex in aplysia. *Science*, 167:1740–1742, 1970.

[70] S. A. Prescott. Interactions between depression and facilitation within neural networks: Updating the dual-process theory of plasticity. *Learning Memory*, 5:446–466, 1998.

[71] C. H. Rankin and T. J. Carew. Dishabituation and sensitization emerge as separate processes during development in aplysia. *J. Neuroscience*, 8:197–211, 1988.

[72] S. G. Rayport and S. Schacher. Synaptic plasticity in vitro: Cell culture of identified aplysia neurons mediating short-term habituation and sensitization. *J. Neuroscience*, 6:759–763, 1986.

[73] A. C. Roberts and D. L. Glanzman. Learning in aplysia: Looking at synaptic plasticity from both sides. *Trends Neuroscience*, 26:662–670, 2003.

[74] S. Schacher, F. Wu, and Z. Sun. Pathway-specific synaptic plasticity: Activity-dependent enhancement and suppression of long-term heterosynaptic facilitation at converging inputs on a single target. *J. Neuroscience*, 17:597–606, 1997.

[75] I. Segev and M. London. Dendritic processing. In M. A. Arbib, editor, *The Handbook of Brain Theory and Neural Networks*, pages 324–332. MIT Press, Cambridge, Massachusetts, 2003.

[76] D. Smetters and A. Zador. Noisy synapses and noisy neurons. *Current Biology*, 6:1217–1218, 1996.

[77] C. F. Stevens and Y. Zhu. Synaptic transmission. In M. A. Arbib, editor, *The Handbook of Brain Theory and Neural Networks*, pages 1133–1135. MIT Press, Cambridge, Massachusetts, 2003.

[78] N. G. Stocks and R. Mannella. Generic noise-enhanced coding in neuronal arrays. *Physical Review E*, 64:030902–1 – 030902–4, 2001.

[79] M. Stopfer and T. J. Carew. Heterosynaptic facilitatio of tail sensory neurons synaptic transmission during habituation in tail-induced tail and siphon withdrawal reflexes of aplysia. *J. Neuroscience*, 16:4933–4948, 1996.

[80] M. Stopfer, X. Chen, Y. Tai, G. S. Huang, and T. J. Carew. Site specificity of short-term and long-term habituation in the tail-elicited siphon withdrawal reflex of aplysia. *J. Neuroscience*, 16:4923–4932, 1996.

[81] J. Tapson. Noise-induced phase locking in a relaxation oscillator: A kramers rate characterization. *Proc. South African Symposium on Communications and Signal Processing*, pages 179–180, 1997.

[82] L. E. Trudeau and V. F. Castellucci. Postsynaptic modifications in long-term facilitation in aplysia: Upregulation of excitatory amino acid receptors. *J. Neuroscience*, 15:1275–1284, 1995.

[83] M. L. Wainwright, H. Zhang, J. H. Byrne, and L. J. Cleary. Localized neuronal outgrowth induced by long-term sensitization training in aplysia. *J. Neuroscience*, 22:4132–4141, 2002.

[84] W. G. Wright, E. A. Marcus, and T. J. Carew. A cellular analysis of inhibition in the siphon withdrawal reflex of aplysia. *J. Neuroscience*, 11:2498–2509, 1991.

[85] A. M. Zador and L. E. Dobrunz. Dynamic synapses in the cortex. *Neuron*, 19:1–4, 1997.

Appendix A

MatLab Code

```
%Function f(ISI) returns value for habituation decrement
%Current function is simply a constant, but an actual function
%could be included
function [decrement] = f(ISI)

decrement = 0.85;



%Function g(meanISI) returns value for habituation
%time constant. A more complex function could be
%implemented at a later stage
function [Trec] = g(meanISI)

Trec = 5.25*meanISI;
```

```
%This is the model sensory neuron. Allows the user to create LE spike trains.
%Also allows for US. All times are in seconds
numpre = 1;
preISI = 180;

numtrials = 10;
ITI = 30;

pokeforce = 4;  %in g/mm^2 on the range 0 to 25
numtet = min(13,round(0.1661*pokeforce^2 - 0.3308*pokeforce + 2.2753))
tetISI = 1/50;

numpost = 1;
postISI = (125);


deltaT = 1e-3;
duration = 5 + preISI*numpre + ((tetISI*numtet)+ITI)*numtrials + postISI*nump
ost + 5;
numpoints = ceil(duration/deltaT);

LEoutput = zeros(1,numpoints);  %SN spikes
MCCspikes = zeros(1,numpoints); %Serotonergic interneuron spikes

USdelay = 0.5;
USstrength = 1;        %on range 0 to 1

pointer = 5;

%MCCspikes(1,(pointer+USdelay)/deltaT) = USstrength;

for i = 1:numpre
    for j = 1:numtet
        LEoutput(1,round(pointer/deltaT)) = 1;
        pointer = pointer + tetISI;
    end
    %MCCspikes(1,(pointer+USdelay)/deltaT) = USstrength;
    pointer = pointer + preISI;
end
%MCCspikes(1,round((pointer+USdelay)/deltaT)) = USstrength;
for i = 1:numtrials
    for j = 1:numtet
        LEoutput(1,round(pointer/deltaT)) = 1;
        pointer = pointer + tetISI;
    end
```

```
    pointer = pointer + ITI;
end

%MCCspikes(1,round((pointer + USdelay + postISI)/deltaT)) = USstrength;
for i = 1:numpost
    pointer = pointer + postISI;
    for j = 1:numtet
        LEoutput(1,round(pointer/deltaT)) = 1;
        pointer = pointer + tetISI;
    end
end
```

```
%Model synapse, including all plasticity. Uses the LE and MCC
%spike trains created by "sensory.m" for inputs. Outputs take
%the form of postsynaptic currents.

x = (deltaT:deltaT:duration);        % X axis vector

PSC = zeros(1,numpoints);
PSC0 = 2e-9;
PSCT = 6*deltaT;

hab0 = 1;
hab = zeros(1,numpoints);
hab(1,1) = hab0;

sens0 = 1;
sens = zeros(1,numpoints);
sens(1,1) = sens0;
Tsens = 300;
Rsens = 0.65e9;

CC = zeros(1,numpoints);
TCC = 60*60;
CC(1,1) = sens0;

Ca = zeros(1,numpoints);
ICa = zeros(1,numpoints);
TCa = 10;
ICa0 = 10;
ICaDuration = round(0.25/deltaT);
CaMax = 1;

HT0 = 0;
HT = zeros(2,numpoints);
IHT = zeros(2,numpoints);
IHT0 = 20e-9;    % 20nM/s
HT(1,1) = HT0;
THT = 9;
HTrisetime = 5/deltaT;

y = zeros(1,numpoints);      %y is the intermediate dishabituation variable
Ty = 7e1;

Thab = 20;
ISImax = 120;
ISImin = 1;
ISI = ISImax;
```

```
meanISI = 0;

Tdishab = 0.8e-6;

numspikes = numpre + numtet + numpost;
spikes = zeros(1,numspikes);
spikecnt = 0;

Thab = g(meanISI);

for i = 2:numpoints

    dPSC = -PSC(1,i-1)/(PSCT * sens(1,i-1));
    PSC(1,i) = PSC(1,i-1) + dPSC * deltaT;


    dhab = 1/Thab * (1-hab(1,i-1)) + y(1,i-1)/Tdishab;
    hab(1,i) = min(1,hab(1,i-1) + deltaT*dhab);

    dHT0 = (IHT(2,i) - HT(2,i-1)/THT);
    HT(2,i) = HT(2,i-1) + dHT0*deltaT;

    dHT = (IHT(1,i) - HT(1,i-1)/THT);
    HT(1,i) = HT(1,i-1) + dHT*deltaT;

    dCa = (-2*Ca(1,i-1) + ICa(1,i)*(CaMax-Ca(1,i-1))/CaMax)/TCa;
    Ca(1,i) = Ca(1,i-1) + dCa*deltaT;

    dy = [HT(1,i) - y(1,i-1)]/Ty;
    y(1,i) = y(1,i-1) + dy*deltaT;

    dCC = [HT(2,i) * Rsens * hab(1,i)^10 + (sens0-CC(1,i-1))*Tsens/TCC]/Tsens
;
    CC(1,i) = CC(1,i-1) + dCC*deltaT;

    dsens = [HT(1,i) * Rsens * hab(1,i)^10 + (CC(1,i-1)-sens(1,i-1))]/Tsens;
    sens(1,i) = sens(1,i-1) + dsens*deltaT;

    ISI = ISI + deltaT;

    if LEoutput(1,i) == 1   %Meaning that a spike has occured

        if (ISI <= ISImax) & (ISI >= ISImin)
            hab(1,i) = hab(1,i) * f(ISI);
            if meanISI == 0
                meanISI = ISI;
```

```
            else
                meanISI = (meanISI*3 + ISI) / 4;
            end
        end

        if (ISI >= ISImin)
            spikecnt = spikecnt + 1;
            spikes(1,spikecnt) = hab(1,i);
        end

        ISI = 0;
        PSC(1,i) = PSC(1,i-1) + PSC0 * hab(1,i);


        for j = i:min(i+ICaDuration,numpoints)
            ICa(1,j) = ICa(1,j) + ICa0;
        end
    end

    if MCCspikes(1,i) ~= 0      %meaning that tail shock has occured
        for j = i:(i + HTrisetime)
            IHT(1,j) = (IHT0 * MCCspikes(1,i));
            IHT(2,j) = (IHT0 * MCCspikes(1,i)) * (Ca(1,i));
        end
    end

end

%figure
%plot(x,IHT(1,:),'r',x,HT(1,:),'k',x,y,'b')%,x,PSC,'g')
%xlabel('Time ( s )')
%ylabel('5-HT concentration ( nM )')
%title('Square I5-HT pulse and resulting 5-HT concentration')
%legend('5-HT current ( nM/s )','5-HT concentration ( nM )')

%plot(x,LEoutput(1,:),'r',x,Ca(1,:),'k')
%figure
%plot(x,sens(1,:),'m',x,CC(1,:),'r')
%subplot(2,1,2),plot(x,LEoutput,'r',x,MCCspikes,'b',x,sens(1,:),'k',x,hab,'m'
)
%xlabel('Time ( s )')
%ylabel('Sens')
%title('Sensitization of Habituated Synapse')
%legend('US time','Sens')
%subplot(1,3,3),plot(spikes.*100,'k-*')
%xlabel('Stimulus Number')
```

```
%ylabel('EPSP Amplitude (% Pretest)')
%title('ISI = 100 s')

%subplot(2,2,2),
%plot(spikes.*100,'k-*')
%axis([0 12 0 100])
%xlabel('Spike Number')
%ylabel('Relative Response ( % )')
%title('ISI = 30 seconds')
%subplot(2,2,4),plot(x,LEoutput(1,:),'r',x,hab(1,:),'k')
%xlabel('Time ( s )')
%ylabel('Hab')

%subplot(1,2,2),plot(x,LEoutput,'r',x,hab,'k')
```

```
%Model motor neuron. Uses PSC produced by "synapse2.m" as input.
%Output is either the resulting PSP, or a vector containing the
%relative areas under the PSPs for each stimulus
R = 65e6;
C = 1.2e-9;
thresh = -51e-3;
urest = -45e-3;

u = zeros(1,numpoints);
u(1,1) = urest;

for i = 2:numpoints

     du = (PSC(1,i) - (u(1,i-1)-urest)/R)/C;
     u(1,i) = u(1,i-1) + du*deltaT;

end

previous = 0;
this = 0;
current = 0;
spikes = zeros(1,1);
numstims = 0;

for i = 1:numpoints
    this = u(1,i)-urest;
    if (this < 0.5e-15)
        this = 0;
    end
    if (this ~= 0)
        current = current + this*deltaT;
    elseif (this == 0)&(previous ~= 0)
        numstims = numstims + 1;
        spikes(1,numstims) = current;
        current = 0;
    end
    previous = this;
end
%spikes(1,1)
%spikes = spikes./spikes(1,1)
%figure
%plot(x,u(1,:),'b')
%v=axis;
%v(1,1) = 4.92;
%v(1,2) = 5.52;
%axis(v);
```

```
%subplot(2,1,2),plot(x,u(1,:))
%xlabel('Time ( ms )');
%ylabel('LFS Membrane Potential ( V )');
%title('PSP');
%subplot(2,1,1),plot(x,PSC(1,:)*1e9)
%xlabel('Time ( ms )');
%ylabel('Postsynaptic Current ( nA )');
%title('PSC');
%subplot(1,2,2),plot(spikes(1,:),'k-*')
%v=axis;
%v(1,3) = 0;
%v(1,2) = length(spikes(1,:))+1;
%axis(v);
%title('Paired (conditioning)')
%xlabel('Stimulus Number')
%ylabel('EPSP amplitude ( % stimulus 1 )')
```